

The Development of Brønsted Acid Catalysis Technologies and Mechanistic Investigations Therein

Thesis by
Diane Elizabeth Carrera

In Partial Fulfillment of the Requirements for the
Degree of
Doctor of Philosophy



California Institute of Technology

Pasadena, California

2009

(Defended 4 September 2009)

© 2009

Diane Elizabeth Carrera

All Rights Reserved

Acknowledgements

First and foremost I need to thank my research advisor, Prof. David MacMillan, for giving me the opportunity to work for him and surrounding me with fellow researchers of the highest caliber. Under his mentorship I have gained a true appreciation for the challenges and rewards inherent in studying organic chemistry and, most importantly, the perspective necessary to push the boundaries of what can be achieved by always thinking big. I would also like to thank the other members of my committee, Professors Jackie Barton, Brian Stoltz, and Peter Dervan for graciously giving their time and thought to my graduate studies as well as dealing with the additional hassles of scheduling exams from three thousand miles away. Without the support staff at both Princeton and Caltech it would have been impossible to do what is written in these pages, so it is with heartfelt appreciation that I thank Dian Buchness, Agnes Tong, Mona Shahgoli, Kim Faulkner, Joe Drew, Caroline Phillips, Istvan Pelczer, Phil Fairall, Kevin Wilkes and Vicky Lloyd. I would also like to thank Allan Watson, Ester Lee and Andrew Dilger for sacrificing their time in the proofreading of this manuscript as well as Hahn Kim, Jeff Van Humbeck, Mark Vanderwal, Spencer Jones and Joe Carpenter for doing the same for my proposals.

To the MacMillan groups members past and present, you have all made these past years as enjoyable as they could possibly be and I will miss the camaraderie and friendships that I've made during my time in the group. In particular, I need to thank the original MacMillan ladies Nikki Goodwin, Sandra Lee, Kate Ashton, Nadine Bremeyer, Maud Reiter, Catherine Larsen, Casey Jones and Teresa Beeson, without whom life both in and outside of lab would not have been nearly as enjoyable. I could not in good faith

complete these sentiments without also recognizing the members of Bay Awesome, which has been, without a doubt, the best place I can think of to spend ridiculous amounts of time storytelling, debating, and even doing chemistry. I'm especially going to miss my baymate of the past two years, David Nagib, whose constant smile and positive attitude have lifted my spirits on many occasions.

I would like to end these notes with a final thank you to the most important people in my life without whom I would never have achieved half of what I have today. To my mom Sarah, no one could have served as a better inspiration and I hope you realize that everything I have accomplished can be attributed directly to you. To my father Carl and stepmother Cheryl, your love and support has served as a true haven for me and helped me to weather the ups and downs of these past few years. To Kate and James, now that we're old enough not to fight about who sits in the middle, I count myself lucky to be able to call you my family. Finally, I dedicate this thesis to the memory of my grandparents whose love and pride in my accomplishments remain with me to this day.

ABSTRACT

The enantioselective reductive amination of ketones with Hantzsch ester has been achieved through Brønsted acid catalysis. A novel triphenylsilyl substituted BINOL-derived phosphoric acid catalyst has been developed for this transformation, imparting high levels of selectivity when used with methyl ketones and aromatic amines. A stereochemical model for the observed selectivity based on torsional effects has been developed through molecular modeling and is further supported by a single crystal x-ray structure of an imine-catalyst complex.

Mechanistic studies have revealed the importance of catalyst buffering and drying agent on reaction efficiency while a Hammett analysis of acetophenone derivatives offers insight into the key factors involved in the enantiodetermining step. Kinetic studies have shown that imine reduction is rate-determining and follows Michaelis-Menten kinetics. Determination of the Eyring parameters for the imine reduction has also been accomplished and suggests that the phosphoric acid catalyst behaves in a bifunctional manner by activating both the imine electrophile and the Hantzsch ester nucleophile.

The intermolecular addition of vinyl, aromatic, and heteroaromatic potassium trifluoroborate salts to non-activating imines and enamines can also be accomplished through Brønsted acid activation. This analog of the Petasis reaction shows a wide substrate scope and is amenable to use with a variety of carbamate protected nitrogen electrophiles in the first example of metal-free 1,2-additions of trifluoroborate nucleophiles. The mechanistic underpinnings of benzyl trifluoroborate addition has also been explored and, in contrast to what is seen with π -nucleophilic species, appears to proceed through an intramolecular alkyl-transfer mechanism.

Table of Contents

Acknowledgements.....	iii
Abstract.....	v
Table of Contents.....	vi
List of Schemes	vii
List of Figures.....	ix
List of Tables.....	xi
List of Abbreviations.....	xiii

Chapter 1: Stereogenic Amines: Biological Importance and Synthesis

I. Introduction.....	1
II. Asymmetric Imine Reduction	3
III. Asymmetric Reductive Amination.....	5

Chapter 2: Development of a Novel Phosphoric Acid Catalyzed Asymmetric Organocatalytic Reductive Amination of Ketones

I. Organocatalytic Activation Modes	10
II. Hydrogen Bonding Catalysis	12
III. Organocatalytic Imine Reduction	15
IV. Asymmetric Organocatalytic Reductive Amination.....	20
V. Conclusion.....	28
Supporting Information.....	30

Chapter 3: Kinetic and Mechanistic Studies of the Brønsted Acid Catalyzed Enantioselective Reductive Amination

I. Limitations in the Ketone Reductive Amination.....	79
---	----

II. Inhibition Studies	82
III. Hammett Study.....	84
IV. Crystal Structure.....	84
V. Role of Drying Agent.....	87
VI. Reaction Kinetics	90
VII. Eyring Activation Parameters	94
VII. Conclusion	96

Supporting Information.....	98
-----------------------------	----

Chapter 4: Development of an Acid Promoted Addition of Organotrifluoroborates to Non-Activating Electrophiles

I. Introduction	127
II. Development of an Organotrifluoroborate Petasis Reaction.....	130
III. Investigations into reaction mechanism.....	135
IV. Enantioselective induction	138
V. Conclusion.....	143

Supporting Information.....	144
-----------------------------	-----

List of Schemes

Chapter 1: Stereogenic Amines: Biological Importance and Synthesis

<i>Number</i>	<i>Page</i>
1. Reductive amination of an amine and a carbonyl compound	2
2. The first reported catalytic asymmetric reductive amination	5
3. Asymmetric reductive amination with alkyl ketones	7
4. Kadyrov's asymmetric reductive amination via transfer hydrogenation.....	7

Chapter 2: Development of a Novel Phosphoric Acid Catalyzed Asymmetric Organocatalytic Reductive Amination of Ketones

<i>Number</i>	<i>Page</i>
1. Hajos-Parrish proline catalyzed cyclization.....	10
2. Phosphoric acid catalyzed Mannich reaction reported by Akiyama	15
3. Evaluation of hydrogen bonding catalysts for imine reduction.....	17

Chapter 4: Development of an Acid Promoted Addition of Organotrifluoroborates to Non-Activating Electrophiles

<i>Number</i>	<i>Page</i>
1. Organocatalyzed Friedel-Crafts addition of organotrifluoroborates	129
2. Acid promoted addition of benzyltrifluoroborate	135
3. Evaluation of diverse acid catalyst structures.....	140

List of Figures

Chapter 1: Stereogenic Amines: Biological Importance and Synthesis

<i>Number</i>	<i>Page</i>
1. Pharmaceuticals containing stereogenic amines	1

Chapter 2: Development of a Novel Phosphoric Acid Catalyzed Asymmetric Organocatalytic Reductive Amination of Ketones

<i>Number</i>	<i>Page</i>
1. Organocatalytic activation modes	11
2. Serine protease active site and mechanism of action.....	12
3. Examples of hydrogen bonding catalysts from the literature.....	14
4. Mechanism of alanine dehydrogenase and proposed mechanism of H-bonding-catalyzed reductive amination	16
5. Computational model and crystal structure	26
6. Substrates with poor reactivity due to electronics	28

Chapter 3: Kinetic and Mechanistic Studies of the Brønsted Acid Catalyzed Enantioselective Reductive Amination

<i>Number</i>	<i>Page</i>
1. Proposed catalytic cycle for imine formation and subsequent reduction.....	80
2. The effect of varying amounts of amine on imine and product formation	82
3. Product inhibition study	83
4. Hammett plot of substituent effects on the reductive amination.....	84
5. Competing mechanistic pathways for the reductive amination.....	85
6. Crystal structure of imine bound catalyst	86
7. Influence of 5 Å MS and catalyst on rate of imine formation.....	66
8. Reaction profile	92
9. Lineweaver-Burk plot of imine concentration versus initial rate.....	93
10. Catalyst linearity for the reductive amination of acetophenone with p-anisidine.....	94
11. Bifunctional transition state model for imine reduction.....	95

12. Eyring activation parameters determined from a linear fit of k_{initial} over a range of temperatures	96
--	----

Chapter 4: Development of an Acid Promoted Addition of Organotrifluoroborates to Non-Activating Electrophiles

<i>Number</i>	<i>Page</i>
1. Mechanism of the Petasis reaction.....	128
2. Hammett study of benzyl trifluoroborate addition	136
3. Mechanism of hemiaminal formation.....	137

List of Tables

Chapter 2: Development of a Novel Phosphoric Acid Catalyzed Asymmetric Organocatalytic Reductive Amination of Ketones

<i>Number</i>	<i>Page</i>
1. Catalyst optimization.....	17
2. Organocatalytic reduction of imines.....	18
3. Impact of water on imine reduction	19
4. Drying agent screen.....	19
5. Drying agent screen for one-pot reductive amination	21
6. Optimization of amine and ketone equivalencies.....	21
7. Temperature screen for the reductive amination	22
8. Catalyst loading screen.....	22
9. Reductive amination with aromatic ketones.....	23
10. Reductive amination with alkyl-methyl ketones	24
11. Reductive amination with aromatic amines.....	25
12. Substrates with poor reactivity due to steric effects	27

Chapter 3: Kinetic and Mechanistic Studies of the Brønsted Acid Catalyzed Enantioselective Reductive Amination

<i>Number</i>	<i>Page</i>
1. Reductive amination with benzyl and alkyl amines	80
2. Effect of Hantzsch ester pyridine on reaction efficiency.....	83
3. Influence of 5Å MS and catalyst on rate of imine formation.....	88
4. Efficiency of water removal by molecular sieves.....	89

Chapter 4: Development of an Acid Promoted Addition of Organotrifluoroborates to Non-Activating Electrophiles

<i>Number</i>	<i>Page</i>
1. Evaluation of nitrogen protecting groups.....	131

2. Effect of solvent on reactivity	131
3. Evaluation of achiral Brønsted acids.....	132
4. Scope of vinyl and aryl trifluoroborate salt nucleophiles.....	133
5. Reaction scope with aryl imines and aliphatic enamines	134
6. Examination of chiral phosphoric acid catalysts	139
7. The effect of solvent on acid catalyzed trifluoroborate addition.....	141
8. Investigation into achiral acid additives to aid turnover.....	141

ABBREVIATIONS

9-BBN	9-borabicyclo[3.3.1]nonane
Ac₂O	acetic anhydride
AcOH	acetic acid
AIBN	azobisisobutyronitrile
Arg	arginine
Asp	aspartate
BINAP	2,2'-bis(diphenylphosphino)-1,1'-binaphthyl;
BINOL	1,1'-bi-2-naphthol
Boc	<i>tert</i> -butyl carbamate
Cbz	carbobenzyloxy
COD	cyclooctadiene
Cp	cyclopentadienyl
CSA	amphorsulfonic acid
Cy	cyclohexyl
DCA	dichloroacetic acid
DIBAL-H	diisobutylaluminum hydride
DME	dimethoxyethane
DMF	dimethylformamide
DMF	dimethylformamide
DMSO	methylsulfoxide
EtOAc	ethyl acetate
EtOH	ethanol
GLC	gas liquid chromatography
Gly	glycine
h	hour
HEH	Hantzsch ester

His	histidine
HOMO	highest occupied molecular orbital
HPLC	high pressure liquid chromatography
IC₅₀	concentration necessary for 50% inhibition
LA	Lewis acid
LUMO	lowest unoccupied molecular orbital
MeCN	acetonitrile
MeOH	methanol
min	minutes
MOM	methoxymethyl
MS	molecular sieves
Ms	methanesulfonyl
NADH	Nicotinamide adenine dinucleotide
NMR	nuclear magnetic resonance
Nu	nucleophile
PMP	<i>para</i> -methoxyphenyl
PPTS	pyridinium <i>p</i> -toluenesulfonate
<i>p</i>-TSA	<i>para</i> -toluenesulfonic acid
Ra/Ni	Raney nickel
Ser	serine
SFC	supercritical fluid chromatography
TADDOL	trans- α,α' -(dimethyl-1,3-dioxolane-4,5-diyl)bisdiphenyl methanol
TBAI	<i>tert</i> -butyl ammonium iodide
TBDPS	<i>tert</i> -butyldiphenylsilyl
TBDPSCI	<i>tert</i> -butylchlorodiphenylsilane
TBS	<i>tert</i> -butyldimethylsilyl
TBSCI	<i>tert</i> -butylchlorodimethylsilane
TBSOTf	<i>tert</i> -butyldimethylsilyl trifluoromethanesulfonate

TFA	trifluoroacetic acid
TFAA	trifluoroacetic anhydride
TfOH	trifluoromethanesulfonic acid
THF	tetrahydrofuran
TLC	thin layer chromatography
TMS	trimethylsilyl
TMSCl	chlorotrimethylsilane
TPS	triphenylsilyl
Ts	tosyl

For my grandparents

Chapter 1

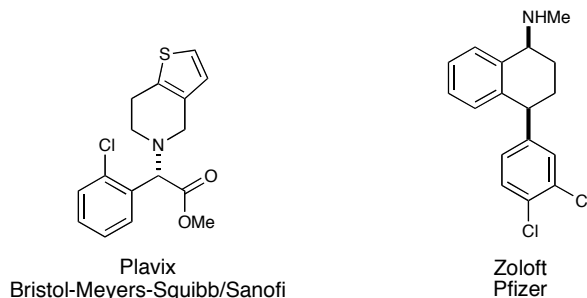
Stereogenic Amines: Biological Importance and Synthesis

1. Introduction

Found widely in both natural products and pharmaceuticals, amines are a key feature of many biologically active compounds. This activity is often not only a result of the presence of amine functionality, but is also tied to the nitrogen's position in three-dimensional space, which affects its ability to interact with biological targets. The blood thinner Plavix and the antidepressant Zoloft, for example, both contain stereogenic carbon-nitrogen bonds in which the molecule containing the opposite stereochemistry with respect to that linkage loses all biological activity (Figure 1).¹ Due to this prevalence of amines in biologically active molecules, methods for the construction of stereogenic carbon-nitrogen bonds have been the focus of a great deal of investigation.

One method that has garnered a great deal of attention is the reduction of an imine or iminium ion formed from the condensation of an amine and an aldehyde or ketone.

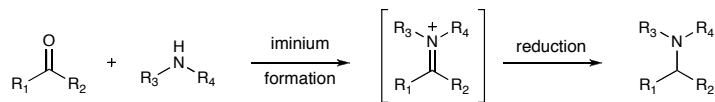
Figure 1: Pharmaceuticals containing stereogenic amines



¹ (a) J. M. Percillo et al. *Drug Metab. Disp.* **2002**, 30(11), 1288. (b) P. Baumann *Int. Clin. Pharmacol.* **1992**, Suppl. 5, 13.

When the formation of the iminium intermediate and subsequent reduction takes place in one chemical step, the process is referred to as reductive amination of the carbonyl or reductive alkylation of the amine (Scheme 1).²

Scheme 1: Reductive amination of an amine and a carbonyl compound



prototypical reducing agents: NaBH_3 , NaBH_3CN , $\text{NaBH}(\text{OAc})_3$

Reductive amination is a powerful transformation because it allows for the convergent construction of complex molecular structures from easily accessible starting materials. The most common reducing reagents used for this transformation are mild hydride sources such as sodium borohydride, sodium cyanoborohydride, and sodium triacetoxyborohydride, which will react preferentially with iminium ions over carbonyls. In spite of their generally utility, a major drawback to using these reagents is that they are non-stereoselective and, in the case where an amine is coupled with a non-symmetrical ketone, give racemic mixtures of product. In order to get around this issue and access enantiomerically enriched products, a number of asymmetric methods have been developed for imine reduction³ and, recently, one pot reductive amination.⁴

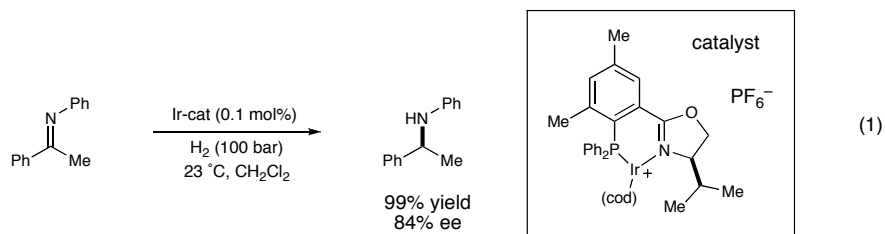
² For a general review of reductive amination see: Ohkuma, T.; Noyori, R. In *Comprehensive Asymmetric Catalysis, Suppl. 1*; Jacobsen, E.N.; Pfaltz, A.; Yamamoto, H., Eds.; Springer: New York, 2004.

³ For a review of asymmetric imine reduction see: Kobayashi, S.; Ishitani, H. *Chem. Rev.* **1999**, 99, 1069.

⁴ For a review of asymmetric reductive amination see: Tararov, V.I.; Börner, A. *Synlett.* **2005**, 203.

II. Asymmetric Imine Reduction

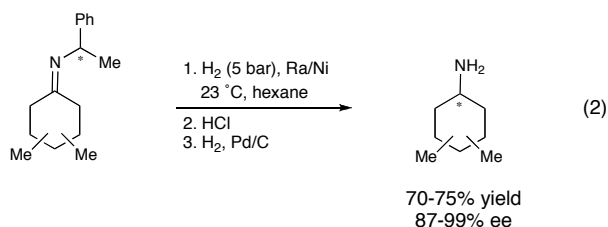
The reduction of imines to form stereogenic amines through the use of chiral metal catalysts and a hydride source has been the subject of extensive investigation for the last forty years. During that time, a wide variety of metals and chiral ligands have been used but most methods rely on molecular hydrogen, borane or silyl species as a source of hydride. Boyle, Scorrano, and Botteghi independently reported the first use of a metal catalyst and H₂ to selectively reduce imines in 1974, albeit with very low levels of selectivity (15-22% ee).⁵ Since that time, early transition metal hydrides have become the most widely used system for asymmetric imine reduction, one of the most successful of which is the iridium based system developed by Pfaltz using a chiral phosphine-oxazolidine ligand to control the stereochemical outcome (eq. 1).⁶ Another approach, developed by Frahm, utilizes a chiral auxiliary on the imine that is later removed to diastereoselectively reduce imines in the presence of molecular hydrogen and Raney nickel (eq. 2).⁷ Though both of these systems provide amine products with high levels of



⁵ (a) Boyle, P. H.; Keating, M.T. *J. Chem. Soc., Chem. Comm.* **1974**, 375. (b) Levi, A.; Modena, G.; Scorrano, G. *J. Chem. Soc., Chem Comm.* **1975**, 6. (c) Botteghi, C.; Bianchi, M.; Benedetti, E.; Matteoli, U. *Chimia* **1975**, 29, 258.

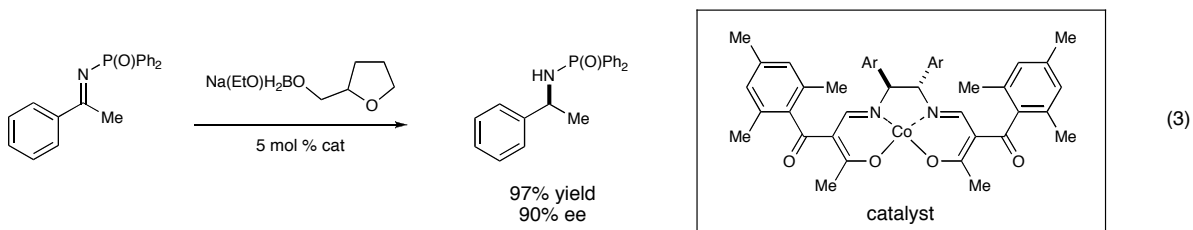
⁶ (a) Schnider, P.; Koch, G.; Prétot, R.; Wang, G.; Bohnen, F. M.; Kruger, C.; Pfaltz, A. *Chem. Eur. J.* **1997**, 3, 887. (b) Pfaltz, A.; Kainz, S.; Brinkmann, A.; Leitner, W. *J. Am. Chem. Soc.* **1999**, 121, 6421. (c) Wang, D-W.; Wang, X-B.; Wang, D-S.; Lu, S-M.; Zhou, Y-G.; Li, Y. X. *J. Org. Chem.* **2009**, 74, 2780.

⁷ (a) Speckenbach, B.; Bisel, P.; Frahm, A. W. *Synthesis* **1997**, 1325. (b) Nugent, T. C.; Wakchaure, V. N.; Ghosh, A. K.; Mohanty, R. R. *Org. Lett.* **2003**, 7, 4967.



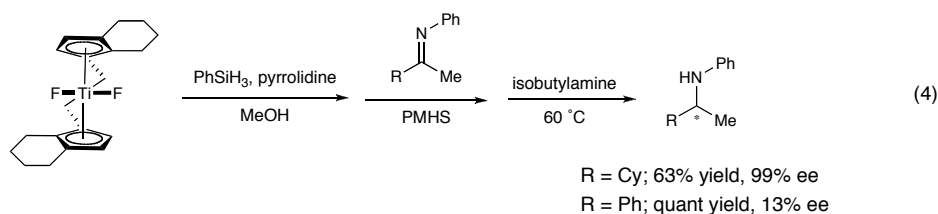
selectivity, the need for high hydrogen pressures make them difficult to use and also place restrictions of substrate scope as additional functionalities, such as olefins, may also be susceptible to reduction.

Though asymmetric imine reduction with borane has not received as much attention as H₂-based systems, Mukaiyama developed a highly enantioselective cobalt catalyst with a modified borohydride to reduce *N*-tosyl and *N*-diphenylphosphinyl imines (eq. 3).⁸ The use of silyl hydrides has been recently shown by Buchwald to be another attractive alternative to using H₂, in this case a titanocene fluoride reacts *in situ* with triphenylsilane to produce the active titanocene hydride species that serves as the reducing agent.⁹ This method works well for dialkyl-substituted imines (eq. 4, 63% yield, 99% ee) but all selectivity is lost in aromatic systems (quant yield, 13% ee). Both the Mukaiyama and Buchwald systems are attractive in that they eliminate the need for



⁸ Sugi, K. D.; Nagata, T.; Yamada, T.; Mukaiyama, T. *Chem. Lett.* **1997**, 493.

⁹ (a) Verdaguer, X.; Lange, U. E. W.; Reding, M. T.; Buchwald, S. L. *J. Am. Chem. Soc.* **1996**, *118*, 6784. (b) Verdaguer, X.; Lange, U. E. W.; Buchwald, S. L. *Angew. Chem. Int. Ed.* **1998**, *37*, 1103. (c) Hansen, M. C.; Buchwald, S. L. *Org. Lett.* **2000**, *2*, 713. For reduction using the same catalyst and H₂ see: (d) Willoughby, C. A.; Buchwald, S. L. *J. Am. Chem. Soc.* **1992**, *114*, 7562. (e) Willoughby, C. A.; Buchwald, S. L. *J. Org. Chem.* **1993**, *58*, 7627. (f) Willoughby, C. A.; Buchwald, S. L. *J. Am. Chem. Soc.* **1994**, *116*, 8952.

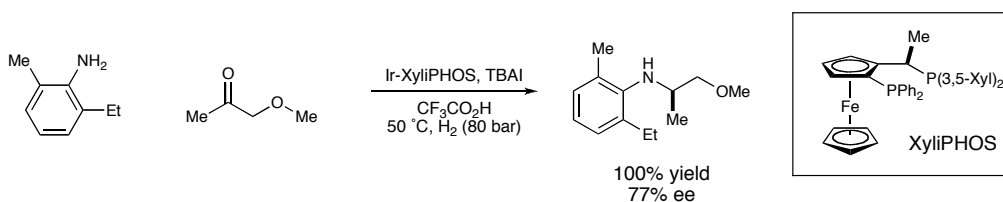


high hydrogen pressure; however, they both have the drawback of limited substrate scope with respect to imine substitution.

III. Asymmetric Reductive Amination

Only within the past ten years have methods for a one-pot catalytic asymmetric reductive amination been reported. The first such report appeared in 1999 when a group from Novartis used an iridium catalyst with a xyliPHOS ligand under H_2 to supply an intermediate compound in their synthesis of metolachlor, a grass herbicide used in agriculture (Scheme 2).¹⁰ They achieved the best results for their system using small amounts of trifluoroacetic acid as an additive to provide the product in quantitative conversion and 77% ee after 16 hours. Both Kadyrov and Zhang employed this strategy of using a chiral metal system in the presence of molecular hydrogen in developing a more general reductive amination method. Kadyrov employed the ligand Deguphos in

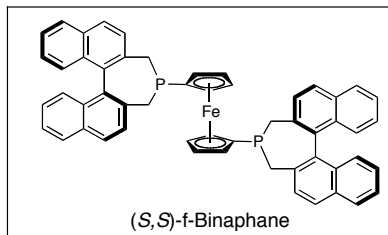
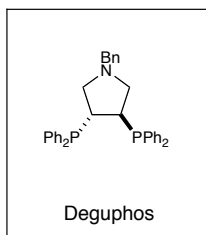
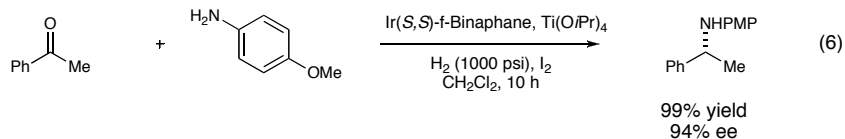
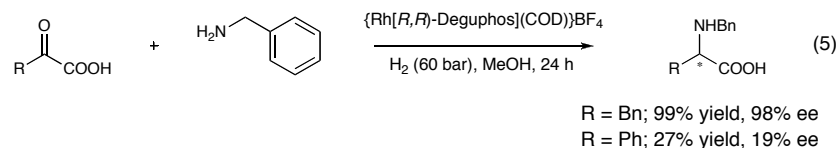
Scheme 2: The first reported catalytic asymmetric reductive amination



¹⁰ Blaser, H. U.; Buser, H. P.; Jalett, H. P.; Pugin, B.; Spindler, F. *Synlett* **1999**, *S1*, 867.

the presence of a rhodium precursor to effect the reductive amination of benzyl substituted α -ketoacids, however the enantioselectivity decreased to only 19% when the benzyl substituent is changed to a phenyl group (eq. 5).¹¹ Aromatic ketones are generally well tolerated by Zhang's iridium catalyst but he does not report any examples utilizing dialkyl or benzyl ketones (eq. 6).¹² An interesting complement to these methods was recently developed by Rubio-Pérez for the reductive amination aniline and alkyl ketones with a preformed [(*R*)-BINAP]PdBr₂ complex and high hydrogen pressure (Scheme 3).¹³ Though unsuccessful when used with aromatic substrates, it is one of the only one-pot metal-based systems that will give alkyl-substituted products with high levels of enantioselectivity.

Though these systems furnish the amine products with good levels of selectivity,

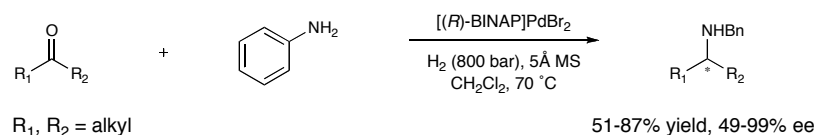


¹¹ Kadyrov, R.; Riermeier, T.; Dingerdissen, U.; Tararov, U. *J. Org. Chem.* **2003**, 68, 4067.

¹² Chi, Y.; Zhou, Y.G.; Zhang, X. *J. Org. Chem.* **2003**, 68, 4120.

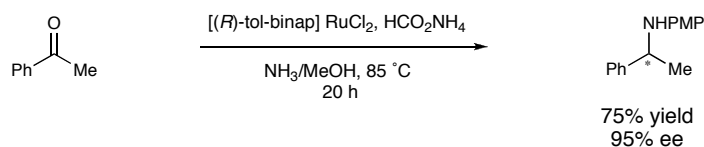
¹³ Rubio-Pérez, L.; Pérez-Flores, F. J.; Sharma, P.; Velasco, L.; Cabrera, A. *Org. Lett.* **2009**, 11, 265.

Scheme 3: Asymmetric reductive amination with alkyl ketones



the use of high hydrogen pressure again prevents these systems from being widely useful on bench scale. Kadyrov addressed this issue by developing a transfer hydrogenation process utilizing ammonium formate as a source of hydrogen and a BINAP ligand on ruthenium to control selectivity (Scheme 4).¹⁴ This process works well with aromatic ketones to give reductive amination products with enantioselectivities ranging in the nineties, however, this selectivity drops to 24% when the dialkyl ketone 2-octanone is used.

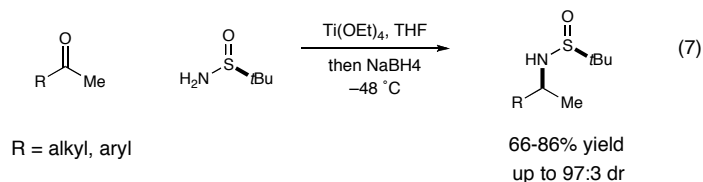
Scheme 4: Kadyrov's asymmetric reductive amination via transfer hydrogenation



One of the most successful systems to date relies on chiral substrate control to provide reductive amination products from aromatic and alkyl ketones in a one-pot fashion. Ellman has shown that a variety of nucleophiles, including hydride, undergo stereoselective addition to a wide range of *N*-*tert*-butanesulfinyl imines to provide protected amine products (eq. 7).¹⁵ In this process, the Lewis acid mediates both imine formation and reduction, overcoming the need for a separate imine formation step.

¹⁴ Kadyrov, R.; Riermeier, T. *Angew. Chem. Int. Ed.* **2003**, 42, 5472.

¹⁵ Borg, G.; Cogan, D. A.; Ellman, J. A. *Tetrahedron Lett.* **1999**, 40, 6709.



Subsequent work by Pannecoucke demonstrated the applicability of this method for the reductive amination of α -fluoroenones in the formation of peptide bond mimics (eq. 8).¹⁶ Of particular note is the observation that a reversal of diastereoselectivity can be achieved through choice of reducing agent with bulky, poorly coordinating reducing agents such as LiBHEt₃, K-Selectride and L-Selectride giving the (*S*, *R*) product while use of sodium borohydride, borane, 9-BBN and DIBAL gives the (*S*, *S*) product.¹⁷

Though the previously described methods represent significant progress toward the development of a general reductive amination procedure, many of them suffer from a number of limitations such as narrow substrate scope and the need for high hydrogen pressures. Furthermore, these methods generally involve use of transition metal catalysts, which have the additional limitations of air and moisture sensitivity and thus add a degree of experimental difficulty as well as toxicity. Recognizing the previously described limitations, the MacMillan group initiated a research program to develop a general

¹⁶ Dutheuil, G.; Couve-Bonnaire, S.; Pannecoucke, X. *Angew. Chem. Int. Ed.* **2007**, *46*, 1290.

¹⁷ Previous reports of this diastereofacial trend: (a) Kochi, T.; Ellman, J. A. *J. Am. Chem. Soc.* **2004**, *126*, 15652. (b) Plobeck, N.; Powell, D. *Tetrahedron: Asymm* **2002**, *13*, 303. (c) Lu, B. Z.; Senanayake, C.; Li, N.; Han, Z.; Bakale, R. P.; Wald, S. A. *Org. Lett.* **2005**, *7*, 2599. (d) Kochi, T.; Tang, T. P.; Ellman, J. A. *J. Am. Chem. Soc.* **2002**, *124*, 6518. (e) Kochi, T.; Tang, T. P.; Ellman, J. A. *J. Am. Chem. Soc.* **2003**, *125*, 11276.

enantioselective reductive amination methodology through the use of mild, non-toxic reagents. The successful accomplishment of these goals through the application of Brønsted acid organocatalysis is described in the subsequent chapter.¹⁸

¹⁸ Following publication of the work described in Ch. 2 a number of methods for enantioselective reductive amination have appeared in the literature: (a) Malkov, A. V.; Stoncius, S.; Kocovsky, P. *Angew. Chem. Int. Ed.* **2007**, *46*, 3722. (b) Malkov, A. V.; Vrankova, K.; Stoncius, S.; Kocovsky, P. *J. Org. Chem.* **2009**, *74*, doi 10.1021/jo900561h. (c) Guizetti, S.; Benaglia, M.; Rossi, S. *Org. Lett.* **2009**, *11*, 2928. (d) Steinhubel, D.; Sun, Y.; Matsumura, K.; Sayo, N.; Saito, T. *J. Am. Chem. Soc.* **2009**, *131*, doi 10.1021/ja905143m.

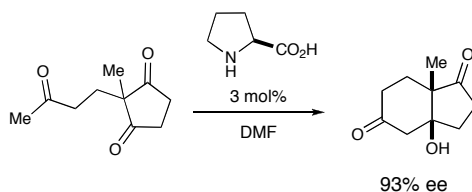
Chapter 2

Development of a Novel Phosphoric Acid Catalyzed Asymmetric Organocatalytic Reductive Amination of Ketones

I. Organocatalytic Activation Modes

In recent years the field of organocatalysis has experienced tremendous growth as chemists have come to realize the myriad benefits of using small, organic molecules as catalysts for transformations previously associated with Lewis acid chemistry. Following the rediscovery of the first reported example of enantioselective catalysis by Hajos and Parrish in 1973 (Scheme 1),¹ the past decade has seen this area experience a true renaissance as researchers around the world have developed a variety of organocatalysts capable of performing a wide range of reactions with excellent levels of reactivity and selectivity.² The MacMillan group has been one of the leaders in the field, advancing the use of secondary amines as extremely useful catalysts for asymmetric transformations ranging from Diels-Alder cyclizations to aldol condensations via the complementary activation modes of iminium and enamine catalysis (Figure 1). In the case of iminium catalysis, a secondary amine condenses with an α,β -unsaturated aldehyde to generate an

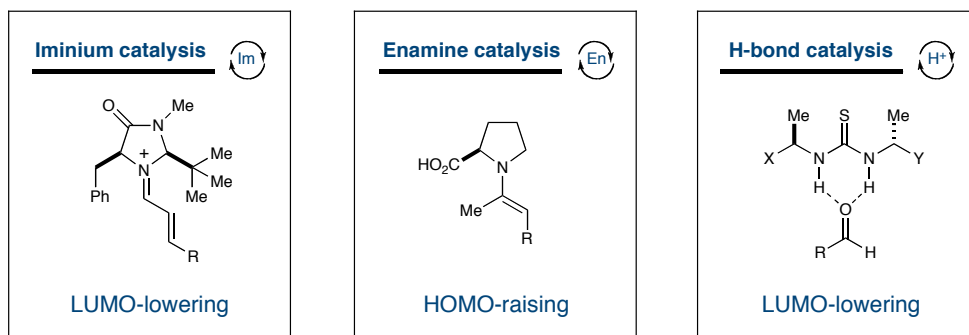
Scheme 1: Hajos-Parrish proline catalyzed cyclization



¹ Hajos, Z. G.; Parrish, D. R. *J. Org. Chem.* **1974**, 39, 1615.

² Berkessel, A.; Gröger, H. *Asymmetric Organocatalysis: From Biomimetic Concepts to Applications in Asymmetric Synthesis*; Wiley-VCH: Weinheim, 2005.

Figure 1: Organocatalytic activation modes



electrophilic LUMO-lowered conjugated iminium ion that is susceptible to 1,4- addition.³ In HOMO-raising enamine catalysis, a secondary amine catalyst condenses with a fully saturated aldehyde to generate a nucleophilic species that will readily undergo α -functionalization with a wide range of electrophiles.⁴

Another area of organocatalysis that has recently garnered attention is that of hydrogen bonding and Brønsted acid catalysis.⁵ Similar to iminium catalysis, in this activation mode imine and carbonyl substrates are activated via donation of a proton or hydrogen bond to generate a LUMO-lowered electrophilic species that is susceptible to subsequent nucleophilic addition. However, in contrast with iminium catalysis, these substrates undergo attack in a 1,2-fashion, giving rise to stereogenic products that are functionalized at the carbonyl carbon. This concept of using hydrogen bonds to activate a substrate towards nucleophilic attack is fairly well known, in fact, it has been recognized for many years that biological systems use hydrogen bonding for just such a purpose. For example, the serine protease family of enzymes makes use of appropriately

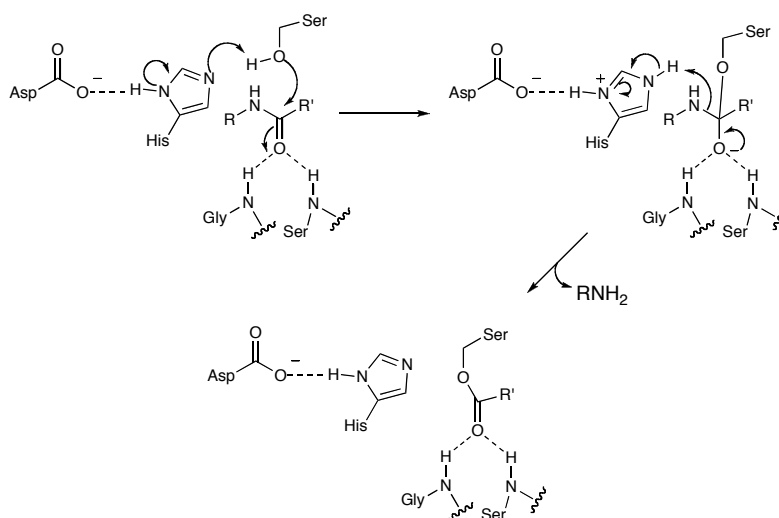
³ For a review of iminium catalysis, see: Errkilä, A.; Majander, I.; Pihko, P. M. *Chem. Rev.* **2007**, *107*, 5416.

⁴ For a review of enamine catalysis, see: Mukherjee, S.; Yang, J. W.; Hoffmann, S.; List, B. *Chem. Rev.* **2007**, *107*, 5471.

⁵ (a) Doyle, A. G.; Jacobsen, E. N. *Chem. Rev.* **2007**, *107*, 5713. (b) Akiyama, T. *Chem. Rev.* **2007**, *107*, 5744

placed hydrogen bond donating amino acids within the active site to catalyze the hydrolysis of amide bonds in proteins. As illustrated by the active site of chymotrypsin (Figure 2), the carbonyl oxygen of the amide bond being broken is positioned into a doubly hydrogen bonded “oxyanion hole” in order to activate it towards nucleophilic attack by a neighboring serine hydroxyl group in the first step of the hydrolysis sequence.⁶

Figure 2: Serine protease active site and mechanism of action



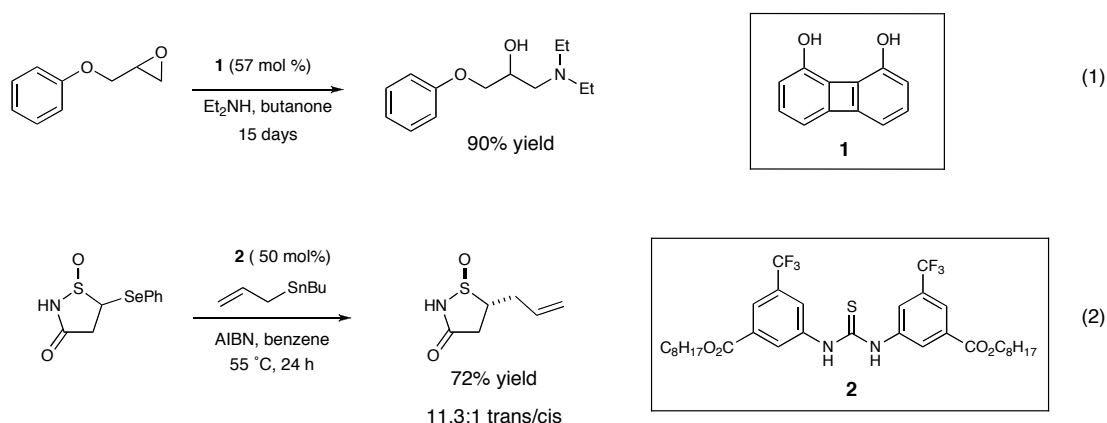
II. Hydrogen Bonding Catalysis

One of the first examples of a hydrogen bonding catalyst appeared in 1985 when Hine and co-workers demonstrated epoxide opening using biphenyldiol catalyst **1** (eq. 1).⁷ Building upon this work, Kelly showed in 1987 that a similar nitro-substituted biphenyldiol could also be used as a Diels-Alder catalyst, though high levels of catalyst

⁶ C. W. Wharton in *Comprehensive Biological Catalysis*, Vol. I (Ed.: M. Sinnott), Academic Press, London, **1998**, pp 345-379.

⁷ Hine, J.; Ahn, K. *J. Org. Chem.* **1987**, *52*, 2089.

loading were required to achieve practical levels of reactivity.⁸ The first example of an asymmetric hydrogen bond catalyzed transformation appeared in 1994 when Curran demonstrated that the double hydrogen bond donating thiourea **2** could be used to catalyze the radical allylation of sulfoxides, but again higher catalyst loadings were necessary to attain good levels of reactivity (eq. 2).⁹



In spite of these early developments, the application of hydrogen bonding catalysis remained largely dormant until 1998 when Jacobsen discovered that the chiral thiourea **3** catalyzed the enantioselective addition of cyanide to *N*-allylbenzalimine in 78% yield and 91% ee (eq. 3).¹⁰ Following discovery of this enantioselective Strecker reaction, the remarkable selectivity of this thiourea framework for the addition of a variety of nucleophiles into aldimines was explored in detail, giving rise to a number of novel asymmetric organocatalytic transformations.¹¹

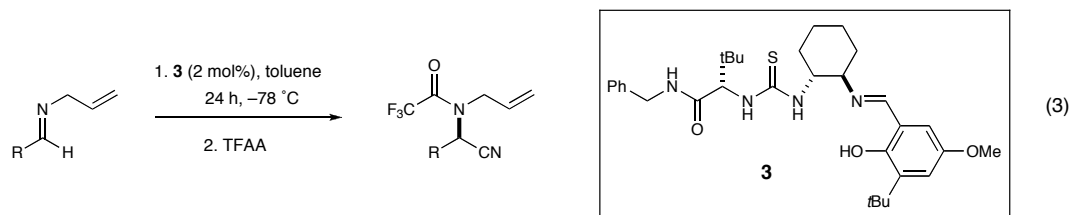
Since that time, a variety of structural classes capable of hydrogen bonding have been used as catalysts including TADDOL, guanidine species, diols, glycolic acids and

⁸ Kelly T. R. *et. al. Tetrahedron Lett.*, **1990**, 31, 3381.

⁹ Curran, D. P.; Kuo, L. H. *J. Org. Chem.* **1994**, 59, 3259.

¹⁰ Sigman, M. S.; Jacobsen, E. N. *J. Am. Chem. Soc.* **1998**, 120, 4901.

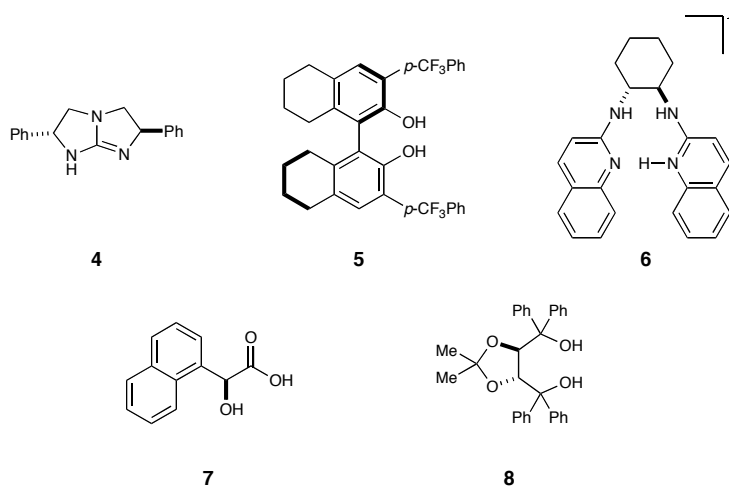
¹¹ For examples see (a) Yoon T. P.; Jacobsen E. N. *Angew. Chem., Int. Ed.* **2005**, 44, 466. (b) Fuerst, D. E.; Jacobsen, E. N. *J. Am. Chem. Soc.* **2005**, 127, 8964.



amidiniums (Figure 3).¹² In particular, the BINOL based phosphoric acid first reported by Terada and Akiyama has proven to be very effective at imine activation and has been used to catalyze aza-Friedel-Crafts alkylation of furans, amido alkylations of α -diazocarbonyls, hydrophosphonylations and Mannich reactions (Scheme 2).¹³

This activation of imines demonstrated by the BINOL phosphoric acids led the MacMillan group to investigate the possibility of performing enantioselective additions to ketimines, which would be a substantial improvement upon the existing methodology that

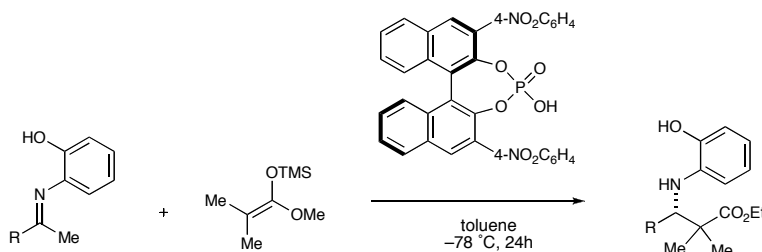
Figure 3: Examples of hydrogen bonding catalysts from the literature



¹² (a) Rawal, V. H.; Huang, Y.; Unni, A. K.; Thadani, A. N. *Nature*, **2003**, 424, 146. (b) Corey, E. J.; Grogan, M. J. *Org. Lett.* **1999**, 1, 157. (c) Nugent, B. M.; Yoder, R. A.; Johnston, J. N. *J. Am. Chem. Soc.* **2004**, 126, 3418. (d) Schaus, S. E.; McDougal, N. T. *J. Am. Chem. Soc.* **2003**, 125, 12094. (e) Yamamoto, H.; Momiyama, N., *J. Am. Chem. Soc.*, **2005**, 127, 1080.

¹³ (a) Akiyama, T.; Itoh, J.; Yokota, K.; Fuchibe, K. *Angew. Chem. Int. Ed.* **2004**, 43, 1566. (b) Akiyama, T.; Morita H.; Itoh J.; Fuchibe, K. *Org. Lett.* **2005**, 7, 2583. (c) Uraguchi, D.; Terada, M. *J. Am. Chem. Soc.* **2004**, 126, 5356. (d) Uraguchi, D.; Sorimachi, K.; Terada, M. *J. Am. Chem. Soc.* **2004**, 126, 11804. (e) Uraguchi, D.; Sorimachi, K.; Terada, M. *J. Am. Chem. Soc.* **2005**, 127, 9360.

Scheme 2: Phosphoric acid catalyzed Mannich reaction reported by Akiyama



until this point, had only been shown to succeed using much more reactive aldimine systems.

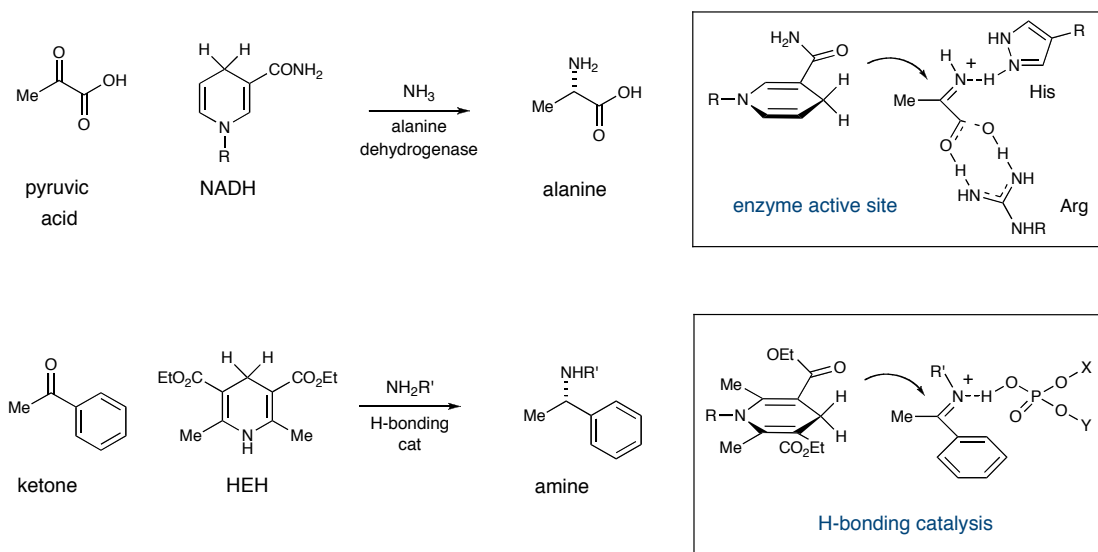
III. Organocatalytic Imine Reduction

In looking for a model as to how this transformation could be accomplished, we turned to the biological world and the action of alanine dehydrogenase for inspiration. This enzyme uses the biological cofactor NADH to enantioselectively reduce the imine formed from the condensation of pyruvic acid and ammonia to generate the amino acid alanine.¹⁴ The ketimine is activated toward reduction through the formation of a hydrogen bond between the imine nitrogen and a histidine residue in the enzyme's active site (Figure 4). We postulated that a similar transformation could be accomplished in a laboratory setting using a chiral hydrogen bonding catalyst and the NADH analog Hantzsch ester¹⁵ (HEH) as a source of hydride. Additionally, we envisioned that this methodology could perhaps be expanded to a reductive amination procedure that takes

¹⁴ (a) Wiame, J. M.; Piérard, A. *Nature* **1955**, 176, 1073. (b) Yoshida, A.; Freese, E. *Biochim. Biophys. Acta* **1964**, 92, 33. (c) Yoshida, A.; Freese, E. *Biochim. Biophys. Acta* **1965**, 96, 248. (d) Yoshida, A.; Freese, E. *Methods Enzymol.* **1970**, 17, 176.

¹⁵ Ouellet, S. G.; Tuttle, J. B.; MacMillan, D. W. C. *J. Am. Chem. Soc.* **2005**, 127, 32.

Figure 4: Mechanism of alanine dehydrogenase and proposed mechanism of H-bonding-catalyzed reductive amination

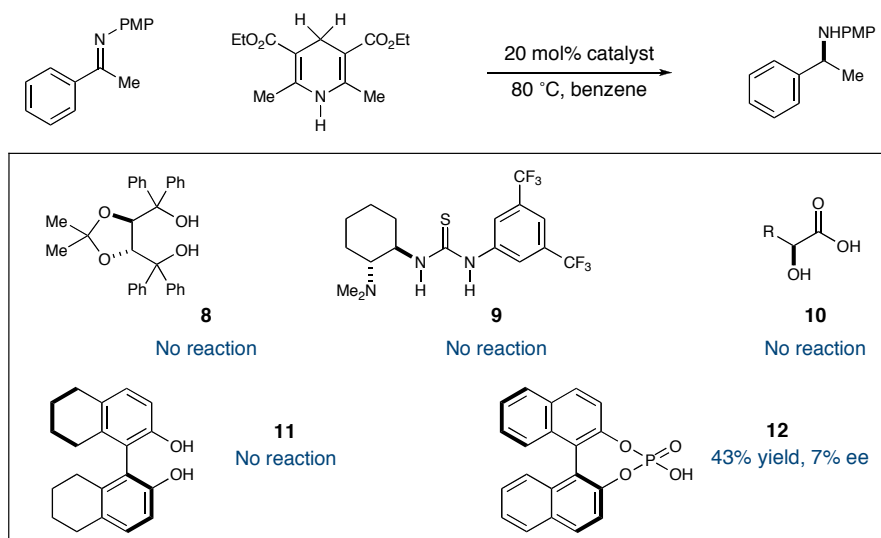


the desired amine and ketone components and couples them together in a simple one-pot process.

As an initial step in this direction, reduction of the preformed imine **15** by Hantzsch ester in the presence of several classes of hydrogen-bonding catalysts was examined and the BINOL based phosphoric acid **12a** was shown to be the most promising (Scheme 3). The *ortho* positions of the BINOL scaffold were substituted with sterically bulky groups in an effort to enhance the enantioselectivity of this transformation by creating a tighter steric environment around the carbon undergoing hydride addition.¹⁶ As seen in Table 1, this strategy proved to be very successful with the novel triphenylsilyl substituted catalyst **14** providing the desired product in 85% ee and 42% conversion (entry 8). Lowering the reaction temperature from 80 to 40 °C further increased the enantioselectivity and also increased the conversion, an observation

¹⁶ (a) Akiyama, T.; Itoh, J.; Yokota, K.; Fuchibe, K. *Angew. Chem. Int. Ed.* **2004**, *43*, 1566. (b) Terada, M.; Uraguchi, D. *J. Am. Chem. Soc.* **2004**, *126*, 5356.

Scheme 3: Evaluation of hydrogen bonding catalysts for imine reduction



attributed to the susceptibility of the Hantzsch to decomposition at elevated temperatures.

Having successfully designed a catalyst to perform the desired reaction with high levels of selectivity, reaction scope with regards to phenyl ring substitution was explored. As seen in Table 2, electron-withdrawing, electron-donating and electron-neutral groups are all well tolerated, undergoing reaction with high levels of selectivity (entries 1-7, 29-

Table 1: Catalyst optimization

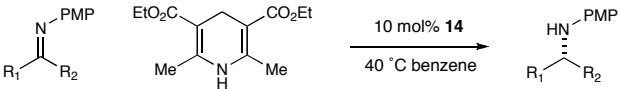
entry	cat.	cat. substitution (R)	temp (°C)	% conv. ^a	% ee ^b
1	12a	H	rt	22	17
2	12b	1-naphthyl	80	72	55
3	12c	2-naphthyl	80	74	46
4	12d	3,5-NO ₂ -phenyl	80	55	11
5	12e	4-NO ₂ -phenyl	rt	6	40
6	13	Si ^t BuPh ₂	80	27	52
7	14	SiPh ₃	80	42	77
8	14	SiPh ₃	40	73	94

^a Conversion determined by GLC analysis relative to an internal standard.

^b Enantiomeric excess determined by chiral GLC analysis.

74% conversion, 52-96% ee). Conversely, changing the imine methyl to ethyl resulted in a lowering of the observed enantioselectivity (entry 8, 46% conversion, 70% ee), suggesting that as the steric bulk of the alkyl chain increases, the catalyst is less able to differentiate between the phenyl and alkyl groups. This observation led to investigation of this transformation with a dialkyl-substituted imine (entry 9, 34% conversion, 80% ee). Though the observed selectivity was somewhat modest when compared to imines with aromatic substitution, the ability of the catalyst to distinguish methyl from ethyl with such high fidelity was quite exciting; such a high level of selectivity had never been previously reported for asymmetric reductive amination catalysts.¹⁷

Table 2: Organocatalytic reduction of imines



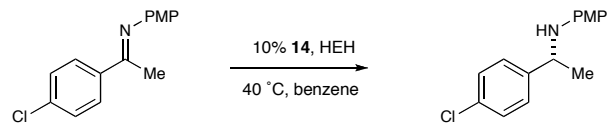
entry	R ₁	R ₂	time (h)	% conv. ^a	% ee ^b
1	Ph	Me	40	51	94
2	4-MeOC ₆ H ₄	Me	48	29	89
3	4-NO ₂ C ₆ H ₄	Me	48	47	94
4	4-ClC ₆ H ₄	Me	96	74	96
5	4-BrOC ₆ H ₄	Me	96	61	95
6	1-naphthyl	Me	48	na	52
7	2-naphthyl	Me	48	na	93
8	Ph	Et	72	46	70
9	Et	Me	48	34	80

^a Conversion determined by GLC analysis relative to an internal standard.

^b Enantiomeric excess determined by chiral GLC and SFC analysis.

Though we were very pleased with the high levels of enantioselectivity seen in this reaction, the problem of low conversion was an issue with nearly all of the substrates examined. We speculated that these low conversions were a result of imine hydrolysis, which was observed to take place when the imine starting materials were exposed to

¹⁷ For a review of asymmetric reductive amination: Tararov, V. I.; Börner, A. *Synlett*, **2005**, 203.

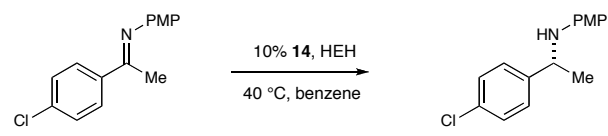
Table 3: Impact of water on imine reduction


entry	eq. H ₂ O	time (h)	% conversion ^a
1	0	48	50
2	0.1	48	32
3	1	48	4
4	2	48	2

^a Conversion determined by GLC analysis relative to an internal standard.

water in the presence of phosphoric acid **14**. In order to test this hypothesis, the *p*-chlorophenyl substituted imine was subjected to the standard reduction conditions in the presence of varying amounts of water (Table 3). The results of this experiment show a clear trend of decreasing reactivity as the amount of water added increases, suggesting that water does indeed have a detrimental effect on the reaction (entries 3-4, 2-4% conversion).

This demonstration of water's detrimental effect on imine reduction led us to reason that addition of a drying agent might lead to increased levels of conversion as it would increase the lifetime of the imine substrate under the reaction conditions. This

Table 4: Drying agent screen


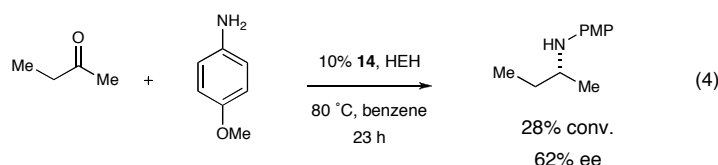
entry	additive	time (h)	% conversion ^a
1	5 Å MS (powder)	24	99
2	4 Å MS (powder)	24	7
3	3 Å MS (powder)	24	6
4	MgSO ₄	24	24
5	Na ₂ SO ₄	24	38

^a Conversion determined by GLC analysis relative to an internal standard.

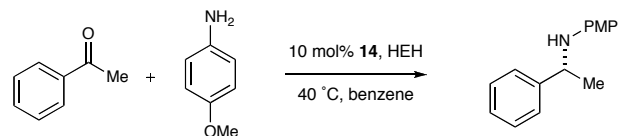
hypothesis was validated as an initial screen of a variety of drying agents showed that the use of 5 Å powdered molecular sieves (5 Å MS) resulted in improved conversion and drastically reduced reaction times (Table 4, entry 1, 99% conversion, 24 hr).

IV. Asymmetric Organocatalytic Reductive Amination

With the issue of low conversion resolved, we next focused on developing a one-pot reductive amination procedure to circumvent the problem of imine instability and associated difficulty in handling preformed imine starting materials. Proof of concept was demonstrated by the reductive amination of 2-butanone with *p*-anisidine, albeit in low conversion and selectivity as high temperature was required in order for the reaction to proceed (eq. 4). This example highlights the advantages of using a one-pot procedure as the preformed imine is extremely unstable and, as in the study of imine reduction, can only be handled as a solution.



This exciting initial result led us to try to improve the reductive amination and broaden the substrate scope to aromatic ketones. Once again, a survey of drying agents showed that 5 Å MS increased the rate of the reductive amination of acetophenone with *p*-anisidine without negatively affecting selectivity (Table 5, entry 1, 87% conversion, 95% ee). Interestingly, in contrast to what was observed with 2-butanone, the reaction does not proceed in the absence of drying agent when acetophenone is used (entry 1),

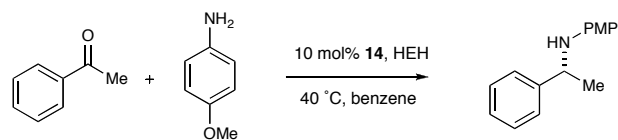
Table 5: Drying agent screen for one-pot reductive amination

entry	additive	time (h)	% conv. ^a	% ee ^b
1	none	23	0	-
2	5 Å MS (powder)	23	87	95
3	4 Å MS (powder)	23	0	-
4	3 Å MS (powder)	23	12	93
5	4 Å MS (bead)	23	21	72
6	3 Å MS (bead)	23	51	83
7	MgSO ₄	23	3	-
8	Na ₂ SO ₄	23	2	-

^a Conversion determined by GLC analysis relative to an internal standard.^b Enantiomeric excess determined by chiral GLC and SFC analysis.

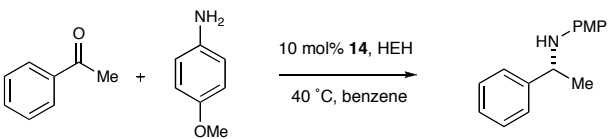
which implies that driving *in situ* imine formation through the removal of water is essential for the one-pot reaction.

With the one-pot procedure in hand, the reaction was optimized with respect to ketone and amine equivalency, temperature and catalyst loading. While increasing the amount of ketone used resulted in a corresponding increase in conversion (Table 6, entry 2, 99% conversion, 94% ee), increasing the amount of amine used resulted in a drastic drop off in conversion (entry 5, 8% conversion). A possible explanation for the low yield

Table 6: Optimization of amine and ketone equivalencies

entry	eq amine	eq ketone	time (h)	% conv. ^a	% ee ^b
1	1	1.5	26	76	94
2	1	2.5	26	99	94
3	1	3.5	26	99	94
4	1.5	1	24	23	93
5	2.5	1	24	8	90

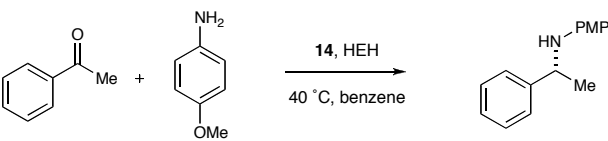
^a Conversion determined by GLC analysis relative to an internal standard.^b Enantiomeric excess determined by chiral GLC analysis.

Table 7: Temperature screen for the reductive amination


entry	temp (°C)	time (h)	% conv. ^a	% ee ^b
1	25	24	4	-
2	40	24	83	95
3	50	24	99	91
4	60	24	99	90
5	70	24	99	88
6	80	24	99	85

^a Conversion determined by GLC analysis relative to an internal standard.^b Enantiomeric excess determined by chiral GLC analysis.

is that the excess amine serves to buffer out the phosphoric acid catalyst, thereby preventing it from entering the catalytic cycle. It was also shown that temperature plays a key role in both reaction rate and selectivity with higher temperatures leading to increased conversion but decreased enantioselectivity (Table 7, entries 16, 4-99% conversion, 85-95% ee). To attain the optimal balance of reaction efficiency and selectivity, 50 °C was chosen as the standard reaction temperature when reaction scope was later explored (entry 3, 99% conversion, 91% ee). The optimal catalyst loading level was shown to be 10%; higher catalyst loading levels do not confer significantly higher reaction rates and lower loadings result in longer reaction times (Table 8, entries 1-4, 69-100% conversion, 94% ee).

Table 8: Catalyst loading screen


entry	mol % 14	time (h)	% conv. ^a	% ee ^b
1	5	24	69	94
2	10	24	97	94
3	15	24	100	94
4	20	24	100	94

^a Conversion determined by GLC analysis relative to an internal standard.^b Enantiomeric excess determined by chiral GLC analysis.

Having established the optimal conditions for the one-pot reductive amination, the scope of both ketone and amine components was explored.¹⁸ Similarly to what was seen in the reduction of imines, a variety of substituted acetophenone derivatives successfully undergo reductive amination with *p*-anisidine, including electron-rich, electron-deficient, as well as *ortho*, *meta* and *para* substituted aryl ketone systems (Table 9, entries 1-9, 60-87% yield, 81-95% ee). Interestingly, acetophenone derivatives with electron withdrawing substituents (entries 4-6, 95% ee) exhibit slightly higher enantioselectivity

Table 9: Reductive amination with aromatic ketones

entry	ketone	yield(%)	%ee ^a	entry	ketone	yield(%)	%ee ^a
1		87	93	7		81	95
2		79	91	8		60	83
3		77	90	9		73	96
4		71	95	10		75	85
5		75	95	11		70	88
6		75	94				

^a Enantiomeric excess determined by chiral GLC and SFC analysis.

¹⁸ MacMillan, D. W. C.; Storer, R. I.; Carrera, D. E.; Ni, Y. *J. Am. Chem. Soc.* **2006**, *128*, 84.

Table 10: Reductive amination with alkyl-methyl ketones

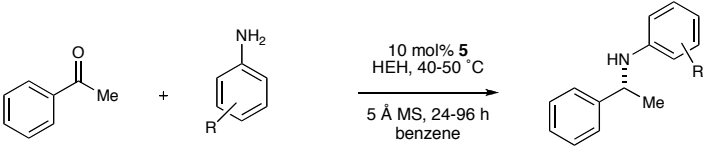
entry	ketone	yield(%)	%ee ^a	entry	ketone	yield(%)	%ee ^a
1		71	83	4		49	86
2		72	91	5		72	81
3		75	94	6		60	90

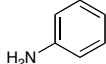
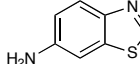
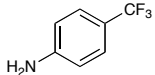
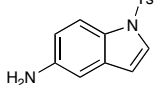
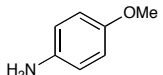
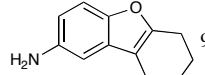
^a Enantiomeric excess determined by chiral GLC and SFC analysis.

than do those with electron donating substituents (entries 2-3, 91-90% ee). Cyclic aryl ketones (entry 10, 75% yield, 85% ee) and α -fluoromethyl ketones (entry 11, 70% yield, 88% ee) are also well tolerated. A broad range of methyl-alkyl substituted ketones were also investigated, all of which undergo reaction with good levels of enantiocontrol (Table 10, entries 1-4, 49-75% yield, 86-94% ee). In particular, the reductive amination of 2-butanone in the presence of 5 Å molecular sieves (Table 10, entry 1) gives both higher conversion and enantioselectivity than what was observed in the case where no sieves were used.

In addition to tolerating a wide range of ketones, the reductive amination was also successfully employed with a variety of electronically diverse aryl amines (Table 11). Electronically rich, neutral and poor aniline derivatives were examined (entries 1-3) as well as more extensively substituted heterocyclic amines (entries 4-6). Mirroring what was observed with acetophenone derivatives, as one moves from the electron-rich *p*-

Table 11: Reductive amination with aromatic amines

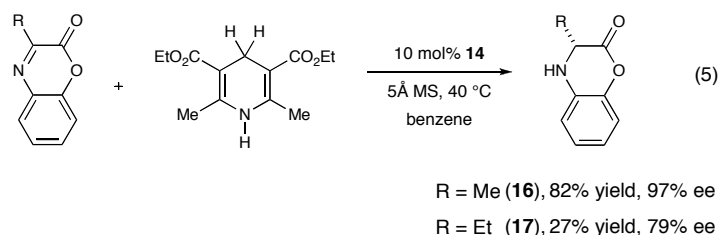


entry	amine	yield(%)	%ee ^a	entry	amine	yield(%)	%ee ^a
1		73	93	4		70	91
2		55	95	5		90	93
3		87	93	6		92	91

^a Enantiomeric excess determined by chiral GLC and SFC analysis.

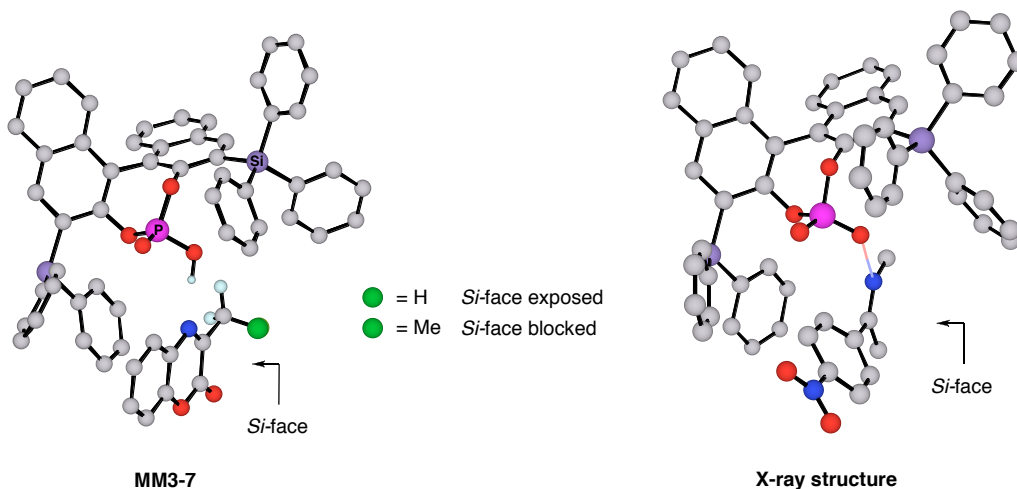
methoxy substituted aniline to the electron-deficient *p*-trifluoromethyl substituted system, there is an observed decrease in yield but increase in enantioselectivity.

The excellent levels of enantiocontrol that were observed for the organocatalytic reductive amination encouraged us to try to develop a stereochemical model that could explain these results. The first step toward this model came from the observation that the pyruvic acid derived imino ester **16** underwent reduction to yield the alanine amino ester in high yield with excellent enantioselectivity (eq. 5). However, when the corresponding ethyl substituted cyclic imine **17** was exposed to the same reaction conditions, a dramatic decrease in both yield and enantioselectivity was observed.



Computational studies revealed that this change in reaction rate as a function of alkyl substituent likely arises from catalyst imposed torsional constraints on substrate conformation (Figure 5).¹⁹ More specifically, imines that incorporate a methyl group are predicted to undergo selective catalyst association wherein the C=N *Si*-face is exposed to hydride addition (**MM3-7**, ● = H). In contrast, the ethyl containing substrate ($R_2 = \text{Et}$, **MM3-7**, ● = Me) is conformationally required to position the terminal CH_3 of the ethyl group away from the catalyst framework, thereby ensuring that both enantiofacial sites of the iminium π -system are shielded (**MM3-7**, ● = Me). This computational model has been validated by a single crystal X-ray structure of a catalyst-bound *p*-nitrophenyl imine that exhibits a remarkable correlation to **MM3-7**.

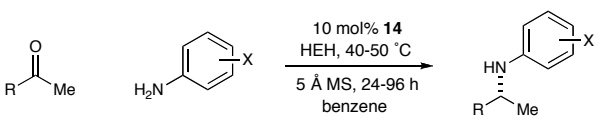
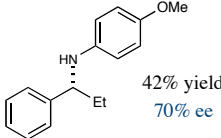
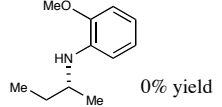
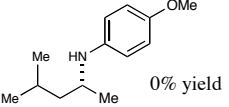
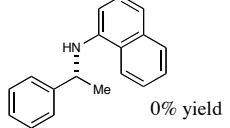
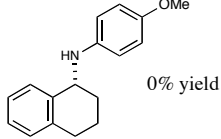
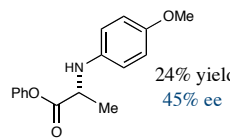
Figure 5: Computational model and crystal structure



Further evidence for this torsional model of stereinduction is provided by the results obtained for the substrates given in Table 12. As these substrates are efficient at imine formation but are unable to undergo catalyzed reduction, it was hypothesized that unfavorable steric interactions are responsible for preventing either catalyst binding or

¹⁹ One phenyl group on the triphenylsilyl substituent has been omitted for clarity.

Table 12. Substrates with poor reactivity due to steric effects

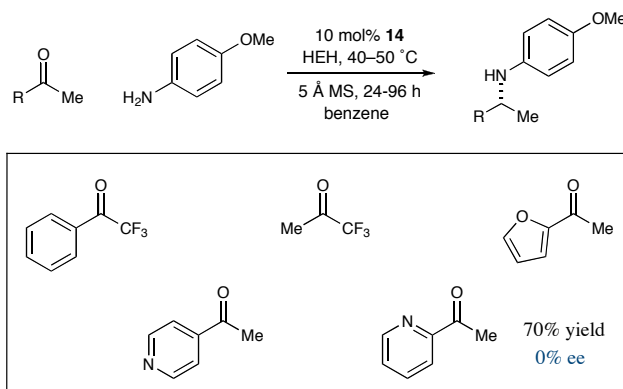
					
entry	product	yield, % ee ^a	entry	product	yield, % ee ^a
1		42% yield 70% ee	4		0% yield
2		0% yield	5		0% yield
3		0% yield	6		24% yield 45% ee

^a Enantiomeric excess determined by chiral GLC and SFC analysis.

hydride delivery. The ethyl substituted acetophenone derivative (entry 1, 42% yield, 70% ee) is analogous to the cyclic imino-esters (eq 4), with the ethyl group effectively preventing hydride delivery to the imine intermediate.

Additionally, it was found that substrates that are unable to adopt flat planar conformations provide none of the reduction product, indicating that they are perhaps unable to fit in the catalyst binding pocket due to steric constraints (entries 2-3). Similarly, the imine intermediates formed from amines with *ortho*-substituents (entries 4-5) are also non-reactive toward reduction with Hantzsch ester. Unlike the earlier examples, however, these substrates can adopt planar conformations, implying that the source of their non-reactivity is instead due to negative steric interactions between the phosphoric acid catalyst and the *ortho* substituents that prevent formation of a hydrogen bond.

Figure 6. Substrates with poor reactivity due to electronics



Similarly, the ketones in Figure 6 are also efficient at imine formation, however, the π -systems of these intermediates are stabilized by a combination of resonance and electron-withdrawing substituents and as such are unable to undergo reduction. Interestingly, it was found that the 2-pyridyl substituted methyl ketone did furnish the desired products in good yields albeit with no selectivity (70% yield, 0% ee). This result led us to conclude that LUMO-lowering activation is most likely occurring via an intramolecular fashion with protonation of the pyridine followed by proton transfer to the imine nitrogen and subsequent reduction.

V. Conclusion

The first direct enantioselective reductive amination procedure was developed using a BINOL-based phosphoric acid catalyst and NADH mimicking Hantzsch ester as reducing agent.^{20,21} The reaction conditions tolerate both aromatic and alkyl ketones as

²⁰ Following completion of the work described in this chapter two examples of organocatalytic imine reduction were reported: (a) Rueping, M.; Sugiono, E.; Azap, C.; Thiessmann, T.; Bolte, M. *Org. Lett.* **2005**, 7, 3781. (b) Hoffmann, S.; Seayad, A. M.; List, B. *Angew. Chem. Int. Ed.* **2005**, 44, 47424.

²¹ Subsequent examples of asymmetric organocatalytic reductive amination: (a) Menche, D.; Hassfeld, J.; Li, J.; Menche, G.; Ritter, A.; Rudolph, S. *Org. Lett.* **2006**, 8, 741. (b) Hoffmann, S.; Nicoletti, M.; List, B. *J. Am. Chem. Soc.* **2006**, 128, 13074. (c) Lindsley, C. W.; Fadey, O. O. *Org. Lett.* **2009**, 11, 943.

well as aryl amines and give products with high levels of enantiocontrol. A stereochemical model to rationalize this high selectivity has been developed using MM3 calculations and is further supported by an X-ray crystal structure of an aryl imine-catalyst complex.

Supporting Information

General Information. Aniline, *p*-trifluoromethyl aniline and commercially available ketones were distilled prior to use. Commercially available *p*-anisidine was purified by vacuum sublimation followed by recrystallization from water. All solvents were purified according to the method of Grubbs.²² Organic solutions were concentrated under reduced pressure on a Büchi rotary evaporator. Sieves (5 Å powdered) were activated by flame under vacuum and stored at 180 °C. Chromatographic purification of products was accomplished using flash chromatography on Silicycle 230-400 mesh silica gel. Thin-layer chromatography (TLC) was carried out on Silicycle 0.25 mm silica gel plates. Visualization of the developed chromatogram was performed by fluorescence quenching, iodine or KMnO₄ staining.

¹H and ¹³C NMR spectra were recorded on a Varian Mercury 300 Spectrometer (300 MHz and 75 MHz respectively), and are internally referenced to residual protic solvent signals (CHCl₃ = 7.24 ppm, DMSO = 2.50 ppm, benzene = 7.16 ppm). Data for ¹H are reported as follows: chemical shift (δ ppm), multiplicity (s = singlet, d = doublet, t = triplet, q = quartet, m = multiplet), integration, coupling constant (Hz) and assignment. Data for ¹³C NMR are reported in terms of chemical shift and in cases where fluorine coupling is seen all observed peaks are reported. IR spectra were recorded on a Perkin Elmer Paragon 1000 spectrometer and are reported in terms of frequency of absorption (cm⁻¹). Mass spectra were obtained from the California Institute of Technology Mass Spectroscopy Facility. X-ray structure analysis was carried out at the California Institute

²² Pangborn, A. B.; Giardello, M. A.; Grubbs, R. H.; Rosen, R. K.; Timmers, F. J. *Organometallics* **1996**, *15*, 1518.

of Technology X-ray Crystallography facility. Gas liquid chromatography (GLC) was carried out on a Hewlett-Packard 6850 Series gas chromatograph equipped with a splitmode capillary injection system and flame ionization detectors using Varian CP-Chirasil-Dex-CB and Bodman Chiraldex Γ -TA (30 m x 0.25 mm) columns. High performance liquid chromatography (HPLC) was performed on Hewlett-Packard 1100 Series chromatographs using a Daicel Chiracel OD-H column (25 cm) and equivalent guard column (5 cm). Analytical supercritical fluid chromatography (SFC) was performed on a Berger Instruments SFC with built-in photometric detector ($\lambda = 214$ nm) using Daicel Chiracel OJ-H, OD-H, AS-H, and AD-H columns (25 cm) as noted. Optical rotations were measured on a Jasco P-1010 polarimeter, and $[\alpha]_D$ values are reported in $10^{-1} \text{ dg cm}^2 \text{ g}^{-1}$; concentration (c) is in g/100 mL.

Synthesis of catalysts:

Catalyst **9** was prepared using the Takemoto procedures.²³

Catalyst **8** (TADDOL) was purchased from Aldrich and used as supplied.

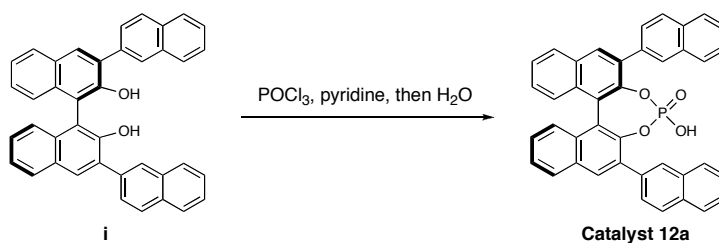
Catalyst **12b** was purchased from Aldrich and used as supplied.

Catalyst **12d** was prepared as described by Akiyama.²⁴

²³ Okino, T.; Hoashi, Y.; Takemoto, Y. *J. Am. Chem. Soc.* **2003**, *125*, 12672.

²⁴ Akiyama, T.; Morita, H.; Itoh, J.; Fuchibe, K. *Org. Lett.* **2005**, *7*, 2583.

Catalyst **12a**:



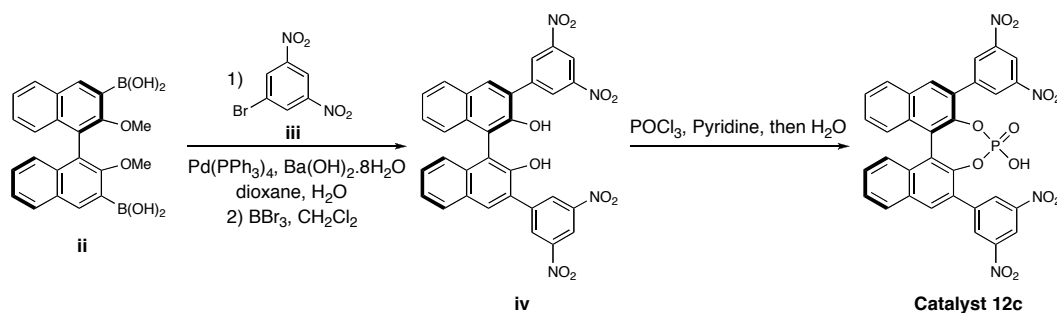
**(*R*)-2,6-Bis-(naphthalen-2-yl)-4-oxo-3,5-dioxo-4 λ^5 -phospha-cyclohepta[2,1-a;3,4-a']
dinaphthalen-4-ol (catalyst 12a)**

Diol **i** was prepared as described by Jørgensen.²⁵ Diol **i** (300 mg, 0.43 mmol) was dissolved in pyridine (1.1 mL). Phosphorous oxychloride (133 mg, 0.081 mL, 0.86 mmol) was added dropwise at room temperature with rapid stirring and the resulting solution was stirred for 6 hours. Water (1.0 mL) was added and the resulting biphasic suspension was stirred at room temperature for a further 30 mins. The reaction mixture was diluted with CH₂Cl₂ and the pyridine extracted by washing with 1 N HCl. The combined organic phase was dried over Na₂SO₄ concentrated and the crude solid was purified by flash column chromatography (1.5% MeOH in CH₂Cl₂) to yield catalyst **3a** as a white solid (280 mg, 86% yield). IR (film) 1253, 1108, 740 cm⁻¹; ¹H NMR (300 MHz, (CD₃)₂SO) δ 7.13 (s, 2H, ArH), 7.36-7.26 (m, 2H, ArH), 7.42-7.62 (m, 6H, ArH), 7.92-8.06 (m, 6H, ArH), 8.12 (d, 2H, J = 8.4 Hz, ArH), 8.23 (s, 2H, ArH), 8.27-8.36 (m, 2H, ArH), 8.51 (s, 2H, ArH); ¹³C NMR (75 MHz, (CD₃)₂SO) δ 122.76, 124.90, 126.00, 126.01, 126.27, 127.02, 127.47, 128.28, 128.51, 128.92, 129.05, 130.23, 130.63, 131.93, 132.15, 132.99, 134.37, 135.79, 147.55, 147.68; HRMS (FAB+) exact mass calculated for [M+H] (C₄₀H₂₆O₄P) requires m/z 601.1569, found m/z 601.1565. $[\alpha]_D^{23} = -322.8^\circ$ ($c =$

²⁵ Simonsen, K. B.; Gothelf, K. V.; Jørgensen, K. A. *J. Org. Chem.* **1998**, 63, 7536.

1.02, CHCl₃).

Catalyst **12c**:



(*R*)-2,6-Bis-(3,5-dinitrophenyl)-4-oxo-3,5-dioxo-4λ⁵-phospha-cyclohepta[2,1-a;3,4-a']dinaphthalen-4-ol (catalyst **12c)**

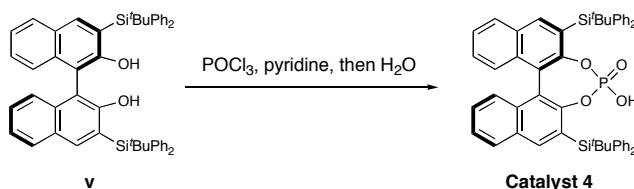
Boronic acid **ii** was prepared as described by Jørgensen.⁴ Degassed dioxane (6.0 mL) and degassed water (2.0 mL) were added to a mixture of boronic acid **ii** (188 mg, 0.47 mmol), bromide²⁶ **iii** (371 mg, 1.50 mmol), barium hydroxide octahydrate (435 mg, 1.38 mmol) and Pd(PPh₃)₄ (58 mg, 0.05 mmol) under argon. The reaction mixture was heated to 70 °C for 48 h, then cooled to room temperature. The dioxane was removed, and the resulting residue was redissolved in CH₂Cl₂, washed with 1 N HCl solution and brine, dried over Na₂SO₄ and concentrated to give crude product as a red oil. The crude oil was dissolved in CH₂Cl₂ (18.0 mL) and cooled to 0 °C. A solution of BBr₃ in CH₂Cl₂ (5.0 mL, 1.0 M) was then added dropwise over 10 mins. The reaction mixture was allowed to warm to room temperature and stirred overnight. The mixture was cooled to 0 °C, then quenched by slow addition of water. The reaction mixture was diluted with CH₂Cl₂, washed with water then brine. The combined organic layers were dried over Na₂SO₄, filtered and concentrated. The crude product was purified by silica flash column

²⁶ Duan, J.; Zhang, L. H.; Dolbier, W. R. Jr. *Synlett* **1999**, 1245.

chromatography (2:1 CH₂Cl₂:hexanes) to yield diol **iv** as an orange solid (187 mg, 65% yield over 2 steps).

Diol **iv** (140 mg, 0.23 mmol) was dissolved in pyridine (0.8 mL). Phosphorous oxychloride (69.3 mg, 0.05 mL, 0.45 mmol) was added dropwise at room temperature with rapid stirring and the resulting solution was stirred for 6 hours. Water (1.0 mL) was added and the resulting biphasic suspension was stirred at room temperature for a further 30 min. The reaction mixture was diluted with CH₂Cl₂ and the pyridine was removed via washing with 1 N HCl. The combined organic phase was dried over Na₂SO₄ and purified by flash column chromatography (1:20 MeOH:CH₂Cl₂) to yield catalyst **3c** as a pale yellow solid (142 mg, 92% yield). IR (film) 1540, 1345, 1107, 732 cm⁻¹; ¹H NMR (300 MHz, (CD₃)₂SO) δ 7.16 (d, 2H, J = 8.7 Hz, ArH), 7.37 (dd, 2H, J = 8.7, 6.9 Hz ArH), 7.51 (dd, 2H, J = 8.1, 6.9 Hz ArH), 8.14 (d, 2H, J = 8.1 Hz, ArH), 8.40 (s, 2H, ArH), 8.89 (t, 2H, J = 2.0 Hz, ArH), 8.89 (d, 4H, J = 2.0 Hz, ArH); ¹³C NMR (75 MHz, (CD₃)₂SO) δ 117.40, 122.82, 125.43, 126.00, 127.31, 128.99, 130.06, 130.23, 130.71, 131.56, 132.50, 141.16, 146.89, 148.00; HRMS (FAB+) exact mass calculated for [M+H] (C₃₂H₁₈N₄O₁₂P) requires m/z 681.0659, found m/z 681.0666. $[\alpha]_D^{23} = -290.4^\circ$ (c = 0.34, CHCl₃).

Catalyst 13:

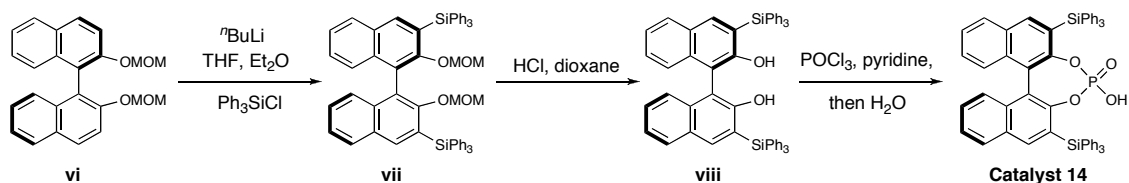


**(*R*)-2,6-Bis-(*tert*-butyldimethylsilyl)-4-oxo-3,5-dioxo-4λ⁵-phospha-cyclohepta
[2,1a;3,4-a'] dinaphthalen-4-ol (catalyst 13)**

Diol **v** was prepared as described by Yamamoto.²⁷ Diol **v** (95 mg, 0.18 mmol) was dissolved in pyridine (1.0 mL). Phosphorous oxychloride (56 mg, 0.04 mL, 0.36 mmol) was added dropwise at room temperature and the resulting solution was heated to 90 °C with stirring for 36 hours. The mixture was cooled to room temperature and water (1.0 mL) was added slowly. The resulting biphasic suspension was stirred for a further 30 mins, then diluted with CH₂Cl₂ and the pyridine was extracted by washing with 1 N HCl. The combined organic phase was dried over Na₂SO₄ concentrated and purified by flash column chromatography (1:20 MeOH:CH₂Cl₂) to yield catalyst **4** as a white solid (61 mg, 58% yield). IR (film) 3070, 2934, 2859, 1427, 1254, 1104, 1091, 984, 702 cm⁻¹; ¹H NMR (300 MHz, (CD₃)₂SO) δ 1.23 (s, 18H, ^tBu), 6.86-6.96 (m, 2H, ArH), 7.20-7.48 (m, 20H, ArH), 7.55-7.64 (m, 2H, ArH), 7.64-7.76 (m, 6H, ArH); ¹³C NMR (75 MHz, (CD₃)₂SO) δ 18.75, 29.45, 121.40, 124.10, 125.23, 126.96, 127.38, 127.57, 128.17, 133.91, 135.23, 135.94, 136.61, 140.81, 154.26, 154.37; HRMS (FAB+) exact mass calculated for [M+Na] (C₅₂H₄₉O₄Si₂PNa) requires *m/z* 847.2805, found *m/z* 847.2795. [α]_D²³ = -171.5° (c = 0.42, CHCl₃).

²⁷ Maruoka, K.; Itoh, T.; Araki, Y.; Shirasaka, T.; Yamamoto, H. *Bull. Chem. Soc. Jpn.* **1988**, *61*, 2975.

Catalyst 14:



(*R*)-2-(methoxymethoxy)-1-(2-(methoxymethoxy)-3-(triphenylsilyl)naphthalen-1-yl)-3-(triphenylsilyl)naphthalene vii

Silylated BINOL derivative **vii** was prepared using a modification of a Snieckus procedure.²⁸ MOM protected (*R*)-BINOL **vi** can be purchased directly or synthesized in quantitative yield following the procedure described by Kobayashi.²⁹ Binol diether **vi** (20.0 g, 53.4 mmol) was dissolved in Et₂O (920 mL) followed by dropwise addition of ⁿBuLi (53.0 mL, 2.3 M, 123 mmol) over 10 mins at room temperature. The resulting suspension was stirred at room temperature for 1 hour 30 mins (note: a color change was observed over the initial 30 mins from a yellow solution to a brown suspension). The mixture was cooled to 0 °C and THF (440 mL) was added. After a further 15 mins at 0 °C a solution of Ph₃SiCl (39.4 g, 133.5 mmol) in THF (100 mL) was added. The reaction mixture was warmed to room temperature and stirred for 30 hours (note: after addition of the THF and Ph₃SiCl the color darkened from light brown to very dark brown over the first hour. The colour faded through green to orange and finally pale yellow over the 30 hour period). The reaction was quenched by addition of sat. NH₄Cl, then extracted into CH₂Cl₂. The organics were washed with brine and dried over Na₂SO₄, filtered and concentrated to yield the crude product as a viscous yellow oil. The product was purified

²⁸ Cox, P. J.; Wang, W.; Snieckus, V. *Tetrahedron Lett.* **1992**, 33, 2253.

²⁹ Kobayashi, S.; Kusakabe, K.; Komiyama, S.; Ishitani, H. *J. Org. Chem.* **1999**, 64, 4220.

by silica flash column chromatography (1:1:20 CH₂Cl₂:Et₂O:pentane) to yield the title product **vii** as a white solid (32.2 g, 68% yield). IR (film) 3068, 1428, 1108, 700 cm⁻¹; ¹H NMR (300 MHz, CDCl₃) δ 2.36 (s, 6H, OCH₃), 3.86 (d, 2H, *J* = 5.0 Hz, OCHHO), 3.93 (d, 2H, *J* = 5.0 Hz, OCHHO), 7.28-7.60 (m, 24H, ArH), 7.65-7.92 (m, 14H, ArH), 7.99 (s, 2H, ArH); ¹³C NMR (75 MHz, CDCl₃) δ 56.41, 98.06, 123.34, 124.81, 126.26, 127.66, 128.06, 128.88, 129.44, 129.67, 130.44, 135.32, 136.41, 136.90, 141.56, 158.50; HRMS (FAB+) exact mass calculated for [M+] (C₆₀H₅₀O₄Si) requires *m/z* 890.3248, found *m/z* 890.3291. [α]_D²³ = +53.4° (c = 1.01, CHCl₃).

(*R*)-1-(2-hydroxy-3-(triphenylsilyl)naphthalen-1-yl)-3-(triphenylsilyl)naphthalen-2-ol
viii⁶

Concentrated HCl (3.0 mL) was added to a solution of MOM protected binol **vii** (25.7 g, 28.8 mmol) in dioxane (200 mL). The resulting solution was heated to 70 °C for 24 h (note: fitted with reflux condensor but not quite refluxing). The reaction mixture was cooled to room temperature and quenched by addition of sat. NaHCO₃ solution. The product was extracted into EtOAc and washed with water, then brine. The combined organics were dried over Na₂SO₄, filtered and concentrated to yield the crude product as a pink solid. Trituration/washing with hot CH₂Cl₂ : Et₂O (1:10) provided pure diol **viii** as a white solid. The washings were concentrated and the procedure repeated on the residue twice to provide a combined yield of pure diol **viii** as a white solid (20.5 g, 89% yield). IR (film) 3521, 3068, 1581, 1428, 1108, 699 cm⁻¹; ¹H NMR (300 MHz, C₆D₆) δ 4.68 (s, 2H, OH), 6.90-7.38 (m, 26H, ArH), 7.80-7.84 (m, 12H, ArH), 8.14 (s, 2H, ArH); ¹³C NMR (75 MHz, C₆D₆) δ 110.84, 124.09, 124.23, 124.39, 127.92, 128.20, 129.45, 129.78,

129.93, 135.09, 135.50, 136.91, 142.42, 156.98; HRMS (FAB+) exact mass calculated for [M⁺] (C₅₆H₄₂O₂Si₂) requires m/z 802.2723, found m/z 802.2700. $[\alpha]_D^{23} = +102.7^\circ$ (c = 1.20, CHCl₃).

(*R*)-2,6-Bis-(triphenylsilyl)-4-oxo-3,5-dioxo-4 λ^5 -phospha-cyclohepta [2,1a;3,4-a']

dinaphthalen-4-ol (catalyst 14)

Diol **v** (9.7 g, 12.1 mmol) was suspended in pyridine (34.0 mL). Phosphorous oxychloride (3.7 g, 2.3 mL, 24.2 mmol) was added dropwise at room temperature with rapid stirring and the resulting suspension was heated to 95 °C. Upon reaching 95 °C all material had dissolved to provide a pale yellow clear solution (note: reaction carried out in a 1-neck flask equipped with a condensor – POCl₃ added via long needle down condensor. Mixture not refluxed). The reaction mixture was stirred for 24 hours at 95 °C until all starting material was deemed consumed by tlc (note: by the end of the reaction a precipitate of pyridine-HCl salt forms). The reaction mixture was cooled to 0 °C and water (10 mL) was added very slowly. The resulting biphasic suspension was heated to 95 °C for an additional 6 h. The reaction mixture was diluted with CH₂Cl₂ and the pyridine was removed via washing with 1 N HCl. The combined organic phase was dried over Na₂SO₄, filtered and concentrated to give crude product as a pale yellow solid. Purification by flash column chromatography (gradient from 1% to 4% MeOH in CH₂Cl₂) yielded catalyst **5** as a white solid (9.02 g, 86% yield). IR (film) 1428, 1106, 701 cm⁻¹; ¹H NMR (300 MHz, (CD₃)₂SO) δ 7.08 (d, 2H, J = 8.1 Hz, ArH), 7.28-7.47 (m, 22H, ArH), 7.52-7.63 (m, 12H, ArH), 7.87 (d, 2H, J = 7.8 Hz, ArH), 8.05 (s, 2H, ArH); ¹³C

NMR (75 MHz, $(\text{CD}_3)_2\text{SO}$) δ 121.19, 125.41, 125.78, 126.17, 127.74, 128.76, 129.51, 129.76, 133.50, 134.01, 136.32, 141.10, 152.10, 152.12; HRMS (FAB+) exact mass calculated for $[\text{M}^+]$ ($\text{C}_{56}\text{H}_{41}\text{O}_4\text{Si}_2\text{P}$) requires m/z 864.2281, found m/z 864.2296. $[\alpha]_D^{23} = -156.0^\circ$ ($c = 1.02$, CHCl_3).

Reductive Amination General Procedure: A 20 mL vial equipped with a magnetic stir bar was charged with amine (123 mg, 1.0 equiv), Hantzsch ester (304 mg, 1.2 equiv), catalyst (86 mg, 10 mol%) and 5 Å molecular sieves (1 g). Benzene (10 mL) was added followed by ketone (3.0 equiv). The reaction mixture was heated with stirring to 40-50 °C as noted and monitored by TLC. Upon completion or 96 hours, the reaction mixture was filtered through a plug of silica, eluting with Et_2O to remove the molecular sieves and unreacted Hantzsch, then concentrated *in vacuo*.

Work-up procedure A: The crude product was dissolved in Et_2O (100 mL) and extracted with 1 N HCl (2×60 mL). The combined aqueous phases were basified to pH 10 with aqueous KOH and extracted with CH_2Cl_2 (2×80 mL). The combined organic phase was dried (MgSO_4) and concentrated *in vacuo*. The product was purified by silica gel chromatography (solvents noted) to yield the title compounds.

Work-up procedure B: The crude product was directly purified by silica gel column chromatography (solvents noted) to yield the title compounds.

Absolute configurations of known compounds were assigned by comparison of HPLC retention times and optical rotations to literature values.

(*R*)-*N*-(4-methoxyphenyl)-[1-(phenyl)-ethyl]amine (Table 9, entry 1):

Prepared according to the general procedure from *p*-anisidine (83 mg, 0.67 mmol) and acetophenone (235 μ L, 2.01 mmol) at 50 °C for 24 h, using work-up procedure B to provide the title compound as a yellow oil (162 mg, 87% yield, 94% ee) following silica gel chromatography (10% Et₂O/pentane). IR (film) 3395, 2977, 1514, 1450, 1235, 1034, 822, 758, 703 cm⁻¹; ¹H NMR (300 MHz, CDCl₃) δ 1.51 (d, 3H, *J* = 6.6 Hz, -CH₃), 3.69 (s, 3H, -OCH₃), 4.41 (q, 1H, *J* = 6.9 Hz, -CHCH₃), 6.47-6.50 (m, 2H, ArH), 6.67-6.70 (m, 2H, ArH), 7.22-7.26 (m, 1H, ArH), 7.26-7.38 (m, 4H, ArH); ¹³C NMR (75 MHz, CDCl₃) δ 25.18, 54.27, 55.75, 114.58, 114.78, 125.93, 126.86, 128.65, 141.59, 145.52, 151.91; HRMS (EI) exact mass calculated for (C₁₅H₁₇NO) requires *m/z* 227.1310, found *m/z* 227.1335. [α]_D²⁵ = +3.9° (c = 0.18, CHCl₃).³⁰ The enantiomeric ratio was determined by GLC using a Chirasil-Dex-CB column (150 °C isotherm for 150 minutes, 1 mL/min); major enantiomer t_r = 81.43 min and minor enantiomer t_r = 79.91 min.

(+)-*N*-(4-methoxyphenyl)-[1-(4-tolyl)-ethyl]amine (Table 9, entry 2):

Prepared according to the general procedure from *p*-anisidine (105 mg, 0.853 mmol) and 4'-methylacetophenone (342 μ L, 2.56 mmol) at 50 °C for 72 h, using work-up procedure B to provide the title compound as a yellow oil (161 mg, 79% yield, 91% ee) following silica gel chromatography (5% Et₂O/pentane). IR (film) 3401, 2962, 2831, 1618, 1511, 1443, 1370, 1295, 1235, 1178, 1140, 1111, 1038, 816, 758 cm⁻¹; ¹H NMR (300 MHz, CDCl₃) δ 1.48 (d, 3H, *J* = 6.9 Hz, CH₃), 2.32 (s, 3H, -C₆H₄CH₃), 3.68 (s, 3H, -OCH₃), 4.38 (q, 1H, *J* = 6.6 Hz, -CHCH₃), 6.45-6.51 (m, 2H, ArH), 6.67-6.72 (m, 2H, ArH),

³⁰ Zhang, X.; Chi, Y.; Zhou, Y. G. *J. Org. Chem.* **2003**, 68, 4120. (reported a rotation of +7.0° (c = 2, CHCl₃) for a product that was 94% ee)

7.11-7.14 (m, 2H, ArH), 7.24-7.27 (m, 2H, ArH); ^{13}C NMR (75 MHz, CDCl_3) δ 21.07, 25.14, 53.96, 55.73, 114.55, 114.73, 125.79, 129.29, 136.34, 141.58, 142.42, 151.84; HRMS (EI) exact mass calculated for ($\text{C}_{16}\text{H}_{19}\text{NO}$) requires m/z 241.1467 found m/z 241.1476. $[\alpha]_D^{28} = +6.9^\circ$ ($c = 0.20$, CHCl_3). The enantiomeric ratio was determined by SFC using a Chiralcel AD-H column (5-50% methanol/ CO_2 , 35 $^\circ\text{C}$, 100 bar, 4 mL/min, ramp rate = 5% /min); major enantiomer $t_r = 3.88$ min and minor enantiomer $t_r = 3.57$ min.

(+)-*N*-(4-methoxyphenyl)-[1-(4-methoxyphenyl)-ethyl]amine (Table 9, entry 3):

Prepared according to the general procedure from *p*-anisidine (110 mg, 0.890 mmol) and 4'-methoxyacetophenone (401 mg, 2.67 mmol) at 50 $^\circ\text{C}$ for 72 h, using work-up procedure A to provide the title compound as a tan solid (177 mg, 77% yield, 90% ee) following silica gel chromatography (3% Et_2O /toluene). IR (film) 3401, 2938, 2834, 1611, 1511, 1463, 1372, 1283, 1236, 1177, 1141, 1111, 1037, 819 cm^{-1} ; ^1H NMR (300 MHz, CDCl_3) δ 1.47 (d, 3H, $J = 6.6$ Hz, $-\text{CH}_3$), 3.69 (s, 3H, $-\text{OCH}_3$), 3.78 (s, 3H, $-\text{OCH}_3$), 4.37 (q, 1H, $J = 6.6$ Hz, $-\text{CHCH}_3$), 6.46-6.49 (m, 2H, ArH), 6.68-6.70 (m, 2H, ArH), 6.84-6.86 (m, 2H, ArH), 7.26-7.29 (m, 2H, ArH); ^{13}C NMR (75 MHz, CDCl_3) δ 25.09, 53.71, 55.24, 55.73, 113.95, 114.66, 114.71, 126.94, 137.39, 141.48, 151.90, 158.42; HRMS (EI) exact mass calculated for ($\text{C}_{16}\text{H}_{19}\text{NO}_2$) requires m/z 257.1416, found m/z 257.1425. $[\alpha]_D^{22} = +16.1^\circ$ ($c = 1.95$, CHCl_3). The enantiomeric ratio was determined by HPLC using a Chiralcel OD-H column (5% isopropanol/hexanes); major enantiomer $t_r = 20.62$ min and minor enantiomer $t_r = 22.64$ min.

(+)-*N*-(4-methoxyphenyl)-[1-(4-nitrophenyl)-ethyl]amine (Table 9, entry 4):

Prepared according to the general procedure from *p*-anisidine (114 mg, 0.927 mmol) and 4'-nitroacetophenone (459 mg, 2.78 mmol) at 50 °C for 72 h, using work-up procedure A to provide the title compound as an orange solid (118 mg, 71% yield, 95% ee) following silica gel chromatography (30% Et₂O/pentane). IR (film) 3402, 2968, 1598, 1511, 1451, 1344, 1235, 1178, 1143, 1109, 1036, 855, 819, 751, 700 cm⁻¹; ¹H NMR (300 MHz, CDCl₃) δ 1.52 (d, 3H, *J* = 6.6 Hz, -CH₃), 3.68 (s, 3H, -OCH₃), 4.49 (q, 1H, *J* = 6.9 Hz, -CHCH₃), 6.38-6.41 (m, 2H, ArH), 6.67-6.70 (m, 2H, ArH), 7.52-7.55 (m, 2H, ArH), 8.16-8.19 (m, 2H, ArH); ¹³C NMR (75 MHz, CDCl₃) δ 24.99, 54.03, 55.68, 114.53, 114.82, 124.04, 126.78, 140.69, 146.99, 152.29, 153.50; HRMS (EI) exact mass calculated for (C₁₅H₁₆N₂O₃) requires *m/z* 272.1161, found *m/z* 272.1164. [α]_D²⁵ = +29.8° (*c* = 0.20, CHCl₃). The enantiomeric ratio was determined by SFC using a Chiralcel OD-H column (10% methanol/CO₂, 35 °C, 100 bar, 4 mL/min); major enantiomer *t*_r = 8.41 min and minor enantiomer *t*_r = 7.88 min.

(+)-*N*-(4-methoxyphenyl)-[1-(4-chlorophenyl)-ethyl]amine (Table 9, entry 5):

Prepared according to the general procedure from *p*-anisidine (101 mg, 0.818 mmol) and 4'-chloroacetophenone (379 mg, 2.45 mmol) at 50 °C for 72 h, using work-up procedure A to provide the title compound as a yellow oil (161 mg, 75% yield, 95% ee) following silica gel chromatography (15% Et₂O/pentane). IR (film) 3401, 2964, 2831, 1618, 1512, 1490, 1464, 1451, 1407, 1372, 1289, 1235, 1204, 1179, 1141, 1092, 1038, 1013, 942, 819, 778, 759 cm⁻¹; ¹H NMR (300 MHz, CDCl₃) δ 1.47 (d, 3H, *J* = 6.9 Hz, -CH₃), 3.69 (s, 3H, -OCH₃), 4.38 (q, 1H, *J* = 6.6 Hz, -CHCH₃), 6.42-6.45 (m, 2H, ArH), 6.67-6.70 (m,

2H, ArH), 7.26-7.29 (m, 4H, ArH); ^{13}C NMR (75 MHz, CDCl_3) δ 25.21, 53.75, 55.73, 114.60, 114.80, 127.36, 128.80, 132.34, 141.28, 144.16, 152.05; HRMS (EI) exact mass calculated for ($\text{C}_{15}\text{H}_{16}\text{NOCl}$) requires m/z 261.0920, found m/z 261.0912. $[\alpha]_D^{24} = +14.8^\circ$ ($c = 1.88$, CHCl_3). The enantiomeric ratio was determined by GLC using a Chirasil-Dex-CB column (160 °C isotherm for 150 minutes, 1 mL/min); major enantiomer $t_r = 134.59$ min and minor enantiomer $t_r = 132.02$ min.

(-)-*N*-(4-methoxyphenyl)-[1-(4-fluorophenyl)-ethyl]amine (Table 9, entry 6):

Prepared according to the general procedure from *p*-anisidine (126 mg, 1.02 mmol) and 4'-fluoroacetophenone (371 μL , 3.07 mmol) at 50 °C for 72 h, using work-up procedure A to provide the title compound as a yellow oil (188 mg, 75% yield, 94% ee) following silica gel chromatography (2% Et_2O /toluene). IR (film) 3402, 2965, 2833, 1603, 1511, 1464, 1414, 1373, 1293, 1235, 1180, 1155, 1140, 1093, 1038, 835, 819, 758 cm^{-1} ; ^1H NMR (300 MHz, CDCl_3) δ 1.48 (d, 3H, $J = 6.6$ Hz, $-\text{CH}_3$), 3.70 (s, 3H, $-\text{OCH}_3$), 4.39 (q, 1H, $J = 6.9$ Hz, $-\text{CHCH}_3$), 6.44-6.47 (m, 2H, ArH), 6.68-6.71 (m, 2H, ArH), 6.96-7.02 (m, 2H, ArH), 7.30-7.35 (m, 2H, ArH); ^{13}C NMR (75 MHz, CDCl_3) δ 25.27, 53.69, 55.72, 114.63, 114.78, 115.27, 115.55, 127.34, 127.45, 141.16, 141.20, 141.36, 152.02, 160.12, 163.35; HRMS (EI) exact mass calculated for ($\text{C}_{15}\text{H}_{16}\text{NFO}$) requires m/z 245.1216, found m/z 245.1206. $[\alpha]_D^{26} = -19.4^\circ$ ($c = 0.29$, CHCl_3). The enantiomeric ratio was determined by SFC using a Chiralcel AD-H column (5-50% methanol/ CO_2 , 35 °C, 100 bar, 4 mL/min, ramp rate = 5%/min); major enantiomer $t_r = 3.30$ min and minor enantiomer $t_r = 2.99$ min.

(-)-*N*-(4-methoxyphenyl)-[1-(3-fluorophenyl)-ethyl]amine (Table 9, entry 7):

Prepared according to the general procedure from *p*-anisidine (122 mg, 0.993 mmol) and 3'-fluoroacetophenone (366 μ L, 2.98 mmol) at 50 °C for 72 h, using work-up procedure B to provide the title compound as a yellow oil (198 mg, 81% yield, 95% ee) following silica gel chromatography (1% Et₂O/toluene). IR (film) 3401, 2966, 2833, 1613, 1590, 1512, 1482, 1449, 1407, 1373, 1341, 1294, 1235, 1173, 1154, 1123, 1038, 895, 819, 786, 697 cm⁻¹; ¹H NMR (300 MHz, CDCl₃) δ 1.49 (d, 3H, *J* = 6.6 Hz, -CH₃), 3.70 (s, 3H, -OCH₃), 4.39 (q, 1H, *J* = 6.9, -CHCH₃), 6.46 (m, 2H, ArH), 6.68-6.71 (m, 2H, ArH), 6.90-6.94 (m, 1H, ArH), 7.05-7.15 (m, 2H, ArH), 7.26-7.31 (m, 1H, ArH); ¹³C NMR (75 MHz, CDCl₃) δ 25.11, 53.97, 55.72, 112.60, 112.88, 113.57, 113.85, 114.53, 114.77, 121.51, 121.55, 130.07, 130.18, 141.23, 148.53, 148.61, 152.05, 161.63, 164.88; HRMS (EI) exact mass calculated for (C₁₅H₁₆NFO) requires *m/z* 245.1216, found *m/z* 245.1209. [α]_D²⁷ = -5.2° (*c* = 0.19, CHCl₃). The enantiomeric ratio was determined by SFC using a Chiralcel AD-H column (5-50% isopropanol/CO₂, 35 °C, 100 bar, 4 mL/min, ramp rate = 5% /min); major enantiomer *t*_r = 3.45 min and minor enantiomer *t*_r = 3.70 min.

(+)-*N*-(4-methoxyphenyl)-[1-(2-fluorophenyl)-ethyl]amine (Table 9, entry 8):

Prepared according to the general procedure from *p*-anisidine (135 mg, 1.10 mmol) and 2'-fluoroacetophenone (400 μ L, 3.29 mmol) at 50 °C for 72 h, using work-up procedure B to provide the title compound as a yellow oil (160 mg, 60% yield, 83% ee) following silica gel chromatography (10% Et₂O/pentane). IR (film) 3401, 2969, 1615, 1586, 1513, 1486, 1451, 1408, 1374, 1354, 1293, 1267, 1236, 1221, 1181, 1156, 1143, 1110, 1084, 1038, 943, 820, 758 cm⁻¹; ¹H NMR (300 MHz, CDCl₃) δ 1.50 (d, 3H, *J* = 6.6 Hz, -CH₃),

3.67 (s, 3H, -OCH₃), 4.72 (q, 1H, $J = 6.6\text{Hz}$, -CHCH₃), 6.45-6.48 (m, 2H, ArH), 6.66-6.69 (m, 2H, ArH), 6.97-7.06 (m, 2H, ArH), 7.14-7.18 (m, 1H, ArH), 7.32-7.37 (m, 1H, ArH); ¹³C NMR (75 MHz, CDCl₃) δ 23.39, 48.23, 48.26, 55.67, 114.51, 114.79, 115.31, 124.36, 124.41, 127.25, 127.32, 128.19, 128.30, 131.86, 132.03, 141.13, 152.07, 158.92, 162.16; HRMS (EI) exact mass calculated for (C₁₅H₁₆FNO) requires m/z 245.1216, found m/z 245.1211. $[\alpha]_D^{27} = +18.8^\circ$ (c = 0.19, CHCl₃). The enantiomeric ratio was determined by SFC using a Chiralcel OJ-H column (5-50% methanol/CO₂, 35 °C, 100 bar, 4 mL/min, ramp rate = 5%/min); major enantiomer $t_r = 3.46$ min and minor enantiomer $t_r = 3.81$ min.

(R)-N-(4-methoxyphenyl)-[1-(naphthalen-2-yl)-ethyl]amine (Table 9, entry 9):

Prepared according to the general procedure from *p*-anisidine (126 mg, 1.02 mmol) and 2'-acetonaphthone (521 mg, 3.06 mmol) at 50 °C for 72 h. Upon completion the reaction was filtered through silica eluting with Et₂O and concentrated *in vacuo*. The crude residue was dissolved in 50 mL Et₂O and stirred for 1 hour with 1 N HCl (100 mL). The white HCl salt was collected *via* gravity filtration, dissolved in CH₂Cl₂ and stirred with saturated aqueous NaHCO₃ for 30 minutes. The layers were separated, the organic phase dried over MgSO₄ and concentrated *in vacuo* to provide the title compound as a light pink solid (207 mg 73% yield, 96% ee). IR (film) 3401, 2963, 2832, 2361, 1601, 1512, 1441, 1373, 1294, 1234, 1179, 1134, 1037, 895, 858, 818, 749 cm⁻¹; ¹H NMR (300 MHz, CDCl₃) δ 1.60 (d, 3H, $J = 6.6$ Hz, -CH₃), 3.67 (s, 3H, -OCH₃), 4.57 (q, 1H, $J = 6.9$ Hz, -CHCH₃), 6.54-6.57 (m, 2H, ArH), 6.65-6.68 (m, 2H, ArH), 7.42-7.53 (m, 3H, ArH), 7.77-7.82 (m, 4H, ArH); ¹³C NMR (75 MHz, CDCl₃) δ 25.19, 54.55, 55.74, 114.67, 114.79, 124.36, 124.50, 125.51, 126.02, 127.71, 127.86, 128.48, 132.77, 133.62, 141.60,

143.07, 151.97; HRMS (EI) exact mass calculated for (C₁₉H₁₉NO) requires m/z 277.1467, found m/z 277.1423. $[\alpha]_D^{25} = +30.9^\circ$ ($c = 0.20$, CHCl₃).³¹ The enantiomeric ratio was determined by HPLC using a Chiralcel OD-H column (3% isopropanol/hexanes); major enantiomer $t_r = 21.96$ min and minor enantiomer $t_r = 26.97$ min.

(+)-*N*-(4-methoxyphenyl)-aminoindane (Table 9, entry 10):

Prepared according to the general procedure from *p*-anisidine (101 mg, 0.823 mmol) and 1-indanone (326 mg, 2.47 mmol) at 50 °C for 72 h, using work-up procedure B to provide the title compound as a brown solid (149 mg, 75% yield, 85% ee) following silica gel chromatography (5% Et₂O/pentane). IR (film) 3370, 3028, 2934, 2826, 2361, 1628, 1511, 1460, 1232, 1178, 1079, 1037, 818, 755 cm⁻¹; ¹H NMR (300 MHz, CDCl₃) δ 1.85-1.97 (m, 1H, -CH(CH₂)₂C₆H₄), 2.51-2.62 (m, 1H, -CH(CH₂)₂C₆H₄), 2.83-2.93 (m, 1H, -CH(CH₂)₂C₆H₄), 2.97-3.07 (m, 1H, -CH(CH₂)₂C₆H₄), 3.71 (s, 3H, -OCH₃), 4.96 (q, 1H, $J = 6.6$ Hz, -CHCH₃), 6.69-6.72 (m, 2H, ArH), 6.80-6.83 (m, 2H, ArH), 7.20-7.27 (m, 3H, ArH), 7.37 (d, 1H, $J = 6.9$ ArH); ¹³C NMR (75 MHz, CDCl₃) δ 30.23, 33.85, 55.85, 59.55, 114.66, 114.99, 124.29, 124.86, 126.59, 127.85, 141.92, 143.60, 144.76, 152.16; HRMS (EI) exact mass calculated for (C₁₆H₁₇NO) requires m/z 239.1310, found m/z 239.1284. $[\alpha]_D^{24} = +45.4^\circ$ ($c = 0.22$, CHCl₃). The enantiomeric ratio was determined by SFC using a Chiralcel AD-H column (5-50% methanol/CO₂, 35 °C, 100 bar, 4 mL/min, ramp rate = 5% /min); major enantiomer $t_r = 5.06$ min and minor enantiomer $t_r = 5.73$ min.

³¹ Nakamura, S.; Yasuda, H.; Toru, T. *Tetrahedron: Asymm.* **2002**, *13*, 1509 (reported HPLC retention times $t_{rR} = 18.1$ min and $t_{rS} = 21.3$ min using a Chiralcel OD-H column, 10% hexane/ⁱPrOH).

(+)-*N*-(4-methoxyphenyl)-[2-fluoro-(1-phenyl)-ethyl]amine (Table 9, entry 11):

Prepared according to the general procedure from *p*-anisidine (53 mg, 0.43 mmol) and 2-fluoroacetophenone (177 μ L, 1.28 mmol) at 5 °C for 96 h, using work-up procedure B to provide the title compound as a yellow oil (71 mg, 70% yield, 88% ee) following silica gel chromatography (7% Et₂O/pentane). IR (film) 3400, 3029, 2951, 2902, 2833, 1618, 1513, 1453, 1293, 1243, 1179, 1094, 1036, 1005, 939, 920, 820, 755, 701 cm⁻¹; ¹H NMR (300 MHz, CDCl₃) δ 3.68 (s, 3H, -OCH₃), 4.37-4.71 (m, 3H, -CHCH₂CH₂F), 6.49-6.52 (m, 2H, ArH), 6.66-6.69 (m, 2H, ArH), 7.24-7.42 (m, 5H, ArH); ¹³C NMR (75 MHz, CDCl₃) δ 55.68, 59.34, 59.59, 84.99, 87.35, 114.74, 115.26, 127.05, 128.00, 128.90, 138.50, 138.58, 141.09, 152.54. HRMS (EI) exact mass calculated for (C₁₅H₁₆NOF) requires m/z 245.1216, found m/z 245.1204. $[\alpha]_D^{28} = +9.8^\circ$ (c = 0.26, CHCl₃). The enantiomeric ratio was determined by SFC using a Chiralcel AD-H column (5-50% methanol/CO₂, 35 °C, 100 bar, 4 mL/min, ramp rate = 5% /min); major enantiomer t_r = 3.80 min and minor enantiomer t_r = 4.46 min.

(-)-*N*-sec-butyl-(4-methoxyphenyl)amine (Table 10, entry 1):

Prepared according to the general procedure from *p*-anisidine (105 mg, 0.853 mmol) and 2-butanone (185 μ L, 2.56 mmol) at 40 °C for 72 h, using work-up procedure B to provide the title compound as a yellow oil (107 mg, 71% yield, 83% ee) following silica gel chromatography (9% Et₂O/pentane). IR (film) 3392, 2963, 2931, 2875, 2832, 1512, 1464, 1407, 1375, 1294, 1232, 1164, 1041, 819, 755 cm⁻¹; ¹H NMR (300 MHz, CDCl₃) δ 0.94 (dd, 3H, J = 7.5, 7.5 Hz, -CH₂CH₃), 1.14 (d, 3H, J = 6.0 Hz, -CH₃), 1.35-1.68 (m, 2H, -CH₂CH₃), 3.31 (sextet, 1H, J = 6.3 Hz, -CHCH₃), 3.71 (s, 3H, -OCH₃), 6.55-6.58 (m,

2H, ArH), 6.76-6.79 (m, 2H, ArH); ^{13}C NMR (75 MHz, CDCl_3) δ 10.40, 20.27, 29.64, 50.80, 55.80, 114.70, 114.94, 141.99, 151.78; HRMS (EI) exact mass calculated for ($\text{C}_{11}\text{H}_{17}\text{NO}$) requires m/z 179.1310, found m/z 179.1302. $[\alpha]_D^{28} = -25.2^\circ$ ($c = 0.24$, CHCl_3). The enantiomeric ratio was determined by GLC using a CP-Chirasil-Dex-CB column (100 °C isotherm for 140 minutes); major enantiomer $t_r = 130.90$ min and minor enantiomer $t_r = 128.72$ min.

(-)-*N*-(4-methoxyphenyl)-[1-(methyl)-heptyl]amine (Table 10, entry 2):

Prepared according to the general procedure from *p*-anisidine (105 mg, 0.853 mmol) and 2-octanone (400 μL , 2.56 mmol) at 40 °C for 96 h, using work-up procedure B to provide the title compound as a clear oil (144 mg, 72% yield, 91% ee) following silica gel chromatography (4% Et_2O /pentane). IR (film) 3393, 2957, 2929, 2856, 2832, 1840, 1618, 1512, 1465, 1407, 1376, 1294, 1234, 1180, 1157, 1108, 1042, 818, 757, 724 cm^{-1} ; ^1H NMR (300 MHz, CDCl_3) δ 0.86 (t, 3H, $J = 6.6$ Hz, $-(\text{CH}_2)_5\text{CH}_3$), 1.12 (d, 3H, $J = 6.3$ Hz, $-\text{CH}_3$), 1.26-1.41 (m, 10H, $-\text{CH}(\text{CH}_2)_5\text{CH}_3$), 3.33 (m, 1H, $J = 6.3$, $-\text{CHCH}_3$), 3.73 (s, 3H, $-\text{OCH}_3$), 6.52-6.55 (m, 2H, ArH), 6.74-6.77 (m, 2H, ArH); ^{13}C NMR (75 MHz, CDCl_3) δ 14.14, 20.82, 22.67, 26.19, 29.44, 31.90, 37.28, 49.50, 55.78, 114.66, 114.94, 142.02, 151.76; HRMS (EI) exact mass calculated for ($\text{C}_{15}\text{H}_{25}\text{NO}$) requires m/z 235.1936, found m/z 235.1932. $[\alpha]_D^{27} = -8.0^\circ$ ($c = 1.14$, CH_2Cl_2). The enantiomeric ratio was determined by SFC using a Chiralcel OJ-H column (5-10% methanol/ CO_2 , 35 °C, 100 bar, 4 mL/min, ramp rate = 0.5%/min); major enantiomer $t_r = 2.70$ min and minor enantiomer $t_r = 2.94$ min.

(*R*)-*N*-(4-methoxyphenyl)-[1-(methyl)-3-phenylpropyl]amine (Table 10, entry 3):

Prepared according to the general procedure from *p*-anisidine (124 mg, 1.01 mmol) and benzylacetone (450 μ L, 3.03 mmol) at 40 °C for 72 h, using work-up procedure A to provide the title compound as a yellow oil (193 mg, 75% yield, 94% ee) following silica gel chromatography (10% Et₂O/pentane). IR (film) 3392, 3025, 2930, 2830, 1714, 1602, 1511, 1453, 1407, 1373, 1293, 1234, 1179, 1153, 1039, 819, 748, 699 cm⁻¹; ¹H NMR (300 MHz, CDCl₃) δ 1.18 (d, 3H, *J* = 6.3 Hz, -CH₃), 1.66-1.76 (m, 1H, -CHCH₂CH₂C₆H₅), 1.78-1.92 (m, 1H, -CHCH₂CH₂C₆H₅), 2.68-2.73 (dd, 2H, *J* = 7.8, -CHCH₂CH₂C₆H₅), 3.33-3.41 (m, 1H, *J* = 7.8, 7.8 Hz, -CHCH₃), 3.72 (s, 3H, -OCH₃), 6.46-6.53 (m, 2H, ArH), 6.71-6.77 (m, 2H, ArH), 7.14-7.19 (m, 3H, ArH), 7.25-7.30 (m, 2H, ArH); ¹³C NMR (75 MHz, CDCl₃) δ 20.90, 32.55, 38.87, 48.99, 55.83, 114.83, 114.99, 125.88, 128.44, 128.50, 141.78, 142.15, 151.93; HRMS (EI) exact mass calculated for (C₁₇H₂₁NO) requires *m/z* 255.1623, found *m/z* 255.1623. [α]_D²⁷ = -2.8° (*c* = 1.20, CH₂Cl₂).³² The enantiomeric ratio was determined by SFC using a Chiralcel AD-H column (5-50% methanol/CO₂, 35 °C, 100 bar, 4 mL/min, ramp rate = 5% /min); major enantiomer *t*_r = 3.88 min and minor enantiomer *t*_r = 4.57 min.

(-)-*N*-(4-methoxyphenyl)-[1-(cyclohexyl)-ethyl]amine (Table 10, entry 4):

Prepared according to the general procedure from *p*-anisidine (123 mg, 1.00 mmol) and cyclohexylmethyl ketone (413 μ L, 3.00 mmol) at 50 °C for 96 h, using work-up procedure B to provide the title compound as a yellow oil (115 mg, 49% yield, 86% ee)

³² Arrasate, S.; Lete, E.; Sotomayor, N. *Tetrahedron: Asymm.* **2001**, *12*, 2077. (reported a rotation of -9.1° (*c* = 1.2, CH₂Cl₂) for a product that was 23% ee and HPLC retention times *t*_R = 23.6 min and *t*_S = 26.6 min using a Chiralcel OD column, 2% hexanes/2-propanol).

following silica gel chromatography (10% Et₂O/pentane). IR (film) 3400, 2924, 2851, 1618, 1511, 1464, 1449, 1407, 1372, 1294, 1236, 1180, 1159, 1102, 1041, 890, 817, 754 cm⁻¹; ¹H NMR (300 MHz, CDCl₃) δ 0.99-1.21 (m, 5H, -C₆H₁₁) 1.06 (d, 3H, *J* = 6.6 Hz, CH₃), 1.39-1.43 (m, 1H, -C₆H₁₁), 1.66-1.75 (m, 5H, -C₆H₁₁), 3.18-3.22 (m, 1H, -CHCH₃), 3.72 (s, 3H, -OCH₃), 6.52-6.55 (m, 2H, ArH), 6.73-6.76 (m, 2H, ArH); ¹³C NMR (75 MHz, CDCl₃) δ 17.35, 26.38, 26.53, 26.69, 28.27, 29.88, 42.86, 54.14, 55.83, 114.53, 114.95, 142.22, 151.60; HRMS (EI) exact mass calculated for (C₁₅H₂₃NO) requires *m/z* 233.1780, found *m/z* 233.1786. $[\alpha]_D^{28} = -4.3^\circ$ (c = 1.09, CHCl₃). The enantiomeric ratio was determined by SFC using a Chiralcel AS-H column (5-25% methanol/CO₂, 35 °C, 100 bar, 4 mL/min, ramp rate = 2% /min); major enantiomer *t_r* = 2.49 min and minor enantiomer *t_r* = 1.90 min.

(+)-*N*-(4-methoxyphenyl)-[1-(methyl)-2-benzoate-ethyl]amine (Table 10, entry 5):

Prepared according to the general procedure from *p*-anisidine (53 mg, 0.43 mmol) and 2-oxopropyl benzoate (230 μL, 1.29 mmol) at 40 °C for 96 h, using work-up procedure B to provide the title compound as a yellow oil (73 mg, 72% yield, 81% ee) following silica gel chromatography (1% Et₂O/ toluene). IR (film) 3392, 2968, 2359, 1719, 1601, 1513, 1451, 1387, 1371, 1315, 1274, 1234, 1177, 1111, 1071, 1027, 821, 712 cm⁻¹; ¹H NMR (300 MHz, CDCl₃) δ 1.30 (d, 3H, *J* = 6.6 Hz, -CH₃), 3.73 (s, 3H, -OCH₃), 3.79-3.84 (m, 1H, -CHCH₃), 4.17-4.22 (m, 1H, -CH₂OCOC₆H₅), 4.41-4.46 (m, 1H, -CH₂OCOC₆H₅), 6.64-6.67 (m, 2H, ArH), 6.74-6.78 (m, 2H, ArH), 7.39-7.45 (m, 2H, ArH), 7.52-7.57 (m, 1H, ArH), 7.98-8.02 (m, 2H, ArH); ¹³C NMR (75 MHz, CDCl₃) δ 18.30, 48.86, 55.78, 67.98, 114.99, 115.08, 128.41, 129.62, 130.02, 133.08, 141.04, 152.39, 166.57. HRMS

(EI) exact mass calculated for (C₁₇H₁₉NO₃) requires m/z 285.1365, found m/z 285.1367. $[\alpha]_D^{26} = +12.8^\circ$ ($c = 0.21$, CH₂Cl₂). The enantiomeric ratio was determined by SFC using a Chiralcel AD-H column (5-50% methanol/CO₂, 35 °C, 100 bar, 4 mL/min, ramp rate = 5%/min); major enantiomer $t_r = 6.80$ min and minor enantiomer $t_r = 4.97$ min.

(-)-N-(4-methoxyphenyl)-[1-(methyl)-pent-4-enyl]amine (Table 10, entry 6):

Prepared according to the general procedure from *p*-anisidine (70 mg, 0.57 mmol) and 5-hexen-2-one (200 µL, 1.70 mmol) at 40 °C for 96 h, using work-up procedure B to provide the title compound as a yellow oil (70 mg, 60% yield, 90% ee) following silica gel chromatography (10% Et₂O/ pentane). IR (film) 3391, 3075, 2960, 2932, 2832, 2852, 2360, 2069, 1840, 1712, 1640, 1618, 1513, 1464, 1442, 1408, 1375, 1293, 1235, 1180, 1157, 1040, 996, 911, 819, 755 cm⁻¹; ¹H NMR (300 MHz, CDCl₃) δ 1.14 (d, 3H, $J = 6.3$ Hz, -CH₃), 1.41-1.54 (m, 1H, -CH₂CH₂CHCH₂), 1.61-1.66 (m, 1H, -CH₂CH₂CHCH₂), 2.10-2.17 (m, 2H, -CH₂CH₂CHCH₂), 3.38 (q, 1H, $J = 6.3$ Hz, -CHCH₃), 3.72 (s, 3H, -OCH₃), 4.93-5.05 (m, 2H, -CH₂CH₂CHCH₂), 5.76-5.85 (m, 1H, -CH₂CH₂CHCH₂), 6.53-6.56 (m, 2H, ArH), 6.74-6.77 (m, 2H, ArH); ¹³C NMR (75 MHz, CDCl₃) δ 20.77, 30.46, 36.26, 49.03, 55.79, 114.73, 114.74, 114.95, 138.45, 141.84, 151.84. HRMS (EI) exact mass calculated for (C₁₃H₁₉NO) requires m/z 205.1467, found m/z 205.1470. $[\alpha]_D^{28} = -3.8^\circ$ ($c = 0.40$, CHCl₃). The enantiomeric ratio was determined by SFC using a Chiralcel OJ-H column (5-50% isopropanol/CO₂, 35 °C, 100 bar, 4 mL/min, ramp rate = 5% /min); major enantiomer $t_r = 2.74$ min and minor enantiomer $t_r = 2.98$ min.

(*R*)-*N*-[1-(phenyl)-ethyl]aniline (Table 11, entry 1):

Prepared according to the general procedure from aniline (93 mg, 1.0 mmol) and acetophenone (351 μ L, 3.00 mmol) at 50 °C for 24 h, using work-up procedure B to provide the title compound as a yellow oil (145 mg, 73% yield, 93% ee) following silica gel chromatography (8% Et₂O/pentane). IR (film) 3410, 3052, 3023, 2966, 2924, 2867, 1947, 1817, 1720, 1601, 1505, 1449, 1428, 1372, 1352, 1319, 1280, 1258, 1206, 1180, 1140, 1077, 1029, 749, 700, 692 cm⁻¹; ¹H NMR (300 MHz, CDCl₃) δ 1.50 (d, 3H, *J* = 6.6 Hz, CH₃), 4.47 (q, 1H, *J* = 6.6 Hz, -CHCH₃), 6.48-6.51 (m, 2H, ArH), 6.60-6.66 (m, 1H, ArH), 7.04-7.10 (m, 2H, ArH), 7.18-7.24 (m, 2H, ArH), 7.27-7.37 (m, 3H, ArH); ¹³C NMR (75 MHz, CDCl₃) δ 25.43, 53.80, 113.69, 117.62, 126.24, 127.26, 129.04, 129.51, 145.63, 147.67; HRMS (EI) exact mass calculated for (C₁₄H₁₅N) requires *m/z* 197.1205 found *m/z* 197.1196. [α]_D²⁸ = -16.9° (*c* = 1.35, CH₃OH).³³ The enantiomeric ratio was determined by HPLC using an OD-H column (2% isopropanol/hexanes); major enantiomer *t*_r = 20.68 min and minor enantiomer *t*_r = 17.46 min.

(-)-*N*-1-(phenylethyl)-[4-(trifluoromethyl)-phenyl]amine (Table 11, entry 2):

Prepared according to the general procedure from *p*-(trifluoromethyl)aniline (124 μ L, 1.00 mmol) and acetophenone (351 μ L, 3.00 mmol) at 40 °C for 24 h, using work-up procedure B to provide the title compound as a clear oil (145.3 mg, 55% yield, 95% ee) following silica gel chromatography (2% Et₂O/pentane). IR (film) 3421, 3064, 3031, 2970, 2928, 2872, 2599, 1892, 1721, 1617, 1531, 1490, 1451, 1328, 1109, 1066, 824, 764, 701 cm⁻¹; ¹H NMR (300 MHz, CDCl₃) δ 1.54 (d, 3H, *J* = 6.6 Hz, CH₃), 4.52 (q, 1H,

³³ Kanth, J. V. B.; Periasamy, M. *J. Org. Chem.* **1993**, 58, 3156. (reported a rotation of -16° (*c* = 1.0, CH₃OH) for a product that was 98% ee)

$J = 6.9$ Hz, $-\text{CHCH}_3$), 6.51 (d, 2H, $J = 8.7$ Hz, Ar-H), 7.23-7.34 (m, 7H, Ar-H); ^{13}C NMR (75 MHz, CDCl_3) δ 24.86, 53.22, 112.45, 125.71, 126.39, 126.44, 126.49, 126.54, 127.20, 128.82, 144.23, 149.60; HRMS (EI) exact mass calculated for $(\text{C}_{15}\text{H}_{14}\text{NF}_3)$ requires m/z 265.1078 found m/z 265.1076. $[\alpha]_D^{28} = -1.4^\circ$ ($c = 0.25$, CHCl_3). The enantiomeric ratio was determined by SFC using a Chiralcel AD-H column (5-50% isopropanol/ CO_2 , 35 °C, 100 bar, 4 mL/min, ramp rate = 5% /min); major enantiomer $t_r = 2.52$ min and minor enantiomer $t_r = 2.91$ min.

(+)-*N*-(6,7,8,9-tetrahydrodibenzo[β,δ]furan-2)-[1-(phenyl)ethyl]amine (Table 11, entry 6):

Prepared according to the general procedure from 6,7,8,9-tetrahydrodibenzo[β,δ]furan-2-amine (106 mg, 0.568 mmol) and acetophenone (170 μL , 1.70 mmol) at 40 °C for 72 h; using work-up procedure B to provide the title compound as a yellow oil (142.4 mg, 92% yield, 91% ee) following silica gel chromatography (100% toluene). IR (film) 3411, 3025, 2927, 2834, 1618, 1595, 1471, 1353, 1276, 1237, 1218, 1188, 1123, 834, 795, 762, 701 cm^{-1} ; ^1H NMR (300 MHz, CDCl_3) δ 1.51 (d, 3H, $J = 6.6$ Hz, $-\text{CH}_3$), 1.73-1.88 (m, 4H, $-\text{C}(\text{CH}_2)_4\text{C}-$), 2.42-2.47 (m, 2H, $-\text{C}(\text{CH}_2)_4\text{C}-$), 2.61-2.65 (m, 2H, $-\text{C}(\text{CH}_2)_4\text{C}-$), 4.49 (q, 1H, $J = 6.6$ Hz, $-\text{CHCH}_3$), 6.42-6.47 (m, 2H, ArH), 7.08-7.11 (m, 1H, ArH), 7.17-7.32 (m, 3H, Ar-H), 7.35-7.39 (m, 2H, Ar-H); ^{13}C NMR (75 MHz, CDCl_3) δ 20.52, 22.76, 23.03, 23.60, 25.13, 54.39, 101.85, 110.74, 110.91, 112.60, 126.01, 126.85, 128.67, 129.51, 143.25, 145.66, 148.11, 154.31; HRMS (EI) exact mass calculated for $(\text{C}_{20}\text{H}_{21}\text{NO})$ requires m/z 291.1623, found m/z 291.1620. $[\alpha]_D^{24} = +32.6^\circ$ ($c = 0.20$, CHCl_3). The enantiomeric ratio was determined by SFC using a Chiralcel AD-H column

(5-50% methanol/CO₂, 35 °C, 100 bar, 4 mL/min, ramp rate = 5%/min); major enantiomer t_r = 6.70 min and minor enantiomer t_r = 5.75 min.

(+)-*N*-(5-benzo[δ]thiazol)-[1-(phenyl)-ethyl]amine (Table 11, entry 4):

Prepared according to the general procedure from benzothiazol-5-ylamine (85.3 mg, 0.568 mmol) and acetophenone (170 μ L, 1.70 mmol) at 50 °C for 72 h; using work-up procedure B to provide the title compound as a yellow oil (93.0 mg, 70% yield, 91% ee) following silica gel chromatography (30% Et₂O/pentane). IR (film) 3412, 3305, 3061, 2967, 1605, 1560, 1482, 1449, 1402, 1373, 1327, 1261, 820, 701 cm⁻¹; ¹H NMR (300 MHz, CDCl₃) δ 1.55 (d, 3H, J = 6.9 Hz, -CH₃), 4.51 (q, 1H, J = 6.6 Hz, -CHCH₃), 6.76-6.85 (m, 2H, Ar-H), 7.22-7.25 (m, 2H, Ar-H), 7.29-7.39 (m, 3H, Ar-H), 7.80-7.83 (m, 1H, Ar-H), 8.59 (s, 1H, Ar-H); ¹³C NMR (75 MHz, CDCl₃) δ 25.07, 53.85, 102.91, 115.06, 123.66, 125.80, 127.14, 128.81, 135.68, 144.53, 145.54, 145.85, 149.12; HRMS (EI) exact mass calculated for (C₁₅H₁₄N₂S) requires m/z 254.0878, found m/z 254.0883. $[\alpha]_D^{25}$ = +85.4° (c = 0.28, CHCl₃). The enantiomeric ratio was determined by SFC using a Chiralcel OJ-H column (5-50% methanol/CO₂, 35 °C, 100 bar, 4 mL/min, ramp rate = 5%/min); major enantiomer t_r = 6.70 min and minor enantiomer t_r = 5.82 min.

(+)-*N*-[1-(phenyl)-ethyl]-1-tosyl-1*H*-indol-5-amine (Table 11, entry 5):

Prepared according to the general procedure from 5-amino-*N*-tosylindole (123 mg, 0.427 mmol) and acetophenone (150 μ L, 1.28 mmol) at 40 °C for 48 h, using work-up procedure B to provide the title compound as a white solid (150 mg, 90% yield, 93% ee) following silica gel chromatography (17% Et₂O/pentane). IR (film) 3412, 2967, 1619,

1596, 1534, 1492, 1467, 1452, 1365, 1305, 1234, 1188, 1176, 1162, 1127, 1092, 1018, 994, 811, 759, 717, 702, 677, 665 cm^{-1} ; ^1H NMR (300 MHz, CDCl_3) δ 1.49 (d, 3H, J = 6.9 Hz, $-\text{CH}_3$), 2.30 (s, 3H, $-\text{SO}_2\text{C}_6\text{H}_4\text{CH}_3$), 4.42 (q, 1H, J = 6.6 Hz, $-\text{CHCH}_3$), 6.36-6.38 (m, 1H, ArH), 6.47-6.48 (m, 1H, ArH), 6.57-6.61 (m, 1H, ArH), 7.05-7.36 (m, 8H, ArH), 7.65-7.71 (m, 3H, ArH); ^{13}C NMR (75 MHz, CDCl_3) δ 21.53, 25.19, 54.05, 103.28, 109.28, 113.22, 114.25, 125.86, 126.54, 126.72, 126.92, 128.00, 128.70, 129.75, 132.00, 135.35, 144.09, 144.59, 145.30. HRMS (EI) exact mass calculated for ($\text{C}_{23}\text{H}_{22}\text{N}_2\text{O}_2\text{S}$) requires m/z 390.1402, found m/z 390.1410. $[\alpha]_D^{28} = +7.1^\circ$ (c = 0.20, CHCl_3). The enantiomeric ratio was determined by SFC using a Chiralcel OJ-H column (5-55% isopropanol/ CO_2 , 35 $^\circ\text{C}$, 100 bar, 4 mL/min, ramp rate 5.5% /min); major enantiomer t_r = 10.09 min and minor enantiomer t_r = 8.42 min.

(-)-3-methyl-3,4-dihydro-benzo-[1,4]-oxazin-2-one (16):

An oven dried 20 mL vial equipped with a magnetic stir bar was charged with imine (200 mg, 0.621 mmol), Hantzsch ester (378 mg, 0.745 mmol) and catalyst (54 mg, 0.031 mmol). Benzene (6.2 mL) was added and the reaction mixture was heated at 40 $^\circ\text{C}$ for 7 h. Upon completion the product was isolated using work-up procedure B to provide the title compound as a white solid (163 mg, 82% yield, 97% ee) following silica gel chromatography (25% Et_2O /pentane). IR (film) 3317, 1752, 1619, 1595, 1503, 1457, 1339, 1306, 1292, 1208, 1197, 1182, 1097, 1040, 748, 690 cm^{-1} ; ^1H NMR (300 MHz, CDCl_3) δ 1.54 (d, 3H, J = 6.6 Hz, $-\text{CH}_3$), 3.98 (q, 1H, J = 6.6 Hz, $-\text{CHCH}_3$), 6.75-6.78 (m, 1H, ArH), 6.84-6.89 (m, 1H, ArH), 6.97-7.26 (m, 2H, ArH); ^{13}C NMR (75 MHz, CDCl_3) δ 17.21, 50.57, 115.02, 116.88, 120.49, 124.91, 132.96, 141.43, 167.25; HRMS (EI)

exact mass calculated for ($\text{C}_9\text{H}_9\text{NO}_2$) requires m/z 163.0633, found m/z 163.0633. $[\alpha]_D^{27} = -38.4^\circ$ ($c = 0.24$, CHCl_3). The enantiomeric ratio was determined by GLC using a Chiraldex Γ -TA column (150 °C isotherm for 30 minutes); major enantiomer $t_r = 20.08$ min and minor enantiomer $t_r = 18.95$ min.

(-)-3-ethyl-3,4-dihydro-benzo-[1,4]-oxazin-2-one (17):

A vial equipped with a magnetic stir bar was charged with imine (100 mg, 0.568 mmol), Hantzsch ester (174 mg, 0.682 mmol) and catalyst (50 mg, 0.057 mmol). Benzene (5.8 mL) was added and the reaction mixture was heated at 40 °C for 50 h. Upon completion the product was isolated using work-up procedure B to provide the title compound as a colorless oil (27 mg, 27% yield, 79% ee) following silica gel chromatography (20% Et_2O /pentane). IR (film) 3365, 2970, 2934, 2878, 1765, 1617, 1501, 1340, 1301, 1191, 746 cm^{-1} ; ^1H NMR (300 MHz, CDCl_3) δ 1.07 (t, 3H, $J = 7.4$ Hz, $-\text{CH}_2\text{CH}_3$), 1.79-2.01 (m, 2H, $-\text{CH}_2\text{CH}_3$), 3.87 (dd, 1H, $J = 7.4, 5.3$ Hz, $-\text{CHNHAr}$), 6.74-6.87 (m, 2H, ArH), 6.96-7.03 (m, 2H, ArH); ^{13}C NMR (75 MHz, CDCl_3) δ 9.59, 24.47, 55.93, 114.99, 116.74, 120.18, 124.91, 132.35, 141.00, 166.47; HRMS (EI) exact mass calculated for ($\text{C}_{10}\text{H}_{11}\text{NO}_2$) requires m/z 177.0790, found m/z 177.0790. $[\alpha]_D^{25} = -23.4^\circ$ ($c = 0.22$, CHCl_3). The enantiomeric ratio was determined by GLC using a Chirasil-Dex-CB column (170 °C isotherm for 30 minutes); major enantiomer $t_r = 11.93$ min and minor enantiomer $t_r = 11.54$ min.

(R)-2-(2-methoxy-phenylamino)-propionic acid methyl ester (proof of absolute stereochemistry for cyclic amine 16):

Cyclic amine (30 mg, 0.18 mmol) was dissolved in methanol (10 mL), followed by addition of PPTS (3 mg). The reaction mixture was stirred for 10 minutes at room temperature then quenched by the addition of saturated Na_2CO_3 (10 mL). Product was extracted into CH_2Cl_2 (4×10 mL) and the combined organics dried over Na_2SO_4 , filtered and concentrated to yield a yellow oil that was used directly in the next reaction. The crude alcohol was dissolved in acetone (2.0 mL). Iodomethane (0.4 mL, 6.4 mmol) was added at RT followed by potassium carbonate (103 mg, 0.75 mmol). The mixture was stirred at room temperature for 4 hours then quenched by addition of saturated NH_4Cl (10 mL). The product was extracted using CH_2Cl_2 (4×10 mL) and the combined organics dried over Na_2SO_4 , filtered and concentrated. The crude oil was purified by flash chromatography (10% Et_2O /pentane) to yield the product as a colorless oil (29 mg, 74% yield). ^1H NMR (300 MHz, CDCl_3) δ 1.51 (d, 3H, $J = 6.9$ Hz, $-\text{CHCH}_3$), 3.71 (s, 3H, $-\text{OCH}_3$), 3.86 (s, 3H, $-\text{CO}_2\text{CH}_3$), 4.14 (q, 1H, $J = 6.9$ Hz, $-\text{CHCH}_3$), 6.51 (d, 1H, $J = 8.1$ Hz, ArH), 6.70-6.86 (m, 3H, ArH); $[\alpha]_D^{27} = +28.0$ ($c = 0.17$, THF).³⁴

³⁴ Norton, J. R; Gately, D. A. *J. Am. Chem. Soc.* **1996**, *118*, 3479. (reported a rotation of -42.8° ($c = 0.15$, THF) for *S* product that was 97% ee)

CALIFORNIA INSTITUTE OF TECHNOLOGY
BECKMAN INSTITUTE
X-RAY CRYSTALLOGRAPHY LABORATORY

Crystal Structure Analysis of:

RIS06

(shown below)

For Investigator: Ian Storer

Advisor: D. W. C. MacMillan

By Michael W. Day e-mail: mikeday@caltech.edu

Contents

Table 1. Crystal data

Figures Figures

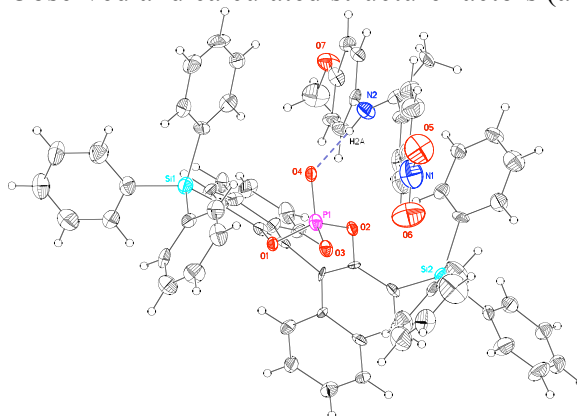
Table 2. Atomic Coordinates

Table 3. Full bond distances and angles

Table 4. Anisotropic displacement parameters

Table 5. Hydrogen bond distances and angles

Table 6. Observed and calculated structure factors (available upon request)



RIS06

Note: The crystallographic data have been deposited in the Cambridge Database (CCDC) and has been placed on hold pending further instructions from me. The deposition number is 287655. Ideally the CCDC would like the publication to contain a footnote of the type: "Crystallographic data have been deposited at the CCDC, 12 Union Road, Cambridge CB2 1EZ, UK and copies can be obtained on request, free of charge, by quoting the publication citation and the deposition number 287655."

Table 1. Crystal data and structure refinement for RIS06 (CCDC 287655).

Empirical formula	$[C_{56}H_{40}O_4PSi_2]^- [C_{15}H_{15}N_2O_3]^+ \cdot 4(C_7H_8) \cdot O$
Formula weight	1519.86

Crystallization Solvent	Toluene
Crystal Habit	Fragment
Crystal size	0.15 x 0.15 x 0.11 mm ³
Crystal color	Yellow

Data Collection

Type of diffractometer	Bruker SMART 1000
Wavelength	0.71073 Å MoK α
Data Collection Temperature	100(2) K
θ range for 7276 reflections used in lattice determination	2.22 to 18.24°
Unit cell dimensions	a = 9.8819(5) Å b = 16.0655(8) Å c = 50.192(3) Å
Volume	7968.3(7) Å ³
Z	4
Crystal system	Orthorhombic
Space group	P2 ₁ 2 ₁ 2 ₁
Density (calculated)	1.267 Mg/m ³
F(000)	3208
θ range for data collection	1.33 to 20.86°
Completeness to $\theta = 20.86^\circ$	94.9 %
Index ranges	-9 \leq h \leq 9, -16 \leq k \leq 15, -47 \leq l \leq 49
Data collection scan type	ω scans at 3 ϕ settings
Reflections collected	46009
Independent reflections	7765 [R _{int} = 0.1370]
Absorption coefficient	0.127 mm ⁻¹
Absorption correction	None
Max. and min. transmission	0.9862 and 0.9813

Table 1 (cont.)**Structure solution and Refinement**

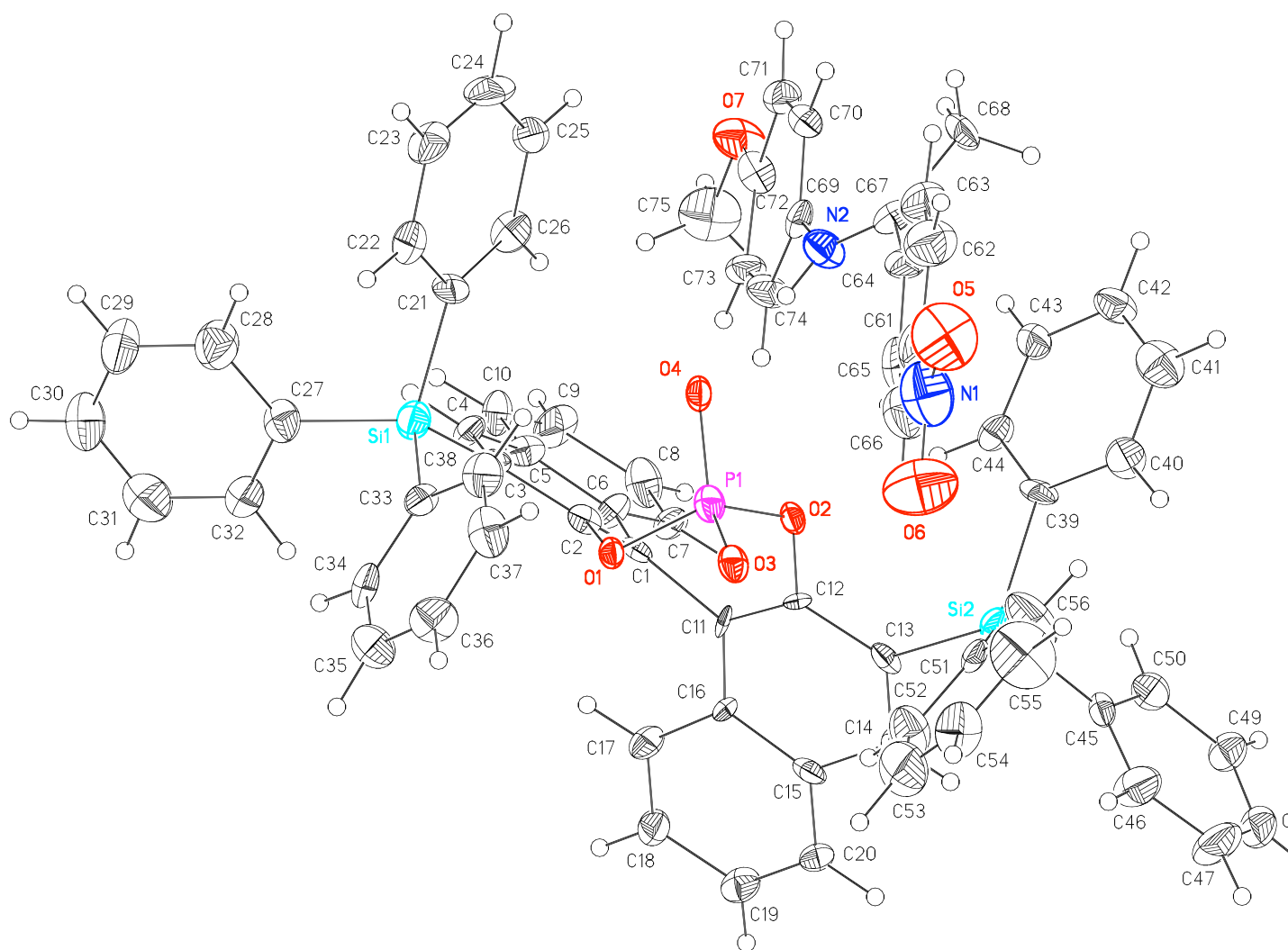
Structure solution program	Bruker XS v6.12
Primary solution method	Direct methods
Secondary solution method	Difference Fourier map
Hydrogen placement	Geometric positions
Structure refinement program	Bruker XS v6.12
Refinement method	Full matrix least-squares on F^2
Data / restraints / parameters	7765 / 960 / 1047
Treatment of hydrogen atoms	Riding
Goodness-of-fit on F^2	1.419
Final R indices [$I > 2\sigma(I)$, 4963 reflections]	$R1 = 0.0601$, $wR2 = 0.0835$
R indices (all data)	$R1 = 0.1161$, $wR2 = 0.0913$
Type of weighting scheme used	Sigma
Weighting scheme used	$w = 1/\sigma^2(F_o^2)$
Max shift/error	0.006
Average shift/error	0.000
Absolute structure parameter	-0.05(15)
Largest diff. peak and hole	0.324 and -0.376 e. \AA^{-3}

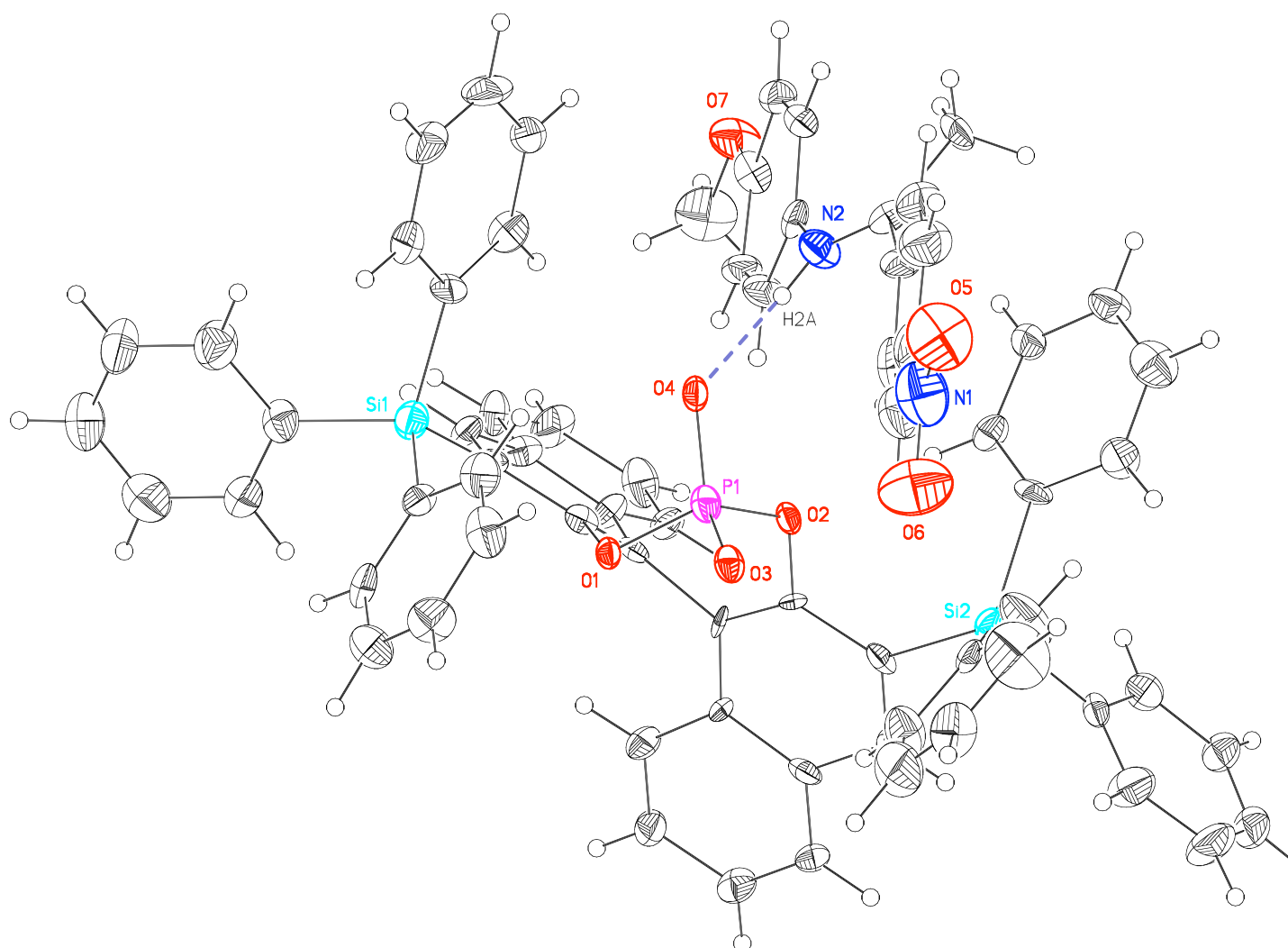
Special Refinement Details

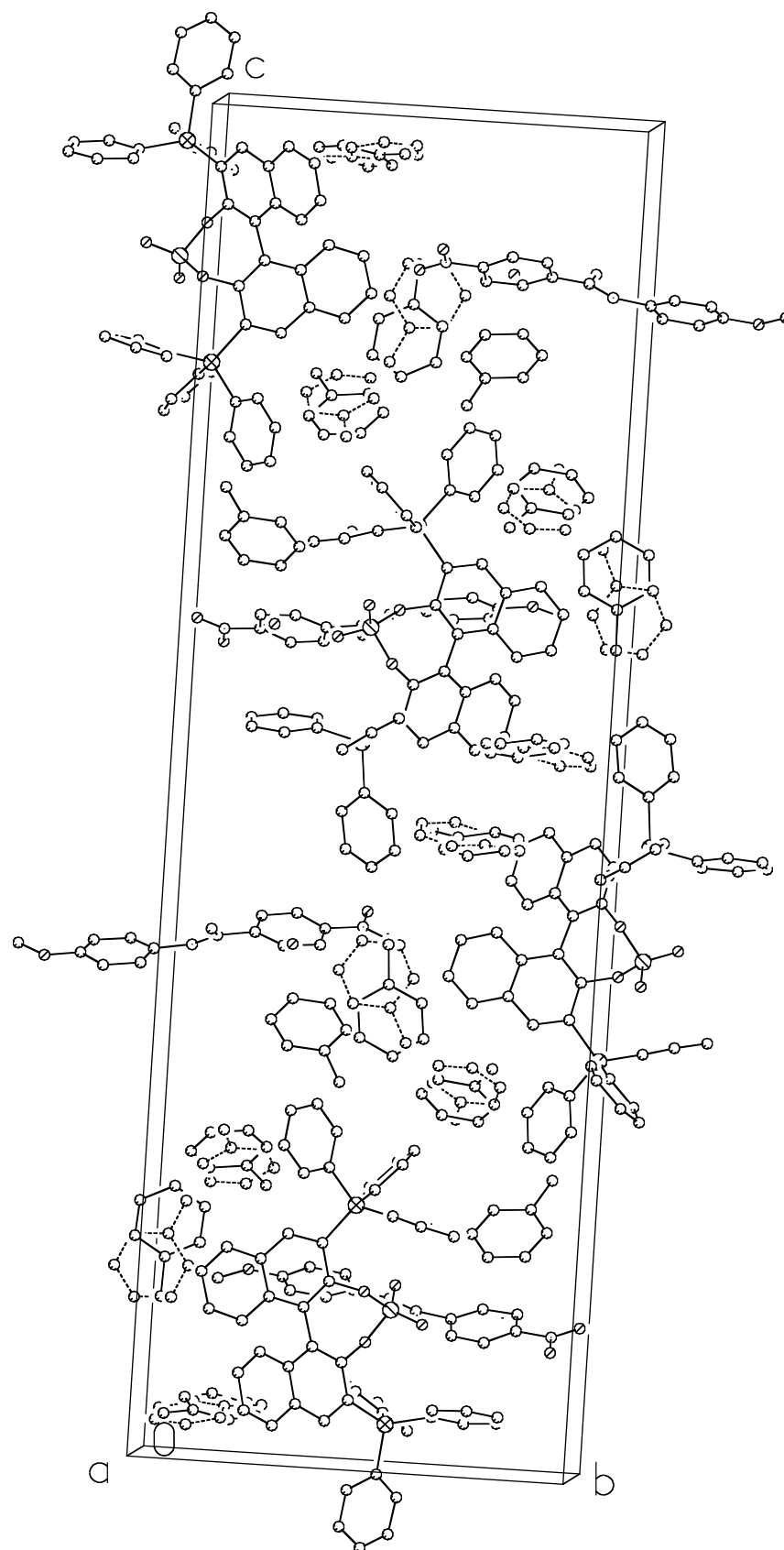
The crystals contain toluene as a solvent of crystallization with four molecules in each asymmetric unit. Three of these toluene molecules are disordered. The geometries of the toluene molecules were restrained to be similar and the six-member rings of these molecules were constrained to be regular hexagons with C-C distances of 1.39Å. For each of the disordered toluene sites the total occupancy of the disordered pair was restrained to sum to one. For two of these sites the minor component was refined with isotropic displacement parameters (see Table 2). The anisotropic displacement parameters of ALL other atoms were restrained to approximate isotropic behavior. Additionally, the asymmetric unit contains a lone atom which was modeled as oxygen.

Refinement of F^2 against ALL reflections. The weighted R-factor (wR) and goodness of fit (S) are based on F^2 , conventional R-factors R are based on F , with F set to zero for negative F^2 . The threshold expression of $F^2 > 2\sigma(F^2)$ is used only for calculating R-factors(gt) etc. and is not relevant to the choice of reflections for refinement. R-factors based on F^2 are statistically about twice as large as those based on F , and R-factors based on ALL data will be even larger.

All esds (except the esd in the dihedral angle between two l.s. planes) are estimated using the full covariance matrix. The cell esds are taken into account individually in the estimation of esds in distances, angles and torsion angles; correlations between esds in cell parameters are only used when they are defined by crystal symmetry. An approximate (isotropic) treatment of cell esds is used for estimating esds involving l.s. planes.







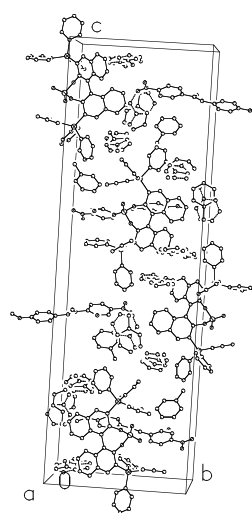
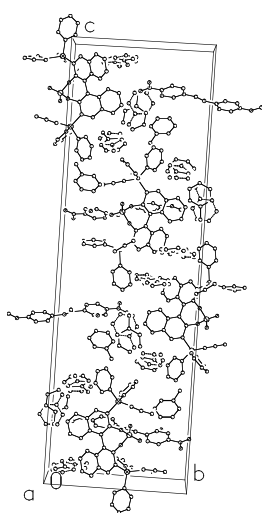


Table 2. Atomic coordinates ($\times 10^4$) and equivalent isotropic displacement parameters ($\text{\AA}^2 \times 10^3$) for RIS06 (CCDC 287655). $U(\text{eq})$ is defined as the trace of the orthogonalized U^{ij} tensor.

	x	y	z	U_{eq}	Occ
P(1)	3582(2)	-762(1)	8811(1)	22(1)	1
Si(1)	4479(2)	146(1)	8049(1)	26(1)	1
Si(2)	3030(2)	-777(1)	9660(1)	23(1)	1
O(1)	4738(4)	-169(3)	8679(1)	16(1)	1
O(2)	3077(4)	-206(3)	9065(1)	17(1)	1
O(3)	4261(4)	-1523(3)	8899(1)	21(1)	1
O(4)	2357(4)	-785(3)	8637(1)	20(1)	1
C(1)	4282(6)	1207(5)	8823(2)	13(2)	1
C(2)	4379(7)	658(5)	8623(2)	21(2)	1
C(3)	4298(6)	868(5)	8342(2)	17(2)	1
C(4)	3952(7)	1674(5)	8294(2)	25(2)	1
C(5)	3697(7)	2274(5)	8493(2)	22(2)	1
C(6)	3840(7)	2027(5)	8767(2)	20(2)	1
C(7)	3485(7)	2622(5)	8959(2)	26(2)	1
C(8)	3049(7)	3412(5)	8891(2)	34(2)	1
C(9)	2955(7)	3641(5)	8620(2)	36(2)	1
C(10)	3300(7)	3080(5)	8427(2)	26(2)	1
C(11)	4576(7)	943(4)	9109(1)	13(2)	1
C(12)	3945(7)	277(5)	9217(2)	13(2)	1
C(13)	4044(6)	70(5)	9492(2)	19(2)	1
C(14)	4916(7)	550(4)	9648(1)	19(2)	1
C(15)	5704(7)	1210(5)	9531(2)	19(2)	1
C(16)	5522(7)	1420(5)	9260(2)	16(2)	1
C(17)	6342(7)	2062(4)	9157(1)	22(2)	1
C(18)	7219(7)	2501(5)	9315(2)	26(2)	1
C(19)	7331(7)	2315(5)	9587(2)	25(2)	1
C(20)	6592(7)	1678(4)	9693(1)	19(2)	1
C(21)	2728(7)	-194(5)	7942(2)	27(2)	1
C(22)	2575(8)	-787(5)	7743(2)	35(2)	1
C(23)	1296(9)	-986(5)	7646(2)	35(2)	1
C(24)	186(8)	-581(5)	7747(2)	40(3)	1
C(25)	323(8)	15(5)	7943(1)	29(2)	1
C(26)	1569(8)	200(5)	8036(1)	33(2)	1
C(27)	5286(8)	785(5)	7776(2)	29(2)	1
C(28)	4855(8)	684(5)	7512(2)	44(3)	1
C(29)	5459(9)	1142(5)	7312(2)	46(3)	1
C(30)	6492(9)	1702(5)	7364(2)	47(3)	1
C(31)	6948(8)	1786(5)	7619(2)	52(3)	1
C(32)	6346(8)	1320(5)	7821(2)	35(2)	1
C(33)	5536(8)	-811(5)	8113(1)	22(2)	1
C(34)	6935(8)	-798(5)	8093(1)	30(2)	1
C(35)	7720(8)	-1482(5)	8149(1)	34(2)	1
C(36)	7116(8)	-2224(5)	8212(2)	38(2)	1
C(37)	5709(9)	-2264(5)	8224(1)	37(2)	1
C(38)	4951(8)	-1546(5)	8180(1)	32(2)	1
C(39)	1141(7)	-633(5)	9592(2)	21(2)	1
C(40)	239(8)	-1187(5)	9720(1)	31(2)	1

C(41)	-1130(8)	-1059(5)	9686(2)	40(3)	1
C(42)	-1629(8)	-399(5)	9543(2)	30(2)	1
C(43)	-744(8)	172(5)	9432(1)	29(2)	1
C(44)	624(8)	35(5)	9453(1)	24(2)	1
C(45)	3284(7)	-658(5)	10031(1)	18(2)	1
C(46)	4039(7)	-1177(5)	10185(2)	40(3)	1
C(47)	4142(8)	-1037(6)	10460(2)	45(3)	1
C(48)	3545(8)	-396(5)	10577(2)	34(2)	1
C(49)	2771(7)	141(5)	10438(2)	28(2)	1
C(50)	2614(7)	24(5)	10166(2)	31(2)	1
C(51)	3739(8)	-1848(5)	9579(1)	19(2)	1
C(52)	5082(8)	-1907(5)	9519(1)	37(2)	1
C(53)	5718(9)	-2715(6)	9503(2)	54(3)	1
C(54)	5005(9)	-3407(5)	9539(2)	42(3)	1
C(55)	3661(10)	-3340(6)	9598(2)	65(3)	1
C(56)	3044(8)	-2563(6)	9621(2)	50(3)	1
C(61)	763(10)	6449(6)	8931(2)	49(3)	1
C(62)	-541(9)	6489(5)	8819(2)	49(3)	1
C(63)	-1116(8)	7307(6)	8802(2)	42(3)	1
C(64)	-390(8)	7998(5)	8882(2)	25(2)	1
C(65)	870(9)	7916(5)	8995(2)	38(3)	1
C(66)	1514(9)	7138(6)	9026(2)	46(3)	1
C(67)	-1008(8)	8832(5)	8845(2)	22(2)	1
C(68)	-2506(6)	8919(4)	8903(1)	29(2)	1
N(1)	1417(9)	5611(5)	8955(2)	59(2)	1
N(2)	-255(6)	9425(4)	8759(1)	31(2)	1
O(5)	730(6)	4997(4)	8882(1)	72(2)	1
O(6)	2574(7)	5570(4)	9060(1)	81(2)	1
O(7)	-1548(5)	12736(3)	8622(1)	39(2)	1
C(69)	-589(8)	10282(5)	8714(1)	21(2)	1
C(70)	-1829(7)	10520(5)	8615(1)	27(2)	1
C(71)	-2105(7)	11360(5)	8580(1)	27(2)	1
C(72)	-1137(8)	11929(5)	8656(2)	24(2)	1
C(73)	128(7)	11692(5)	8743(1)	26(2)	1
C(74)	380(7)	10855(5)	8772(2)	28(2)	1
C(75)	-577(7)	13386(5)	8692(2)	54(3)	1
C(1A)	4195(8)	4255(5)	9672(2)	55(4)	0.822(9)
C(2A)	3052(6)	3630(4)	9645(1)	35(3)	0.822(9)
C(3A)	1773(7)	3884(3)	9563(1)	29(3)	0.822(9)
C(4A)	744(5)	3301(5)	9533(1)	30(3)	0.822(9)
C(5A)	994(6)	2465(4)	9585(2)	48(4)	0.822(9)
C(6A)	2272(8)	2212(3)	9668(1)	27(3)	0.822(9)
C(7A)	3301(5)	2795(5)	9698(1)	29(5)	0.822(9)
C(1B)	1240(40)	2138(19)	9591(11)	25(18)	0.178(9)
C(2B)	1980(30)	2964(16)	9611(8)	80(20)	0.178(9)
C(3B)	3330(30)	2990(18)	9688(8)	20(20)	0.178(9)
C(4B)	3940(30)	3750(20)	9747(8)	60(20)	0.178(9)
C(5B)	3190(40)	4480(18)	9730(8)	120(30)	0.178(9)
C(6B)	1840(40)	4454(16)	9653(8)	110(30)	0.178(9)
C(7B)	1230(30)	3696(19)	9594(8)	9(16)	0.178(9)

C(1C)	5854(10)	4796(8)	8883(2)	40(4)	0.756(8)
C(2C)	6222(8)	4745(5)	8586(1)	50(4)	0.756(8)
C(3C)	6611(9)	5443(4)	8441(2)	65(6)	0.756(8)
C(4C)	6977(8)	5363(5)	8175(2)	74(5)	0.756(8)
C(5C)	6956(9)	4586(6)	8054(1)	84(6)	0.756(8)
C(6C)	6567(9)	3888(4)	8199(2)	45(4)	0.756(8)
C(7C)	6201(7)	3967(4)	8465(2)	57(4)	0.756(8)
C(1D)	6990(40)	4300(20)	8158(6)	73(18)	0.244(8)
C(2D)	6440(30)	4686(14)	8413(5)	97(19)	0.244(8)
C(3D)	6220(30)	5538(13)	8430(5)	29(14)	0.244(8)
C(4D)	5890(20)	5897(14)	8673(6)	68(15)	0.244(8)
C(5D)	5790(30)	5400(20)	8900(4)	90(20)	0.244(8)
C(6D)	6020(40)	4550(20)	8883(5)	450(90)	0.244(8)
C(7D)	6350(40)	4193(14)	8640(6)	110(20)	0.244(8)
C(1E)	-157(9)	5868(6)	7814(2)	121(4)	1
C(2E)	672(5)	6282(4)	8030(1)	64(3)	1
C(3E)	1601(6)	5853(3)	8187(1)	66(3)	1
C(4E)	2417(5)	6283(4)	8365(1)	60(3)	1
C(5E)	2304(5)	7143(4)	8388(1)	44(3)	1
C(6E)	1376(6)	7572(3)	8231(1)	52(3)	1
C(7E)	560(5)	7142(4)	8053(1)	59(3)	1
C(1F)	60(15)	2395(10)	7980(4)	81(7)	0.582(10)
C(2F)	1225(10)	2816(7)	7836(2)	40(5)	0.582(10)
C(3F)	2131(12)	2361(5)	7682(2)	50(9)	0.582(10)
C(4F)	3214(11)	2760(8)	7559(2)	70(7)	0.582(10)
C(5F)	3390(10)	3612(8)	7591(2)	63(8)	0.582(10)
C(6F)	2483(13)	4067(5)	7744(2)	50(6)	0.582(10)
C(7F)	1401(11)	3669(6)	7867(2)	44(7)	0.582(10)
C(1G)	3720(20)	3300(16)	7561(6)	74(11)	0.418(10)
C(2G)	2376(14)	3162(10)	7702(3)	56(8)	0.418(10)
C(3G)	1733(17)	3806(8)	7837(4)	73(13)	0.418(10)
C(4G)	541(17)	3654(10)	7976(3)	88(10)	0.418(10)
C(5G)	-9(14)	2858(12)	7979(3)	85(12)	0.418(10)
C(6G)	633(18)	2214(9)	7845(4)	71(10)	0.418(10)
C(7G)	1826(17)	2365(9)	7706(3)	76(15)	0.418(10)
O(1A)	5426(6)	-3028(4)	8846(1)	100(2)	1

Table 3. Bond lengths [Å] and angles [°] for RIS06 (CCDC 287655).

P(1)-O(3)	1.463(5)
P(1)-O(4)	1.492(4)
P(1)-O(1)	1.628(5)
P(1)-O(2)	1.633(4)
Si(1)-C(3)	1.883(7)
Si(1)-C(21)	1.892(7)
Si(1)-C(33)	1.886(8)
Si(1)-C(27)	1.889(8)
Si(2)-C(45)	1.888(7)
Si(2)-C(13)	1.889(7)
Si(2)-C(51)	1.902(7)
Si(2)-C(39)	1.912(7)
O(1)-C(2)	1.403(8)
O(2)-C(12)	1.387(7)
C(1)-C(2)	1.344(8)
C(1)-C(6)	1.416(9)
C(1)-C(11)	1.524(9)
C(2)-C(3)	1.448(9)
C(3)-C(4)	1.361(9)
C(4)-C(5)	1.410(9)
C(5)-C(10)	1.393(9)
C(5)-C(6)	1.438(9)
C(6)-C(7)	1.404(9)
C(7)-C(8)	1.383(9)
C(8)-C(9)	1.415(8)
C(9)-C(10)	1.366(9)
C(11)-C(12)	1.352(9)
C(11)-C(16)	1.425(9)
C(12)-C(13)	1.420(9)
C(13)-C(14)	1.399(9)
C(14)-C(15)	1.440(9)
C(15)-C(20)	1.412(8)
C(15)-C(16)	1.414(8)
C(16)-C(17)	1.409(8)
C(17)-C(18)	1.369(8)
C(18)-C(19)	1.404(8)
C(19)-C(20)	1.364(9)
C(21)-C(26)	1.392(9)
C(21)-C(22)	1.387(9)
C(22)-C(23)	1.391(9)
C(23)-C(24)	1.373(9)
C(24)-C(25)	1.378(9)
C(25)-C(26)	1.350(9)
C(27)-C(32)	1.374(9)
C(27)-C(28)	1.399(9)
C(28)-C(29)	1.383(9)
C(29)-C(30)	1.385(10)
C(30)-C(31)	1.366(10)
C(31)-C(32)	1.391(9)
C(33)-C(38)	1.358(9)
C(33)-C(34)	1.386(9)
C(34)-C(35)	1.375(9)

C(35)-C(36)	1.369(9)
C(36)-C(37)	1.393(9)
C(37)-C(38)	1.392(9)
C(39)-C(44)	1.380(9)
C(39)-C(40)	1.413(9)
C(40)-C(41)	1.379(9)
C(41)-C(42)	1.370(9)
C(42)-C(43)	1.384(9)
C(43)-C(44)	1.373(8)
C(45)-C(46)	1.359(9)
C(45)-C(50)	1.449(9)
C(46)-C(47)	1.405(9)
C(47)-C(48)	1.324(9)
C(48)-C(49)	1.347(9)
C(49)-C(50)	1.387(8)
C(51)-C(52)	1.364(9)
C(51)-C(56)	1.355(10)
C(52)-C(53)	1.443(10)
C(53)-C(54)	1.330(10)
C(54)-C(55)	1.366(10)
C(55)-C(56)	1.394(10)
C(61)-C(62)	1.407(10)
C(61)-C(66)	1.416(10)
C(61)-N(1)	1.500(11)
C(62)-C(63)	1.435(10)
C(63)-C(64)	1.381(9)
C(64)-C(65)	1.374(9)
C(64)-C(67)	1.484(9)
C(65)-C(66)	1.410(10)
C(67)-N(2)	1.284(8)
C(67)-C(68)	1.515(8)
N(1)-O(5)	1.252(8)
N(1)-O(6)	1.260(8)
N(2)-C(69)	1.435(8)
O(7)-C(72)	1.369(8)
O(7)-C(75)	1.461(8)
C(69)-C(74)	1.359(9)
C(69)-C(70)	1.378(9)
C(70)-C(71)	1.387(9)
C(71)-C(72)	1.376(9)
C(72)-C(73)	1.379(9)
C(73)-C(74)	1.375(9)
C(1A)-C(2A)	1.517(7)
C(2A)-C(3A)	1.3900
C(2A)-C(7A)	1.3900
C(3A)-C(4A)	1.3900
C(4A)-C(5A)	1.3900
C(5A)-C(6A)	1.3900
C(6A)-C(7A)	1.3900
C(1B)-C(2B)	1.519(8)
C(2B)-C(3B)	1.3900
C(2B)-C(7B)	1.3900
C(3B)-C(4B)	1.3900
C(4B)-C(5B)	1.3900

C(5B)-C(6B)	1.3900
C(6B)-C(7B)	1.3900
C(1C)-C(2C)	1.536(7)
C(2C)-C(3C)	1.3900
C(2C)-C(7C)	1.3900
C(3C)-C(4C)	1.3900
C(4C)-C(5C)	1.3900
C(5C)-C(6C)	1.3900
C(6C)-C(7C)	1.3900
C(1D)-C(2D)	1.518(7)
C(2D)-C(3D)	1.3900
C(2D)-C(7D)	1.3900
C(3D)-C(4D)	1.3900
C(4D)-C(5D)	1.3900
C(5D)-C(6D)	1.3900
C(6D)-C(7D)	1.3900
C(1E)-C(2E)	1.514(6)
C(2E)-C(3E)	1.3900
C(2E)-C(7E)	1.3900
C(3E)-C(4E)	1.3900
C(4E)-C(5E)	1.3900
C(5E)-C(6E)	1.3900
C(6E)-C(7E)	1.3900
C(1F)-C(2F)	1.520(8)
C(2F)-C(3F)	1.3900
C(2F)-C(7F)	1.3900
C(3F)-C(4F)	1.3900
C(4F)-C(5F)	1.3900
C(5F)-C(6F)	1.3900
C(6F)-C(7F)	1.3900
C(1G)-C(2G)	1.527(8)
C(2G)-C(3G)	1.3900
C(2G)-C(7G)	1.3900
C(3G)-C(4G)	1.3900
C(4G)-C(5G)	1.3900
C(5G)-C(6G)	1.3900
C(6G)-C(7G)	1.3900
O(3)-P(1)-O(4)	121.9(3)
O(3)-P(1)-O(1)	106.8(3)
O(4)-P(1)-O(1)	110.2(3)
O(3)-P(1)-O(2)	111.2(3)
O(4)-P(1)-O(2)	102.8(3)
O(1)-P(1)-O(2)	102.2(2)
C(3)-Si(1)-C(21)	108.3(4)
C(3)-Si(1)-C(33)	114.9(3)
C(21)-Si(1)-C(33)	108.6(4)
C(3)-Si(1)-C(27)	105.8(3)
C(21)-Si(1)-C(27)	109.7(4)
C(33)-Si(1)-C(27)	109.4(3)
C(45)-Si(2)-C(13)	107.3(3)
C(45)-Si(2)-C(51)	104.7(3)
C(13)-Si(2)-C(51)	111.1(3)
C(45)-Si(2)-C(39)	107.0(3)

C(13)-Si(2)-C(39)	110.6(3)
C(51)-Si(2)-C(39)	115.5(4)
C(2)-O(1)-P(1)	117.3(4)
C(12)-O(2)-P(1)	123.2(4)
C(2)-C(1)-C(6)	118.9(7)
C(2)-C(1)-C(11)	120.7(7)
C(6)-C(1)-C(11)	120.4(7)
C(1)-C(2)-O(1)	119.3(7)
C(1)-C(2)-C(3)	124.8(7)
O(1)-C(2)-C(3)	115.5(7)
C(4)-C(3)-C(2)	114.1(7)
C(4)-C(3)-Si(1)	118.1(6)
C(2)-C(3)-Si(1)	127.6(6)
C(3)-C(4)-C(5)	124.7(7)
C(10)-C(5)-C(4)	121.1(8)
C(10)-C(5)-C(6)	120.8(7)
C(4)-C(5)-C(6)	118.1(7)
C(7)-C(6)-C(1)	125.0(8)
C(7)-C(6)-C(5)	116.4(7)
C(1)-C(6)-C(5)	118.6(7)
C(8)-C(7)-C(6)	122.2(7)
C(7)-C(8)-C(9)	119.8(8)
C(10)-C(9)-C(8)	119.7(8)
C(9)-C(10)-C(5)	121.0(7)
C(12)-C(11)-C(16)	121.1(7)
C(12)-C(11)-C(1)	120.6(7)
C(16)-C(11)-C(1)	118.3(7)
C(11)-C(12)-O(2)	120.4(7)
C(11)-C(12)-C(13)	122.8(7)
O(2)-C(12)-C(13)	116.6(7)
C(14)-C(13)-C(12)	117.3(7)
C(14)-C(13)-Si(2)	118.2(6)
C(12)-C(13)-Si(2)	124.5(6)
C(13)-C(14)-C(15)	120.6(7)
C(20)-C(15)-C(16)	120.3(7)
C(20)-C(15)-C(14)	119.5(7)
C(16)-C(15)-C(14)	120.1(7)
C(17)-C(16)-C(15)	117.0(7)
C(17)-C(16)-C(11)	125.3(7)
C(15)-C(16)-C(11)	117.7(7)
C(18)-C(17)-C(16)	122.0(7)
C(17)-C(18)-C(19)	120.2(7)
C(20)-C(19)-C(18)	119.6(7)
C(19)-C(20)-C(15)	120.7(7)
C(26)-C(21)-C(22)	117.8(7)
C(26)-C(21)-Si(1)	121.6(6)
C(22)-C(21)-Si(1)	120.2(6)
C(23)-C(22)-C(21)	120.6(7)
C(24)-C(23)-C(22)	119.2(8)
C(23)-C(24)-C(25)	121.0(8)
C(26)-C(25)-C(24)	119.2(7)
C(25)-C(26)-C(21)	122.2(7)
C(32)-C(27)-C(28)	117.3(8)
C(32)-C(27)-Si(1)	122.9(7)

C(28)-C(27)-Si(1)	119.6(7)
C(29)-C(28)-C(27)	119.7(8)
C(28)-C(29)-C(30)	121.8(8)
C(31)-C(30)-C(29)	119.0(9)
C(30)-C(31)-C(32)	119.2(9)
C(27)-C(32)-C(31)	123.0(8)
C(38)-C(33)-C(34)	117.2(8)
C(38)-C(33)-Si(1)	121.0(6)
C(34)-C(33)-Si(1)	121.8(7)
C(35)-C(34)-C(33)	122.3(8)
C(36)-C(35)-C(34)	119.8(8)
C(35)-C(36)-C(37)	119.0(8)
C(38)-C(37)-C(36)	119.5(8)
C(33)-C(38)-C(37)	122.0(8)
C(44)-C(39)-C(40)	119.1(7)
C(44)-C(39)-Si(2)	123.1(6)
C(40)-C(39)-Si(2)	117.4(6)
C(41)-C(40)-C(39)	117.9(8)
C(42)-C(41)-C(40)	122.2(8)
C(41)-C(42)-C(43)	119.6(8)
C(44)-C(43)-C(42)	119.1(8)
C(43)-C(44)-C(39)	121.8(7)
C(46)-C(45)-C(50)	116.7(7)
C(46)-C(45)-Si(2)	124.8(6)
C(50)-C(45)-Si(2)	118.5(6)
C(45)-C(46)-C(47)	120.0(8)
C(48)-C(47)-C(46)	121.9(8)
C(47)-C(48)-C(49)	121.5(8)
C(48)-C(49)-C(50)	119.1(8)
C(49)-C(50)-C(45)	120.8(7)
C(52)-C(51)-C(56)	117.9(8)
C(52)-C(51)-Si(2)	118.0(6)
C(56)-C(51)-Si(2)	123.1(7)
C(51)-C(52)-C(53)	119.9(8)
C(54)-C(53)-C(52)	120.9(8)
C(53)-C(54)-C(55)	118.6(9)
C(54)-C(55)-C(56)	120.9(9)
C(51)-C(56)-C(55)	121.7(8)
C(62)-C(61)-C(66)	125.4(9)
C(62)-C(61)-N(1)	117.9(9)
C(66)-C(61)-N(1)	116.7(9)
C(61)-C(62)-C(63)	115.3(8)
C(64)-C(63)-C(62)	120.9(8)
C(63)-C(64)-C(65)	120.9(8)
C(63)-C(64)-C(67)	118.4(8)
C(65)-C(64)-C(67)	120.7(8)
C(64)-C(65)-C(66)	122.7(8)
C(65)-C(66)-C(61)	114.7(8)
N(2)-C(67)-C(64)	118.2(7)
N(2)-C(67)-C(68)	124.2(7)
C(64)-C(67)-C(68)	117.5(7)
O(5)-N(1)-O(6)	125.0(9)
O(5)-N(1)-C(61)	116.7(8)
O(6)-N(1)-C(61)	118.2(9)

C(67)-N(2)-C(69)	129.2(7)
C(72)-O(7)-C(75)	116.8(6)
C(74)-C(69)-C(70)	121.1(7)
C(74)-C(69)-N(2)	117.1(8)
C(70)-C(69)-N(2)	121.8(8)
C(69)-C(70)-C(71)	119.3(7)
C(72)-C(71)-C(70)	118.4(7)
C(73)-C(72)-O(7)	124.8(8)
C(73)-C(72)-C(71)	122.3(8)
O(7)-C(72)-C(71)	112.9(7)
C(72)-C(73)-C(74)	117.9(8)
C(69)-C(74)-C(73)	120.8(8)
C(3A)-C(2A)-C(7A)	120.0
C(3A)-C(2A)-C(1A)	120.7(6)
C(7A)-C(2A)-C(1A)	119.3(6)
C(4A)-C(3A)-C(2A)	120.0
C(5A)-C(4A)-C(3A)	120.0
C(6A)-C(5A)-C(4A)	120.0
C(7A)-C(6A)-C(5A)	120.0
C(6A)-C(7A)-C(2A)	120.0
C(3B)-C(2B)-C(7B)	120.00(6)
C(3B)-C(2B)-C(1B)	120.5(10)
C(7B)-C(2B)-C(1B)	118.7(10)
C(2B)-C(3B)-C(4B)	120.0
C(5B)-C(4B)-C(3B)	120.00(6)
C(4B)-C(5B)-C(6B)	120.00(7)
C(7B)-C(6B)-C(5B)	120.0
C(6B)-C(7B)-C(2B)	120.0
C(3C)-C(2C)-C(7C)	120.0
C(3C)-C(2C)-C(1C)	122.0(6)
C(7C)-C(2C)-C(1C)	118.0(6)
C(4C)-C(3C)-C(2C)	120.0
C(5C)-C(4C)-C(3C)	120.0
C(4C)-C(5C)-C(6C)	120.0
C(7C)-C(6C)-C(5C)	120.0
C(6C)-C(7C)-C(2C)	120.0
C(3D)-C(2D)-C(7D)	120.0
C(3D)-C(2D)-C(1D)	120.4(6)
C(7D)-C(2D)-C(1D)	119.1(6)
C(2D)-C(3D)-C(4D)	120.0
C(5D)-C(4D)-C(3D)	120.0
C(6D)-C(5D)-C(4D)	120.0
C(5D)-C(6D)-C(7D)	120.0
C(6D)-C(7D)-C(2D)	120.0
C(3E)-C(2E)-C(7E)	120.0
C(3E)-C(2E)-C(1E)	122.9(5)
C(7E)-C(2E)-C(1E)	116.8(5)
C(2E)-C(3E)-C(4E)	120.0
C(5E)-C(4E)-C(3E)	120.0
C(4E)-C(5E)-C(6E)	120.0
C(7E)-C(6E)-C(5E)	120.0
C(6E)-C(7E)-C(2E)	120.0
C(3F)-C(2F)-C(7F)	120.0
C(3F)-C(2F)-C(1F)	121.3(8)

C(7F)-C(2F)-C(1F)	118.7(8)
C(2F)-C(3F)-C(4F)	120.0
C(5F)-C(4F)-C(3F)	120.0
C(4F)-C(5F)-C(6F)	120.0
C(5F)-C(6F)-C(7F)	120.0
C(6F)-C(7F)-C(2F)	120.0
C(3G)-C(2G)-C(7G)	120.0
C(3G)-C(2G)-C(1G)	121.1(9)
C(7G)-C(2G)-C(1G)	118.8(9)
C(4G)-C(3G)-C(2G)	120.0
C(3G)-C(4G)-C(5G)	120.0
C(6G)-C(5G)-C(4G)	120.0
C(5G)-C(6G)-C(7G)	120.0
C(6G)-C(7G)-C(2G)	120.0

Table 4. Anisotropic displacement parameters ($\text{\AA}^2 \times 10^4$) for RIS06 (CCDC 287655). The anisotropic displacement factor exponent takes the form: $-2\pi^2 [h^2 a^{*2} U^{11} + \dots + 2 h k a^* b^* U^{12}]$

	U^{11}	U^{22}	U^{33}	U^{23}	U^{13}	U^{12}
P(1)	227(13)	208(15)	214(15)	16(13)	37(13)	-35(13)
Si(1)	285(15)	270(16)	215(15)	21(14)	8(13)	-27(13)
Si(2)	244(14)	220(15)	212(15)	33(13)	-14(12)	17(13)
O(1)	160(30)	190(30)	130(30)	10(30)	40(20)	10(30)
O(2)	150(30)	190(30)	160(30)	0(30)	40(30)	-40(30)
O(3)	230(30)	170(30)	220(30)	0(30)	40(30)	-60(30)
O(4)	210(30)	260(30)	140(30)	-10(30)	50(30)	-50(30)
C(1)	80(40)	130(50)	190(50)	-110(50)	20(40)	-10(40)
C(2)	150(40)	160(50)	320(60)	180(50)	-20(40)	-30(40)
C(3)	140(40)	170(50)	200(50)	-50(40)	-30(40)	60(40)
C(4)	260(50)	350(50)	160(50)	80(50)	-60(40)	-60(40)
C(5)	240(50)	160(50)	260(50)	10(50)	-70(40)	-20(40)
C(6)	300(50)	170(50)	150(50)	-10(50)	-40(40)	20(40)
C(7)	240(50)	310(50)	220(50)	130(50)	-50(40)	0(40)
C(8)	390(50)	260(50)	370(60)	0(50)	110(40)	-50(40)
C(9)	480(50)	240(50)	350(60)	190(50)	-110(50)	-60(40)
C(10)	360(50)	190(50)	240(50)	70(50)	70(40)	-40(40)
C(11)	190(50)	150(50)	50(50)	40(40)	50(40)	130(40)
C(12)	90(40)	190(40)	120(40)	20(30)	-50(30)	10(30)
C(13)	110(50)	190(50)	260(50)	30(40)	40(40)	-20(40)
C(14)	140(40)	290(50)	130(50)	100(40)	30(40)	40(40)
C(15)	90(40)	240(50)	240(50)	-50(40)	0(40)	-20(40)
C(16)	140(50)	240(50)	90(50)	40(40)	-20(40)	10(40)
C(17)	280(50)	210(50)	150(50)	-50(40)	-40(40)	-20(40)
C(18)	270(50)	330(50)	180(50)	0(40)	0(40)	-70(40)
C(19)	300(50)	250(50)	210(50)	-80(40)	-40(40)	10(40)
C(20)	190(50)	190(50)	200(50)	30(40)	-50(40)	40(40)
C(21)	190(50)	390(50)	230(50)	-80(50)	-40(40)	-140(40)
C(22)	370(60)	480(60)	200(50)	-20(50)	40(40)	-20(50)
C(23)	450(60)	350(60)	240(50)	-50(40)	-70(50)	-150(50)
C(24)	320(50)	550(60)	340(60)	-100(50)	-170(50)	-60(50)
C(25)	230(50)	430(60)	230(50)	-50(50)	20(40)	70(50)
C(26)	390(50)	390(50)	200(50)	-180(40)	-10(50)	-50(50)
C(27)	330(50)	280(50)	250(50)	-90(50)	60(40)	0(50)
C(28)	510(60)	460(60)	370(60)	30(50)	0(50)	-140(50)
C(29)	610(60)	500(60)	290(50)	40(50)	80(50)	-80(50)
C(30)	560(60)	440(60)	420(60)	70(50)	140(50)	-60(50)
C(31)	400(60)	610(60)	560(60)	70(60)	10(50)	-80(50)
C(32)	360(50)	410(60)	270(50)	50(50)	-10(50)	-20(50)
C(33)	240(50)	230(50)	190(50)	10(40)	-30(40)	-10(40)
C(34)	400(50)	350(50)	150(50)	80(40)	50(40)	-10(50)
C(35)	290(50)	300(50)	420(60)	-50(50)	50(40)	40(50)
C(36)	390(60)	320(60)	440(60)	0(50)	-10(50)	120(50)
C(37)	440(60)	290(60)	370(50)	-90(50)	100(50)	-70(50)
C(38)	370(50)	320(50)	280(50)	-100(50)	40(40)	40(50)
C(39)	120(40)	260(50)	260(50)	-110(40)	-40(40)	-60(40)
C(40)	300(50)	280(50)	360(50)	70(50)	20(50)	50(40)

C(41)	380(60)	330(60)	490(60)	-70(50)	20(50)	-70(40)
C(42)	190(50)	300(50)	420(50)	40(40)	0(40)	30(40)
C(43)	210(50)	370(50)	280(50)	80(50)	20(40)	40(50)
C(44)	300(50)	200(50)	210(50)	60(40)	-30(40)	50(40)
C(45)	190(50)	200(50)	170(50)	-40(40)	50(40)	-60(40)
C(46)	410(50)	460(60)	330(60)	0(50)	-90(50)	80(40)
C(47)	520(60)	510(60)	330(60)	140(50)	-150(50)	100(50)
C(48)	370(50)	430(60)	210(50)	-90(50)	10(50)	-100(50)
C(49)	330(50)	300(50)	220(50)	-60(50)	-10(40)	0(40)
C(50)	280(50)	340(50)	300(50)	20(50)	-10(40)	-110(40)
C(51)	250(50)	210(50)	110(50)	60(40)	0(40)	70(40)
C(52)	370(60)	290(50)	460(60)	70(50)	110(50)	10(50)
C(53)	460(60)	640(60)	510(60)	-30(60)	140(50)	230(60)
C(54)	580(60)	210(50)	470(60)	80(50)	70(50)	90(50)
C(55)	780(70)	230(60)	950(70)	10(50)	50(60)	-40(50)
C(56)	310(50)	390(60)	790(60)	20(50)	170(50)	70(50)
C(61)	570(60)	460(60)	450(60)	220(50)	60(50)	80(60)
C(62)	490(60)	480(60)	510(60)	70(50)	-90(50)	-30(50)
C(63)	380(50)	500(60)	380(50)	120(50)	-50(50)	110(50)
C(64)	240(50)	240(50)	260(50)	-30(40)	-90(40)	-100(50)
C(65)	480(60)	300(60)	360(50)	80(50)	180(50)	-20(50)
C(66)	480(60)	420(60)	480(60)	10(50)	70(50)	-80(50)
C(67)	320(50)	150(50)	190(50)	-50(40)	-80(40)	50(40)
C(68)	140(50)	400(50)	340(50)	30(40)	80(40)	50(40)
N(1)	640(50)	460(60)	670(60)	-40(50)	180(50)	80(50)
N(2)	230(40)	290(50)	400(50)	40(40)	10(40)	-30(40)
O(5)	810(50)	480(50)	860(50)	-70(40)	40(40)	-30(40)
O(6)	770(50)	780(50)	870(50)	0(40)	-240(40)	130(40)
O(7)	340(30)	280(40)	560(40)	10(30)	-70(30)	-150(30)
C(69)	300(50)	200(50)	140(50)	60(40)	30(40)	40(50)
C(70)	180(50)	350(60)	280(50)	60(40)	10(40)	-30(40)
C(71)	260(50)	290(50)	250(50)	10(50)	-40(40)	-40(50)
C(72)	270(50)	120(50)	330(50)	-50(40)	60(40)	0(40)
C(73)	210(50)	290(50)	290(50)	40(40)	-60(40)	50(40)
C(74)	220(50)	240(50)	390(50)	40(50)	-50(40)	-80(50)
C(75)	570(60)	320(50)	730(60)	20(50)	-70(50)	140(50)
C(1A)	610(70)	280(60)	760(80)	40(60)	-170(60)	-120(60)
C(2A)	450(70)	480(70)	130(60)	-100(60)	100(50)	-130(60)
C(3A)	260(60)	430(70)	170(60)	80(50)	0(60)	210(60)
C(4A)	300(60)	210(60)	390(60)	-10(60)	10(50)	-50(60)
C(5A)	390(70)	470(80)	590(80)	-100(70)	-20(60)	-90(70)
C(6A)	340(60)	260(60)	210(60)	-60(50)	80(50)	90(50)
C(7A)	290(80)	260(70)	310(80)	-70(50)	110(50)	170(50)
C(1C)	310(60)	450(80)	430(70)	-120(60)	-160(50)	30(50)
C(2C)	170(60)	560(80)	760(80)	-120(70)	10(60)	180(60)
C(3C)	720(90)	540(90)	700(90)	230(70)	90(70)	10(70)
C(4C)	970(80)	530(80)	730(90)	-10(70)	0(70)	-40(70)
C(5C)	1140(90)	690(90)	690(80)	-100(80)	60(70)	150(70)
C(6C)	450(70)	450(80)	450(80)	-180(60)	110(60)	-80(60)
C(7C)	390(70)	490(80)	820(80)	-80(70)	-40(70)	-10(60)

C(1E)	1280(80)	1210(80)	1130(70)	-480(70)	-520(70)	-60(70)
C(2E)	640(60)	610(60)	660(60)	-150(60)	-40(60)	-40(60)
C(3E)	720(60)	700(60)	550(60)	110(60)	-200(50)	-90(60)
C(4E)	740(60)	540(60)	500(60)	40(50)	-140(50)	-20(50)
C(5E)	460(60)	520(60)	340(60)	-20(50)	110(50)	-50(50)
C(6E)	390(50)	590(60)	560(60)	-240(50)	180(50)	-10(50)
C(7E)	550(60)	610(60)	620(60)	-80(60)	110(50)	40(60)
C(1F)	780(100)	830(100)	800(110)	-40(90)	-160(80)	120(80)
C(2F)	440(90)	430(90)	330(80)	90(70)	-80(70)	30(70)
C(3F)	510(100)	540(120)	450(110)	-10(80)	-240(80)	120(80)
C(4F)	710(100)	770(100)	630(100)	60(80)	-10(80)	70(80)
C(5F)	580(110)	770(110)	550(100)	160(80)	-210(80)	-50(80)
C(6F)	600(90)	500(90)	410(90)	140(70)	-130(70)	150(80)
C(7F)	490(100)	440(100)	400(100)	-50(80)	-210(80)	30(80)
C(1G)	760(140)	810(140)	670(140)	50(90)	-60(90)	0(100)
C(2G)	490(110)	720(120)	480(110)	70(90)	-90(90)	80(90)
C(3G)	780(150)	780(150)	630(150)	60(90)	-50(90)	130(90)
C(4G)	810(130)	910(130)	930(130)	-10(90)	-90(90)	-150(90)
C(5G)	870(140)	810(140)	870(140)	110(100)	-150(90)	30(90)
C(6G)	720(130)	670(130)	750(130)	90(90)	40(90)	-40(90)
C(7G)	780(170)	790(170)	710(170)	0(90)	-70(90)	280(90)
O(1A)	1170(50)	920(50)	910(50)	30(40)	90(40)	140(40)

Table 5. Hydrogen bonds for RIS06 (CCDC 287655) [\AA and $^\circ$].

D-H...A	d(D-H)	d(H...A)	d(D...A)	<(DHA)
N(2)-H(2A)...O(4)#1	0.88	1.81	2.674(7)	168.7

Symmetry transformations used to generate equivalent atoms:
 #1 x,y+1,z

Chapter 3

Kinetic and Mechanistic Studies of the Brønsted Acid Catalyzed Enantioselective Reductive Amination

I. Limitations in the Ketone Reductive Amination

Having demonstrated a wide substrate scope with regards to the ketone coupling partner in the asymmetric organocatalytic reductive amination of ketones (eq. 1), we turned our attention toward examining the scope of the amine component. While variously substituted aromatic amines provide the reductive amination products in good overall yield and enantioselectivity (Ch. 2, Tables 9-10), when this methodology was extended to benzyl and alkyl amines, a dramatic drop-off in the level of reactivity and selectivity was observed (Table 1). Intrigued by these observations, studies were undertaken to probe the mechanistic and kinetic details of this reaction with the aim of rationalizing these results and allowing us to broaden the scope of this transformation with respect to the amine component.

Upon examination of Table 1, the clear relationship between reactivity and pK_a is made apparent. Thus, it was hypothesized that the lack of reactivity of alkyl and benzyl amines resulted from their higher levels of basicity (pK_a = 9.34-9.82). This trend can be rationalized by examination of the catalytic cycle given in Figure 1.

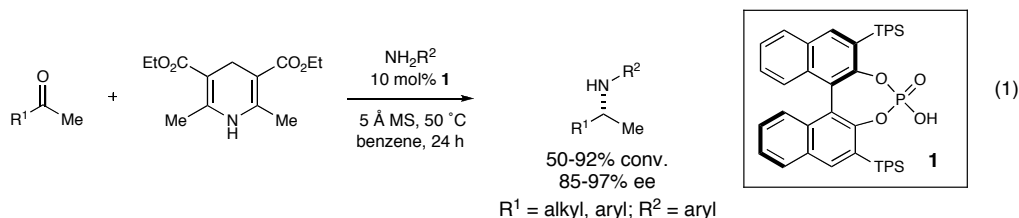
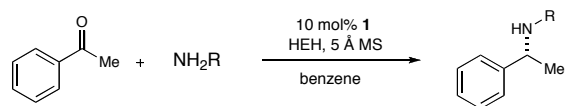
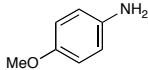
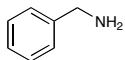
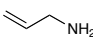
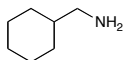
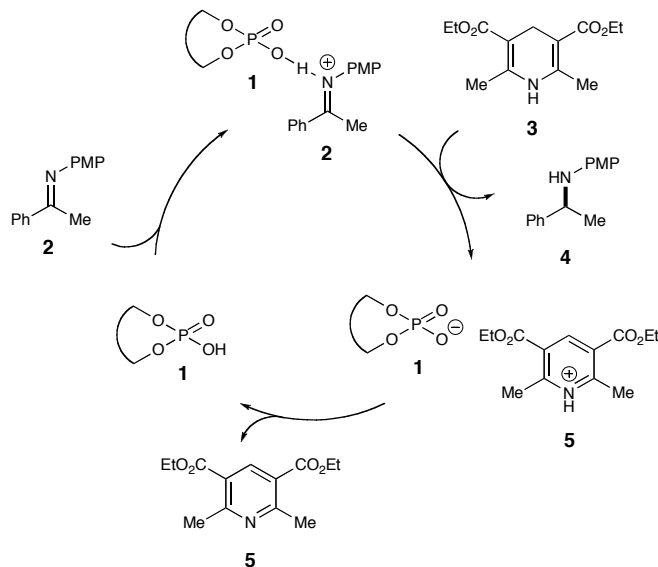


Table 1: Reductive amination with benzyl and alkyl amines


amine	pKa	temp (°C)	time (h)	% conv. ^a	% ee ^b
	4.6	50	24	97	94
	9.34	50 80	72 72	36 84	nd nd
	9.69	80	72	0	na
	9.82	80	72	0	na

^aConversion determined by GLC analysis. ^bEnantiomeric excess determined by chiral GLC analysis (Varian CP-chirasil-dex-CB).

Following condensation of the amine and ketone starting materials, the imine intermediate **2** is activated by catalyst **1** through either a hydrogen bonding or protonation event. Coordination of the catalyst to the imine nitrogen sufficiently lowers the LUMO of the carbonyl π system to allow it to undergo hydride delivery from the Hantzsch ester **3** to furnish the desired product **4**. Proton transfer from Hantzsch ester pyridinium

Figure 1. Proposed catalytic cycle for imine formation and subsequent reduction

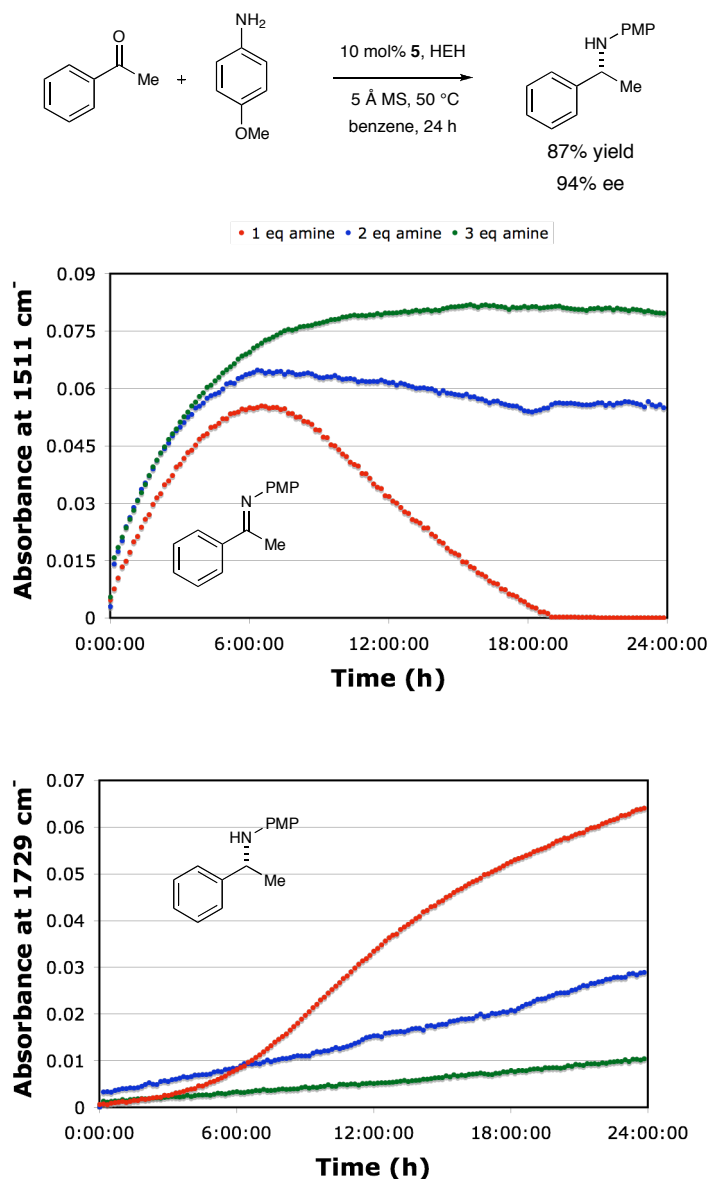
by-product **5** regenerates the phosphoric acid catalyst and turns over the catalytic cycle. If this proton is sequestered at any point in this catalytic cycle, it could result in the lower observed levels of reactivity seen with alkyl and benzyl amines. In order to test the validity of this theory, a series of inhibition studies were undertaken to determine if the proton could be removed from the catalytic cycle by any of the reaction components.

II. Inhibition Studies

The first set of experiments undertaken revealed that the amine starting material is most likely culprit shutting down the catalytic cycle via proton sequestration. As seen in Figure 2, for the reductive amination of *p*-anisidine with acetophenone, increasing the equivalents of amine starting material leads, as expected, to increased rates of imine formation. Conversely, this same increase has the opposite effect on the rate of reduction, slowing it down significantly in the case of two equivalents (40% conv, 24h) and stopping it almost completely with three equivalents (9% conv, 24h). As the imine concentration in this case is relatively high, this inhibition of the reduction pathway must be due to buffering of the proton required for LUMO activation by the excess amine starting material. These observations account for the lower reactivity of more basic amines in the reductive amination as their higher pKa's indicate that they are better able to buffer out the acid catalyst and shut down the catalytic cycle.

Due to the fact that they contain basic functionality that could inhibit the imine reduction step, the effect of both the Hantzsch ester pyridine and the secondary amine product on reaction efficiency was also examined. Although the Hantzsch ester pyridine

Figure 2: The effect of varying amounts of amine on imine and product formation



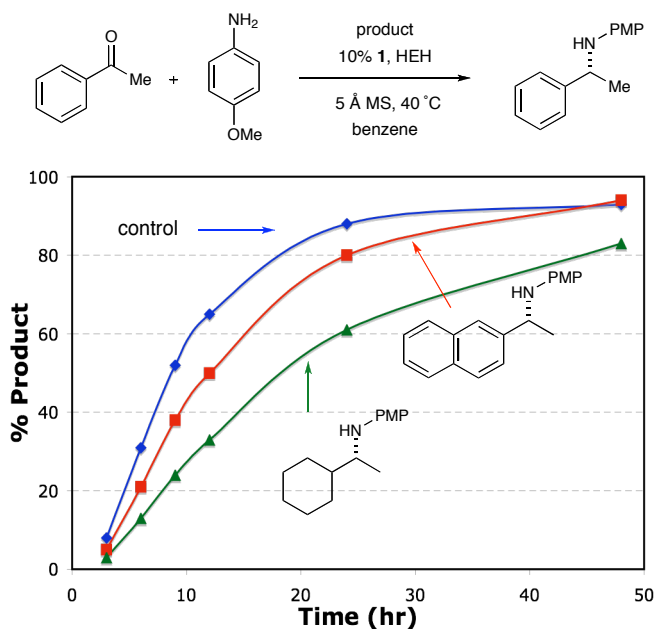
was shown to exert a minimal influence on the rate of product formation (Table 2), the secondary amine product proved to have a significant effect on reaction rate that is dependent upon the substitution pattern about the carbon undergoing reduction (Figure 3). When compared to a control reaction, addition of a naphthyl substituted amine product resulted in a slight retardation of reaction rate, however this effect is nearly negligible as the two reactions achieve comparable levels of conversion after 48 hours.

Table 2: Effect of Hantzsch ester pyridine on reaction efficiency

entry	eq pyridine	time (h)	% conv. ^a	% ee ^b
1	0	48	95	94
2	1	48	88	93
3	2	48	75	91

^a Conversion determined by GLC analysis. ^b Enantiomeric excess determined by chiral GLC analysis.

Contrasting this result is the observation that addition of a cyclohexyl substituted secondary amine has a significant effect on reaction rate, inhibiting the reaction to a greater degree than is seen with the naphthyl amine product (60% conversion, 24 h). This suggests that product inhibition is one possible explanation for the lower levels of conversion that are seen for the reductive amination of alkyl ketones as compared with aromatic ketones.

Figure 3: Product inhibition study

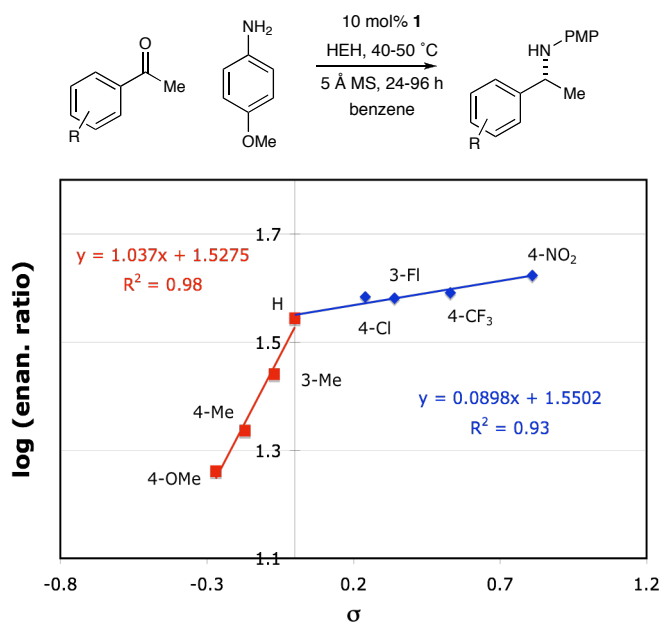
^a Conversion determined by GLC analysis.

III. Hammett Study

As these studies indicate the sensitive interplay between the phosphoric acid catalyst and other reaction components, we were led to consider the effect of the electronic nature of the reactive iminium intermediate and hoped an examination of enantioselectivity trends would lend insight into what is taking place. Toward this end, the reductive amination of *p*-anisidine with a wide range of variously substituted aromatic ketones was performed, and the results were used to construct a Hammett plot. Interestingly, this plot of σ values versus the enantiomeric ratios of the secondary amine products gives a pair of lines with a distinct break at zero, suggesting either a change in mechanism of the stereochemistry-determining step or the appearance of a competing mechanistic pathway (Figure 4).

As all substrates exhibited high levels of enantioselectivity, it was postulated that this break does not indicate a change in mechanism, but rather appearance of a competing

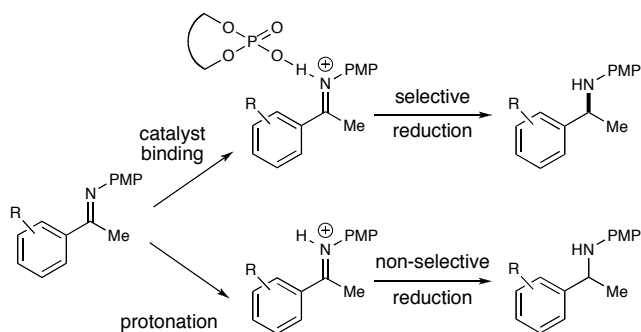
Figure 4: Hammett plot of substituent effects on the reductive amination



^a Enantiomeric excess determined by chiral GLC and SFC analysis.

non-selective pathway for imine reduction. One likely possibility is that this second pathway is non-catalyst associated protonation and subsequent reduction of the imine resulting in an erosion of product enantiopurity (Figure 5). This is in accord with the observation that ketones with electron donating substituents generally give lower levels of selectivity, as there is greater electron density on the imine nitrogen they are more likely to participate in the non-selective protonation pathway. Conversely, ketones with electron-withdrawing substituents undergo reaction with consistently high levels of selectivity, suggesting that they undergo reaction via a selective pathway only, i.e., through association with the catalyst. Combined with the earlier studies on the effect of basic reaction components, these results imply that the catalyst operates through hydrogen-bonding activation as opposed to pure acid catalysis.

Figure 5: Competing mechanistic pathways for the reductive amination

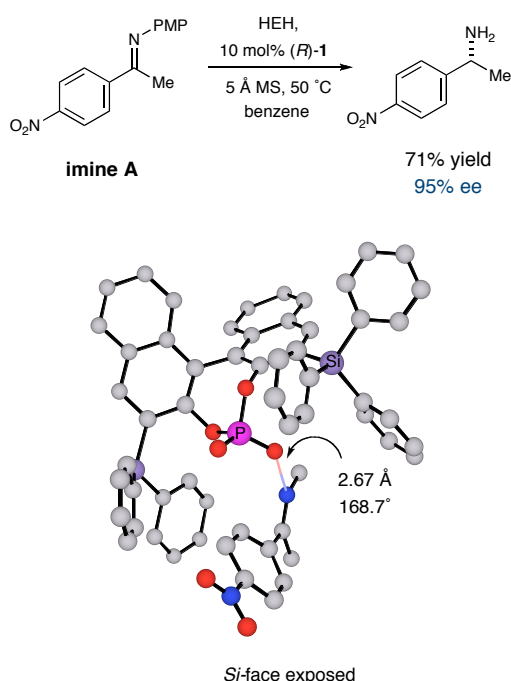


IV. Crystal Structure

Additional evidence for hydrogen bond activation is seen in a crystal structure obtained for the imine bound catalyst complex, showing an O-H-N bond length of 2.67 Å

and bond angle of 168.7° , both of which fall within known values¹ for hydrogen bonding interactions (Figure 6).² Attempts to obtain ^1H NMR evidence of hydrogen bonding were also made, however, no measurable difference in chemical shift was observed when the imine and catalyst were combined in a one-to-one ratio, and the only change observed over time was decomposition of the imine to its ketone and amine starting materials.

Figure 6: Crystal structure of imine bound catalyst



V. Role of Drying Agent

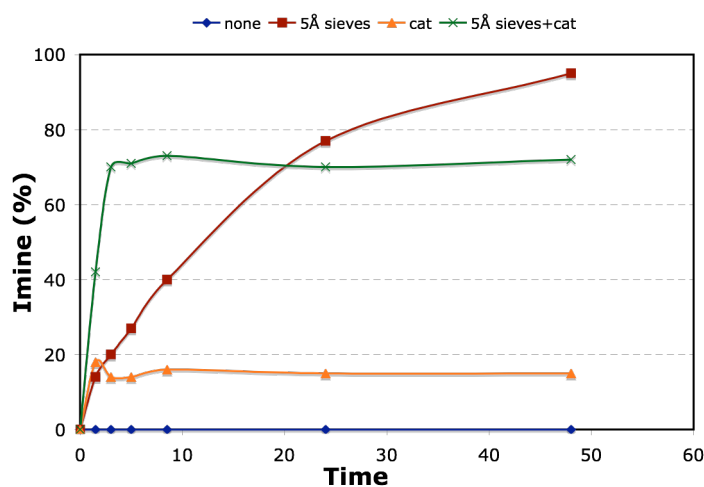
Having gained valuable insight into the role of the phosphoric acid catalyst in the reduction step of the reductive amination, we next turned our attention to the imine

¹ *Modern Physical Organic Chemistry*; Anslyn, R. A.; Dougherty, D. A.; University Science Books: Sausalito, 2006.

² The crystallographic data has been deposited at the CCDC, 12 Union Road, Cambridge, CB2 1EZ, UK and copies can be obtained on request, free of charge, by quoting the publication citation and the deposition number.

formation step of the process and specifically why the 5 Å molecular sieves were more effective than other drying agents examined. Given the evidence that 5 Å MS are required for the one pot reaction but not reduction of the pre-formed imine, it was speculated that their key role is mediating the rate of imine formation. Imine formation is an equilibrium process therefore in the absence of drying agent, the water generated is able to hydrolyze the imine back to starting materials, resulting in low concentration of imine substrate for organocatalyzed reduction. However, if a drying agent is present to remove the water the equilibrium is driven towards imine formation, increasing the concentration of reduction substrate and increasing the overall rate of reductive amination. In order to probe how large of an impact the sieves have, the rate of imine formation in the presence and absence of 5 Å molecular sieves and catalyst was monitored by ^1H NMR (Figure 7).

Figure 7: Influence of 5 Å MS and catalyst on rate of imine formation



The results of these experiments are quite intriguing. In the absence of both 5 Å MS and catalyst, no imine formation is observed, even after 48 hours at 40 °C, implying

that the equilibrium lies completely on the side of starting materials. In the presence of sieves only, imine formation occurs steadily over time, reaching 95% after 48 hours, showing that by simply removing water from the system the equilibrium can be shifted completely to the side of product. In the presence of catalyst only, imine is formed rapidly but reaches an equilibrium position of 15% that remains constant over 48 hours. Most interestingly, combining catalyst and sieves results in rapid imine formation (70%, 1.5 h) that also remains constant over time but never approaches the near quantitative levels that are seen when only sieves are used. One possible explanation for this behavior is that the larger pore size of the 5 Å sieves are unable to completely sequester all of the water present and, given that acids catalyze imine hydrolysis, the reaction reaches an equilibrium position where a certain amount of imine is continually undergoing hydrolysis.

Presuming that driving imine formation is the primary role of the molecular sieves in the one pot reaction, we were curious as to the reasons behind the 5 Å MS superior performance relative to other drying agents. Once again, the rate of imine formation from acetophenone and *p*-anisidine heated in benzene was monitored by ¹HNMR and taken as a measure of the drying agents' effectiveness. As seen in Table 3, the 5 Å MS

Table 3: Influence of 5Å MS and catalyst on rate of imine formation

entry	additive	time (hr)	% conv. ^a
1	5 Å MS	4	97
2	4 Å MS	4	66
3	3 Å MS	4	65
4	MgSO ₄	4	28
5	Na ₂ SO ₄	4	20

^a Conversion determined by GLC analysis.

perform the best, giving 97% imine after only four hours (entry 1). The 4 Å MS and 3 Å MS lead to less rapid formation of imine, 66% after four hours and 65% after four hours respectively (entries 2, 3). However, the salt based drying agents MgSO_4 and Na_2SO_4 perform quite poorly, even after 24 hours imine formation is well below 50% (entries 4, 5).

In order to explain why the 5 Å sieves resulted in faster rates of imine formation, it was put forth that this rate increase was perhaps due to their greater efficiency at removing water as compared to other sieve varieties. To verify this experimentally, a Karl-Fisher apparatus was used to measure the rate of water removal from benzene by 3, 4 and 5 Å MS powders (Table 4). A stock solution of 0.025 M water in benzene was prepared, the drying agent added and an aliquot removed and titrated with the Karl-Fisher apparatus to give a value of water content in parts per million (ppm). After an initial value of approximately 625 ppm, the 5 Å MS were shown to dry the fastest, effectively removing all the water after two minutes. The 3 Å sieves dried the solution after three minutes while the 4 Å sieves required ten minutes. The ability of the 5 Å sieves to more rapidly remove water from the system explains their superior performance in the reductive amination in that because they are able to generate a higher concentration of imine during the course of the reaction, the rate determining reduction

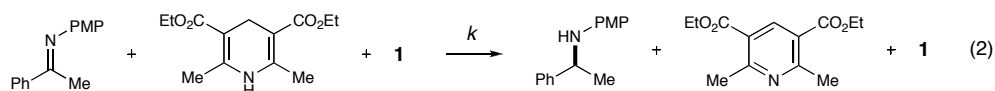
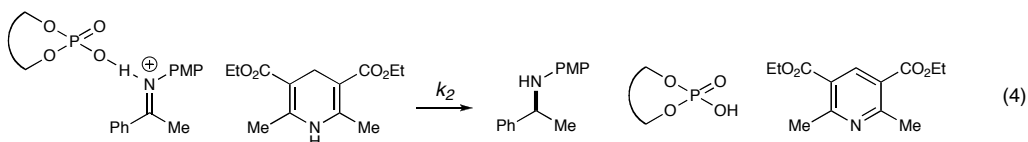
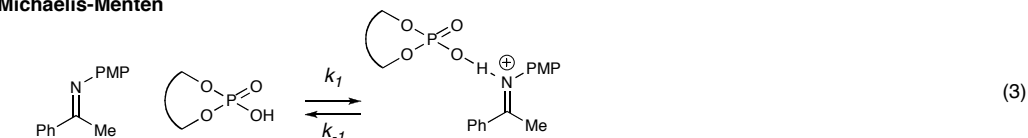
Table 4. Efficiency of water removal by molecular sieves

entry	sieves	H ₂ O content (ppm)			
		0 min	2 min	3 min	10 min
1	3 Å	701	15.1	-2.61	nd
2	4 Å	596	51.4	15.6	-2.35
3	5 Å	625	-3.52	1.21	nd

step is able to proceed at closer to its maximum rate. Though the 3 Å sieves might be better at sequestering water from the system, i.e., once a water molecule is adsorbed it is less likely to diffuse out of the zeolite due to its small pore size, the larger pore size of the 5 Å sieves results in more rapid kinetic adsorption of water. As imine reduction is an irreversible process, it provides a funnel through which the imine intermediate is removed and prevents the system from reaching equilibrium levels of imine hydrolysis, thereby negating the thermodynamic advantage of using 3 Å sieves.

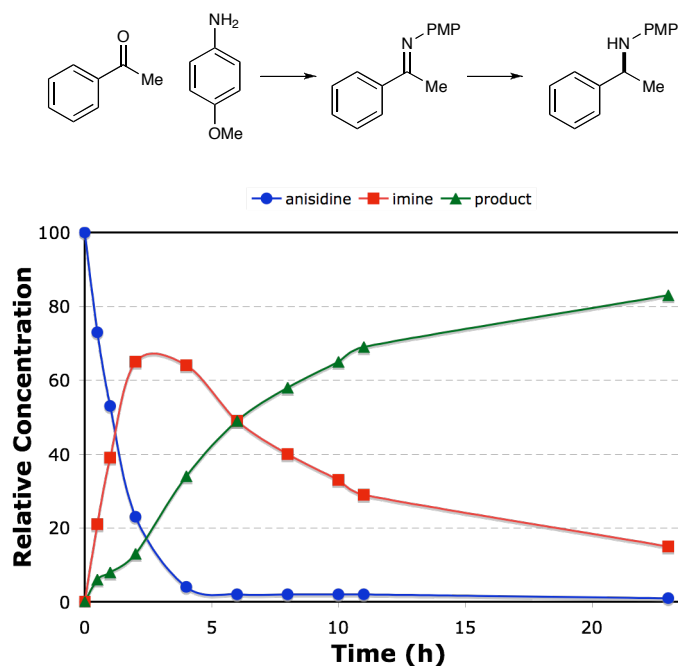
VI. Reaction Kinetics

Following completion of the previously described mechanistic studies, we decided to explore the fundamental steps of the reductive amination by examining the reaction kinetics. The first study performed was a gas chromatographic (GC) analysis of the reaction profile to measure the amounts of *p*-anisidine, imine and product present over time relative to an internal standard (Figure 8). As expected, the reaction profile demonstrates that there are two distinct steps occurring in the reductive amination, the first being condensation of the amine and ketone to furnish the imine intermediate followed by a second reduction step to provide the secondary amine product. The data in Figure 8 shows that imine formation occurs primarily within the first two hours and reaches a maximum concentration of 65%. Imine concentration remains at approximately this level for an additional two hours and decays gradually thereafter. Initial product formation is slow ($t = 0\text{-}2$ hr) but increases rapidly over a period

Concerted Ternary**Michaelis-Menten**

corresponding to when imine concentration is at a maximum (2-4 hr). Interestingly, the concentration of *p*-anisidine decreases dramatically and approaches zero after only four hours. This drop coincides with the time of greatest increase in the rate of product formation (from 13% to 34% over 2 hr). This overlap between the jump in product formation and disappearance of amine agrees with the hypothesis that the amine starting material inhibits the reduction step via deprotonation of the acid catalyst; only after nearly all of the *p*-anisidine has been converted to imine is the catalyst able to initiate the reduction cycle. Since imine formation is known to be rapid and reversible, we decided to focus our kinetic studies on the reduction step. We postulated that this reduction step could occur by two possible mechanisms, either a concerted ternary process or a steady-state intermediate process.

In the concerted ternary process imine, catalyst and Hantzsch ester would come together in a single fundamental step to irreversibly generate the product at a rate dependent on a single rate constant *k* (eq. 2). The second possibility is a Michaelis-

Figure 8: Reaction profile

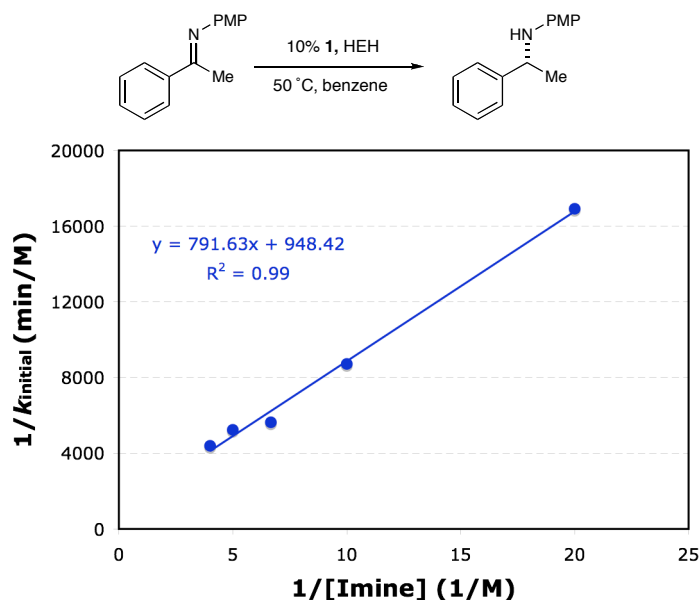
Menten situation where the first step is reversible formation of a steady-state amount of an activated imine-catalyst complex that then undergoes a second irreversible reduction step to furnish the product (eq. 3, 4). Examination of reactant order would differentiate between these mechanistic scenarios as a ternary process will display first order kinetics for all three reagents, while the steady-state process will exhibit saturation behavior with regards to imine concentration.

The rate of imine reduction was measured by gas chromatography over a range of imine concentrations (0.05 M – 0.25 M) and the initial rate constant was obtained from the best-fit line of the plot of time versus product concentration. For this and subsequent kinetic studies the initial rate constant was used as this reaction is long lived (complete conversion obtained after 24 hr at 40 °C) and to ensure monitoring of true catalyst associated reduction as opposed to a divergent pathway. The imine reduction exhibited

saturation behavior and fit a Lineweaver-Burk plot (Figure 9, $V_{\max} = 5.972 \times 10^{-4} \pm 1.706 \times 10^{-4}$, $K_m = 0.4031\text{M} \pm 0.1681\text{M}$)³ indicating that the organocatalytic reductive amination follows a Michaelis-Menten pathway.

Initial investigations into the order of the Hantzsch ester proved to be inconclusive due to poor solubility of the reagent in benzene.⁴ As the order of Hantzsch ester could not be established, we turned to an investigation of kinetic isotope effects (KIE) in the hopes of gaining some insight into the role of the Hantzsch in the reaction. Imine reduction exhibited a significant KIE of 3.06, indicating that the Hantzsch ester is involved in the rate-determining step. While this result does not distinguish between the mechanisms given in equations 2-4, a similar result was obtained when the full reductive amination was performed, revealing that hydride delivery, not imine formation, is indeed

Figure 9: Lineweaver-Burk plot of imine concentration versus initial rate



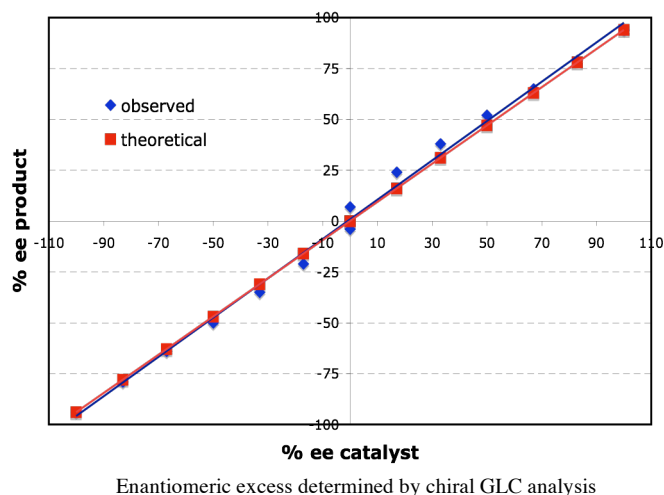
³ Michaelis-Menten parameters and associated errors were obtained by fitting the initial rate constants versus [imine] to a Lineweaver-Burk plot using the Enzyme Kinetics Module 1.2 with SigmaPlot 9.1 software.

⁴ The solubility limit of the Hantzsch ester in benzene at 40 °C in the presence of the phosphoric acid catalyst was shown to be 0.06M.

the rate-determining step for the one pot process.

As an investigation into the order of the phosphoric acid catalyst in the reductive amination, (*S*)-**1** was synthesized, and the reaction was run with varying levels of catalyst enantiopurity. As expected, the enantiopurity of the secondary amine product was shown to track in a linear fashion with the enantiopurity of the catalyst (Figure 10). The absence of a non-linear effect proves that only one molecule of catalyst is involved in the enantiodetermining step of the reaction, a result that is in agreement with previous observations concerning the role of catalyst in the reaction.⁵

Figure 10: Catalyst linearity for the reductive amination of acetophenone with *p*-anisidine



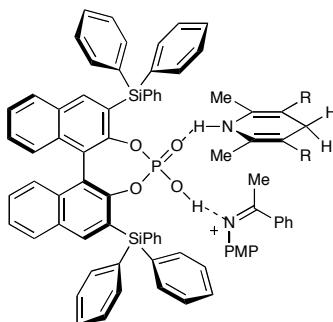
VII. Eyring Activation Parameters

The final kinetic study undertaken was a determination of the Eyring activation parameters of the rate-determining imine reduction step. Our interest in defining these parameters stems from the recent assertions in the literature that this class of BINOL

⁵ For more information on nonlinear effects in catalysis see: Kagan, H. B.; Guillaneux, D.; Zhao, S-H.; Samuel, O.; Rainford, D. *J. Am. Chem. Soc.* **1994**, *116*, 9430.

derived phosphoric acid catalysts operate through a bifunctional activation mode whereby the phosphoric acid moiety activates both the electrophile and the nucleophile via hydrogen bonding.⁶ This situation could also theoretically take place in the reductive amination with the phosphoric acid activating both the imine and Hantzsch ester via hydrogen bonding (Figure 11). As this hypothesis implies a highly ordered transition state, obtaining the value of ΔS^\ddagger for the reaction would either lend support for or call into question this hypothesis.

Figure 11: Bifunctional transition state model for imine reduction



The initial rate of imine reduction at temperatures ranging from 40-80 °C was examined and the Eyring activation parameters were determined from the graph of $1000/T$ versus $\ln(k_{\text{initial}}/T)$ (Figure 12).⁷ The fairly large negative value obtained for ΔS^\ddagger of -30.11 eu is suggestive of bifunctional catalysis as it indicates a large degree of preorganization in the transition state. Though this experiment is not definitive proof of bifunctional catalysis, this theory was recently lent additional support by the calculations of Goodman⁸ who determined that the transition state depicted in Figure 11 is stabilized

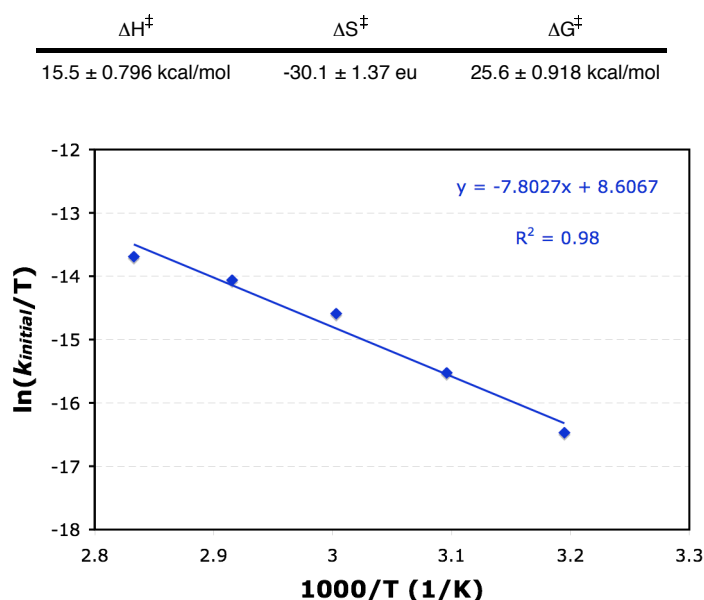
⁶ (a) Akiyama, T.; Morita H.; Itoh J.; Fuchibe, K. *Org. Lett.* **2005**, 7, 2583. (b) Terada, M.; Machioka, K.; Sorimacho, K. *Angew. Chem. Int. Ed.* **2006**, 45, 2254.

⁷ For Eyring error calculation see: Girolami, G.S.; Morse, P. M.; Spencer, M. D.; Wilson, S. R. *Organometallics* **1994**, 13, 1646.

⁸ Goodman, J. M.; Simon, L. J. *J. Am. Chem. Soc.* **2008**, 130, 8741.

by up to 10 kcal/mol with respect to the case where binding takes place solely between the imine and phosphoric acid catalyst. Taken in combination, the experimental results regarding substrate specificity, experimentally determined entropy of activation and calculated stabilization values are suggestive evidence that this class of phosphoric acid catalysts are operating through bifunctional activation of both electrophiles and nucleophiles.

Figure 12: Eyring activation parameters determined from a linear fit of k_{initial} over a range of temperatures



VIII. Conclusion

A number of mechanistic and kinetic studies have been undertaken to examine in detail the organocatalytic reductive amination of ketones with a novel trialkylsilyl substituted BINOL derived phosphoric acid catalyst. The sensitivity of this acid catalyst to buffering by any number of reaction components explains several experimental observations including the lack of reactivity with benzyl and alkyl amines as well as lower yields obtained with alkyl substituted ketones. A Hammett study of

enantioselectivity trends lends supports to the theory that the phosphoric acid catalyst is activating the imine substrate via hydrogen bonding as opposed to a full protonation event while a break in the plot suggests the appearance of a non-selective competitive pathway for imine activation through non-catalyst associated protonation. Evidence for a hydrogen bond in a crystal structure of an imine-catalyst complex lends further support to this hypothesis. An examination of kinetic isotope effects for the Hantzsch ester reducing agent has shown that hydride delivery is the rate-determining step in both the one pot and imine reduction processes. Additionally, it has been shown through an examination of imine order that the reduction step follows Michaelis-Menten kinetics with reversible catalyst binding occurring prior to irreversible hydride delivery. A determination of the Eyring activation parameters for imine reduction revealed that the entropy of activation is large and negative, suggesting a bifunctional role of the catalyst activating both the imine electrophile and Hantzsch ester nucleophile.

Supporting Information

I. General Information.

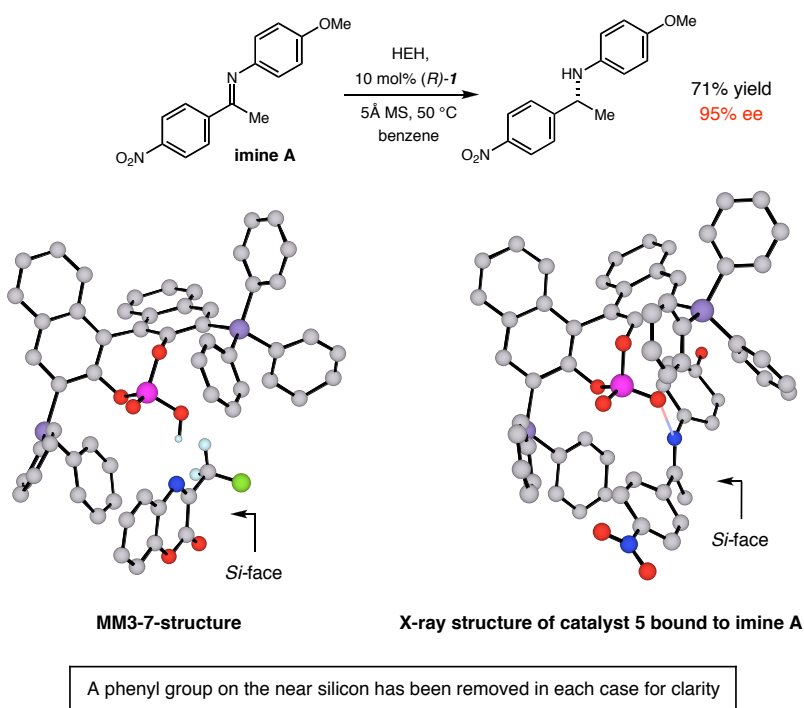
Benzylamine, cyclohexylamine, allylamine and commercially available ketones were distilled prior to use while commercially available *p*-anisidine was purified by vacuum sublimation followed by recrystallization from water. All solvents were purified according to the method of Grubbs.⁹ Organic solutions were concentrated under reduced pressure on a Büchi rotary evaporator. Sieves (5Å powdered) were activated by flame under vacuum and stored at 180 °C. Chromatographic purification of products was accomplished using flash chromatography on Silicycle 230-400 mesh silica gel. Thin-layer chromatography (TLC) was carried out on Silicycle 0.25mm silica gel plates. Visualization of the developed chromatogram was performed by fluorescence quenching, iodine or KMnO₄ staining.

¹HNMR spectra were recorded on a Varian Mercury 300 Spectrometer (300 MHz), and are internally referenced to residual protic solvent signals (CHCl₃ = 7.24 ppm). X-ray structure analysis was carried out at the California Institute of Technology X-ray Crystallography facility. Gas liquid chromatography (GLC) was carried out on a Hewlett-Packard 6850 Series gas chromatograph equipped with a splitmode capillary injection system and flame ionization detectors using Varian CP-Chirasil-Dex-CB and Bodman Chiraldex Γ-TA (30 m x 0.25 mm) columns. High performance liquid chromatography (HPLC) was performed on Hewlett-Packard 1100 Series chromatograph using a Daicel Chiracel OD-H column (25 cm) and equivalent guard column (5 cm).

⁹ Pangborn, A.B; Giardello, M.A.; Grubbs, R. H.; Rosen, R.K.; Timmers, F.J. *Organometallics* **1996**, *15*, 1518.

Analytical supercritical fluid chromatography (SFC) was performed on a Berger Instruments SFC with built-in photometric detector ($\lambda = 240$ nm) using Daicel Chiracel OJ-H, OD-H, AS-H, and AD-H columns (25 cm) as noted. All react IR data was collected on a Mettler Toledo ReactIR iC10 instrument.

Figure 1. X-ray Crystal Structure.



Representative Procedure I: Reductive Amination with (*R*)-1

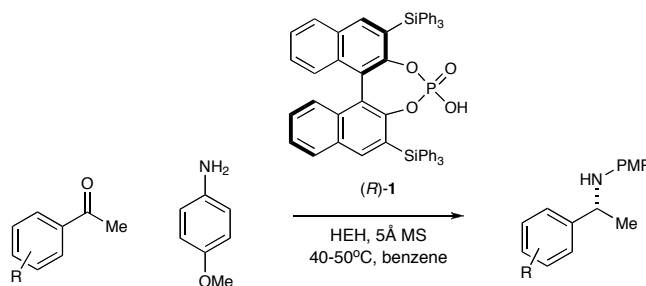
A 20 mL vial equipped with a magnetic stir bar was charged with amine (1.0 equiv), Hantzsch ester (1.2 equiv), catalyst (10 mol%) and 5 Å molecular sieves (1 g/mmol). Benzene (0.1 M) was added followed by ketone (3.0 equiv). The reaction

mixture was heated with stirring to 40-50 °C as noted and monitored by TLC. Upon completion or 96 hours, the reaction mixture was filtered through a plug of silica, eluting with Et₂O to remove the molecular sieves and unreacted Hantzsch ester, then concentrated *in vacuo*.

Workup procedure A: The crude product was dissolved in Et₂O (100 mL) and extracted with 1N HCl (2 × 60 mL). The combined aqueous phases were basified to pH 10 with aqueous KOH and extracted with CH₂Cl₂ (2 × 80 mL). The combined organic phase was dried (MgSO₄) and concentrated *in vacuo*. The product was purified by silica gel chromatography (solvents noted) to yield the title compounds.

Workup procedure B: The crude product was directly purified by silica gel column chromatography (solvents noted) to yield the title compounds.

2. Hammett Analysis



entry	R	% ee	enantiomeric ratio	log (enantiomeric ratio)	σ
1	4-Me	91	21.67574	1.33597	-0.17
2	4-OMe	90	18.23262	1.26085	-0.27
3	3-Me	93	30.18179	1.47974	-0.07
4	H	94	34.98261	1.54385	0.00
5	4-NO ₂	95	42.02926	1.62355	0.78
6	4-Cl	95	38.32889	1.58353	0.23
7	3-F	95	38.15427	1.58154	0.34
8	4-CF ₃	95	39.70928	1.59889	0.54

(+)-*N*-(4-methoxyphenyl)-[1-(4-tolyl)-ethyl]amine (entry 1):

Prepared according to representative procedure I from *p*-anisidine (105 mg, 0.853 mmol) and 4'-methylacetophenone (342 μ L, 2.56 mmol) at 50 °C for 72 h, using workup procedure B to provide the title compound as a yellow oil (161 mg, 79% yield, 91% ee) following silica gel chromatography (5% Et₂O/pentane).¹⁰ The enantiomeric ratio was determined by SFC using a Chiralcel AD-H column (5-50% methanol/CO₂, 35 °C, 100 bar, 4 mL/min, ramp rate = 5%/min); major enantiomer t_r = 3.88 min and minor enantiomer t_r = 3.57 min.

(+)-*N*-(4-methoxyphenyl)-[1-(4-methoxyphenyl)-ethyl]amine (entry 2):

Prepared according to representative procedure I from *p*-anisidine (110 mg, 0.890 mmol) and 4'-methoxyacetophenone (401 mg, 2.67 mmol) at 50 °C for 72 h, using workup procedure A to provide the title compound as a tan solid (177 mg, 77% yield, 90% ee) following silica gel chromatography (3% Et₂O/toluene).² The enantiomeric ratio was determined by HPLC using a Chiralcel OD-H column (5% isopropanol/hexanes); major enantiomer t_r = 20.62 min and minor enantiomer t_r = 22.64 min.

¹⁰ For full characterization see: MacMillan, D. W. C.; Storer, R. I.; Carrera, D. E.; Ni, Y. *J. Am. Chem. Soc.* **2006**, 128, 84.

(-)-*N*-(4-methoxyphenyl)-[1-(3-methylphenyl)-ethyl]amine (entry 3):

Prepared according to representative procedure I from *p*-anisidine (8.6 mg, 0.0694 mmol) and 3'-methylacetophenone (28 μ L, 0.21 mmol) at 40 °C for 24 h, using workup procedure B to provide the title compound as a pale yellow oil (14.3 mg, 86% yield, 93% ee) following silica gel chromatography (10% Et₂O/pentane).¹¹ The enantiomeric ratio was determined by SFC using a Chiralcel AD-H column (5-50% isopropanol/CO₂, 35 °C, 100 bar, 4 mL/min, ramp rate = 5%/min); major enantiomer *t_r* = 3.76 min and minor enantiomer *t_r* = 4.03 min.

(*R*)-*N*-(4-methoxyphenyl)-[1-(phenyl)-ethyl]amine (entry 4):

Prepared according to representative procedure I from *p*-anisidine (83 mg, 0.67 mmol) and acetophenone (235 μ L, 2.01 mmol) at 50 °C for 24 h, using workup procedure B to provide the title compound as a yellow oil (162 mg, 87% yield, 93% ee) following silica gel chromatography (10% Et₂O/pentane).² The enantiomeric ratio was determined by GLC using a Chirasil-Dex-CB column (150 °C isotherm for 150 minutes, 1 mL/min); major enantiomer *t_r* = 81.43 min and minor enantiomer *t_r* = 79.91 min.

(+)-*N*-(4-methoxyphenyl)-[1-(4-nitrophenyl)-ethyl]amine (entry 5):

Prepared according to representative procedure I from *p*-anisidine (114 mg, 0.927 mmol) and 4'-nitroacetophenone (459 mg, 2.78 mmol) at 50 °C for 72 h, using workup procedure A to provide the title compound as an orange solid (118 mg, 71% yield, 95% ee) following silica gel chromatography (30% Et₂O/pentane).² The enantiomeric ratio

¹¹ For full characterization see: Reuping, M.; Azap, C.; Sugiono, E.; Theissmann, T *Synlett*. **2005**, No. 5, 2367.

was determined by SFC using a Chiralcel OD-H column (10% methanol/CO₂, 35 °C, 100 bar, 4 mL/min); major enantiomer t_r = 8.41 min and minor enantiomer t_r = 7.88 min.

(+)-*N*-(4-methoxyphenyl)-[1-(4-chlorophenyl)-ethyl]amine (entry 6):

Prepared according to representative procedure I from *p*-anisidine (101 mg, 0.818 mmol) and 4'-chloroacetophenone (379 mg, 2.45 mmol) at 50 °C for 72 h, using workup procedure A to provide the title compound as a yellow oil (161 mg, 75% yield, 95% ee) following silica gel chromatography (15% Et₂O/pentane).² The enantiomeric ratio was determined by GLC using a Chirasil-Dex-CB column (160 °C isotherm for 150 minutes, 1 mL/min); major enantiomer t_r = 134.59 min and minor enantiomer t_r = 132.02 min.

(-)-*N*-(4-methoxyphenyl)-[1-(3-fluorophenyl)-ethyl]amine (entry 7):

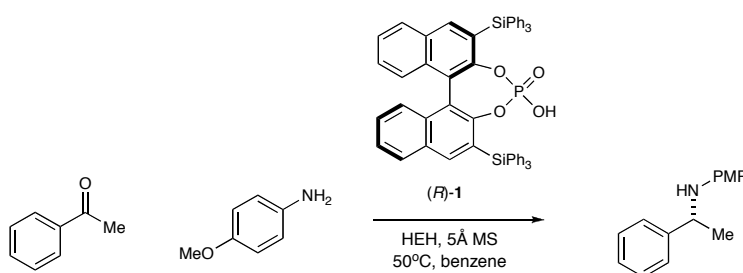
Prepared according to representative procedure I from *p*-anisidine (122 mg, 0.993 mmol) and 3'-fluoroacetophenone (366 μL, 2.98 mmol) at 50 °C for 72 h, using workup procedure B to provide the title compound as a yellow oil (198 mg, 81% yield, 95% ee) following silica gel chromatography (1% Et₂O/toluene).² The enantiomeric ratio was determined by SFC using a Chiralcel AD-H column (5-50% isopropanol/CO₂, 35 °C, 100 bar, 4 mL/min, ramp rate = 5%/min); major enantiomer t_r = 3.45 min and minor enantiomer t_r = 3.70 min.

(-)-*N*-(4-methoxyphenyl)-[1-(4-trifluoromethylphenyl)-ethyl]amine (entry 8):

Prepared according to representative procedure I from *p*-anisidine (53.0 mg, 0.427 mmol) and 4'-trifluoromethylacetophenone (244.0 mg, 1.28 mmol) at 50 °C for 72 h, using

workup procedure B to provide the title compound as a yellow oil (54 mg, 43% yield, 95% ee) following silica gel chromatography (1% Et₂O/pentane).³ The enantiomeric ratio was determined by GLC using a Chirasil-Dex-CB column (150 °C isotherm for 85 minutes, 1 mL/min); major enantiomer t_r = 77.457 min and minor enantiomer t_r = 75.806 min.

3. Amine Equivalency Investigation



The effect of varying amine equivalency was examined by measuring the amount of imine and product present in the reaction over time via ReactIR. An 25 mL oven dried roundbottom flask equipped with a magnetic stir bar was charged with catalyst (86.5 mg, 0.10 mmol, 0.1 eq), *p*-anisidine (123.15-369.3 mg, 1.00-3.00 mmol, 1.0-3.0 eq), Hantzsch ester (304 mg, 1.20 mmol, 1.2 eq) and 5 Å molecular sieves (950 mg). Benzene (10.0 mL, 0.1M) was added, the reaction mixture was heated with stirring to 50 °C and a background scan was taken. Upon completion of the background scan, acetophenone (117 µL mg, 1.00 mmol, 1.0 eq) was added in one portion and scans were taken every 10 minutes over a 24 h period. The imine peak was recorded over 1506-1511cm⁻¹ and the product peak recorded over 1735-1741cm⁻¹.

1 equivalent *p*-anisidine:

Time	Imine	Product	Time	Imine	Product	Time	Imine	Product
0:00:50	0.004673	0.000588	8:00:50	0.052441	0.01516	16:00:50	0.011362	0.047373
0:10:50	0.007564	0.000697	8:10:50	0.052519	0.015672	16:10:51	0.010756	0.047848
0:20:51	0.010347	0.000536	8:20:51	0.051358	0.016542	16:20:51	0.009658	0.048267
0:30:50	0.013312	0.000849	8:30:50	0.051175	0.017287	16:30:51	0.009068	0.048634
0:40:51	0.01481	0.00101	8:40:51	0.050559	0.018008	16:40:50	0.00882	0.049075
0:50:51	0.017141	0.001112	8:50:50	0.049154	0.018879	16:50:51	0.007544	0.049795
1:00:51	0.01987	0.001255	9:00:51	0.04905	0.019715	17:00:51	0.007382	0.049978
1:10:50	0.021274	0.001039	9:10:51	0.047241	0.020467	17:10:51	0.00621	0.050437
1:20:50	0.023669	0.001262	9:20:51	0.047113	0.021323	17:20:51	0.00598	0.050792
1:30:51	0.025756	0.001472	9:30:51	0.045267	0.022037	17:30:50	0.005573	0.051169
1:40:51	0.026937	0.001445	9:40:51	0.044968	0.022984	17:40:51	0.004625	0.051684
1:50:50	0.029613	0.001783	9:50:51	0.043967	0.023586	17:50:51	0.00424	0.052184
2:00:51	0.031363	0.001682	10:00:51	0.042846	0.024419	18:00:51	0.003316	0.052567
2:10:50	0.032442	0.001833	10:10:51	0.04216	0.025212	18:10:51	0.002831	0.053003
2:20:50	0.034773	0.002037	10:20:51	0.040671	0.025939	18:20:50	0.00253	0.053255
2:30:51	0.035766	0.002106	10:30:50	0.040104	0.026703	18:30:51	0.001541	0.053566
2:40:51	0.037211	0.002113	10:40:51	0.03968	0.027549	18:40:51	0.001525	0.053949
2:50:50	0.039423	0.00257	10:50:50	0.037724	0.028093	18:50:51	0.001158	0.054175
3:00:51	0.040167	0.002506	11:00:51	0.037675	0.029003	19:00:51	0.000233	0.054725
3:10:51	0.041663	0.002722	11:10:51	0.036488	0.02979	19:10:50	0.000223	0.055039
3:20:50	0.043227	0.003041	11:20:50	0.034987	0.030619	19:20:51	0.000213	0.055297
3:30:51	0.043844	0.003158	11:30:51	0.034152	0.031328	19:30:51	0.000203	0.055572
3:40:50	0.045161	0.003378	11:40:51	0.033815	0.031855	19:40:50	0.000193	0.055972
3:50:50	0.046678	0.003712	11:50:51	0.031903	0.03255	19:50:51	0.000183	0.056429
4:00:51	0.047609	0.003868	12:00:51	0.031686	0.033409	20:00:50	0.000173	0.057
4:10:50	0.048089	0.00397	12:10:51	0.03051	0.034018	20:10:51	0.000163	0.057189
4:20:51	0.049778	0.004598	12:20:51	0.029953	0.034809	20:20:50	0.000153	0.057654
4:30:50	0.050022	0.004545	12:30:51	0.028866	0.035575	20:30:51	0.000143	0.057569
4:40:50	0.050864	0.004926	12:40:51	0.027691	0.036294	20:40:50	0.000133	0.058045
4:50:51	0.052033	0.005337	12:50:51	0.027275	0.036836	20:50:51	0.000123	0.058428
5:00:50	0.052031	0.005595	13:00:51	0.025725	0.037078	21:00:50	0	0.058703
5:10:50	0.053337	0.005956	13:10:51	0.025316	0.038075	21:10:50	0	0.05879
5:20:51	0.053513	0.006288	13:20:50	0.024778	0.038622	21:20:51	0	0.059455
5:30:51	0.053784	0.006683	13:30:51	0.023491	0.03916	21:30:50	0	0.059834
5:40:50	0.054603	0.007288	13:40:51	0.02348	0.039767	21:40:51	0	0.059915
5:50:51	0.054381	0.007679	13:50:51	0.021892	0.040419	21:50:50	0	0.06017
6:00:51	0.054934	0.008077	14:00:51	0.021292	0.040851	22:00:51	0	0.060699
6:10:50	0.054767	0.008514	14:10:51	0.019987	0.041862	22:10:51	0	0.06099
6:20:51	0.055009	0.008821	14:20:51	0.019556	0.042156	22:20:50	0	0.061353
6:30:51	0.055414	0.0096	14:30:51	0.018232	0.042946	22:30:51	0	0.061571
6:40:50	0.055297	0.010086	14:40:51	0.01734	0.043175	22:40:51	0	0.061867
6:50:51	0.054809	0.010648	14:50:51	0.016855	0.043933	22:50:51	0	0.062456
7:00:51	0.055028	0.011232	15:00:50	0.016371	0.044226	23:00:50	0	0.062505
7:10:51	0.055024	0.011891	15:10:51	0.014638	0.044967	23:10:50	0	0.062771
7:20:50	0.054451	0.012544	15:20:50	0.014494	0.045309	23:20:50	0	0.063345
7:30:51	0.054693	0.013173	15:30:51	0.013387	0.046013	23:30:51	0	0.063704
7:40:51	0.053483	0.013931	15:40:51	0.013	0.046492	23:40:51	0	0.063841
7:50:51	0.053371	0.014537	15:50:51	0.011807	0.046816	23:50:51	0	0.064051

2 equivalent *p*-anisidine:

Time	Imine	Product	Time	Imine	Product	Time	Imine	Product
0:00:50	0.002974	0	8:00:50	0.063551	0.010446	16:00:50	0.057185	0.018842
0:10:50	0.01406	0.003281	8:10:50	0.06362	0.010466	16:10:51	0.056716	0.018957
0:20:51	0.017344	0.003354	8:20:51	0.063851	0.010617	16:20:51	0.056196	0.018997
0:30:50	0.020158	0.003253	8:30:50	0.064064	0.010902	16:30:51	0.056616	0.019505
0:40:51	0.023846	0.003621	8:40:51	0.063754	0.011055	16:40:50	0.056709	0.019985
0:50:51	0.026249	0.003763	8:50:50	0.063257	0.011011	16:50:51	0.056069	0.019403
1:00:51	0.028865	0.00401	9:00:51	0.062826	0.010972	17:00:51	0.05579	0.01961
1:10:50	0.030758	0.004016	9:10:51	0.062783	0.010998	17:10:51	0.055507	0.02011
1:20:50	0.033616	0.004162	9:20:51	0.063003	0.011611	17:20:51	0.055429	0.020022
1:30:51	0.03525	0.004121	9:30:51	0.062955	0.011905	17:30:50	0.055333	0.020161
1:40:51	0.037116	0.004231	9:40:51	0.063364	0.01181	17:40:51	0.054818	0.020468
1:50:50	0.038934	0.00447	9:50:51	0.062752	0.012112	17:50:51	0.054135	0.020359
2:00:51	0.041185	0.004869	10:00:51	0.062336	0.012106	18:00:51	0.054011	0.020789
2:10:50	0.043125	0.005239	10:10:51	0.062468	0.012434	18:10:51	0.053801	0.020624
2:20:50	0.044259	0.004902	10:20:51	0.062542	0.0128	18:20:50	0.054144	0.021167
2:30:51	0.045692	0.004847	10:30:50	0.062341	0.012512	18:30:51	0.054327	0.021584
2:40:51	0.047578	0.005513	10:40:51	0.061722	0.012782	18:40:51	0.054834	0.022052
2:50:50	0.048932	0.005669	10:50:50	0.06194	0.013009	18:50:51	0.054903	0.022216
3:00:51	0.049835	0.005502	11:00:51	0.061752	0.013276	19:00:51	0.05571	0.022698
3:10:51	0.051027	0.005902	11:10:51	0.061773	0.013659	19:10:50	0.05611	0.023124
3:20:50	0.052479	0.005999	11:20:50	0.061802	0.013924	19:20:51	0.056225	0.023214
3:30:51	0.05323	0.006245	11:30:51	0.061782	0.014508	19:30:51	0.056087	0.023292
3:40:50	0.054871	0.006579	11:40:51	0.062191	0.014907	19:40:50	0.056099	0.023735
3:50:50	0.055363	0.006373	11:50:51	0.061768	0.01512	19:50:51	0.056152	0.023965
4:00:51	0.056161	0.006584	12:00:51	0.061409	0.015296	20:00:50	0.055985	0.024367
4:10:50	0.057424	0.006895	12:10:51	0.061566	0.015332	20:10:51	0.055897	0.024512
4:20:51	0.058103	0.006902	12:20:51	0.060839	0.015114	20:20:50	0.055691	0.024514
4:30:50	0.058508	0.006998	12:30:51	0.061371	0.015868	20:30:51	0.055662	0.024579
4:40:50	0.05888	0.007026	12:40:51	0.061075	0.015894	20:40:50	0.055667	0.025066
4:50:51	0.059855	0.007113	12:50:51	0.06066	0.016145	20:50:51	0.05585	0.025215
5:00:50	0.061151	0.007526	13:00:51	0.06045	0.016136	21:00:50	0.056231	0.025656
5:10:50	0.061479	0.007689	13:10:51	0.060015	0.016252	21:10:50	0.056214	0.026087
5:20:51	0.06131	0.007586	13:20:50	0.060115	0.016152	21:20:51	0.055508	0.026003
5:30:51	0.062562	0.008075	13:30:51	0.060143	0.016449	21:30:50	0.056066	0.026513
5:40:50	0.062968	0.008174	13:40:51	0.059862	0.016778	21:40:51	0.055634	0.026517
5:50:51	0.063599	0.008394	13:50:51	0.059872	0.016891	21:50:50	0.056171	0.026868
6:00:51	0.06385	0.00832	14:00:51	0.059441	0.016876	22:00:51	0.056145	0.026949
6:10:50	0.064142	0.008878	14:10:51	0.058677	0.016497	22:10:51	0.05654	0.027378
6:20:51	0.064801	0.009329	14:20:51	0.059446	0.017403	22:20:50	0.056443	0.027458
6:30:51	0.064571	0.009373	14:30:51	0.058733	0.01751	22:30:51	0.056267	0.02778
6:40:50	0.063973	0.009229	14:40:51	0.058664	0.017282	22:40:51	0.056004	0.027858
6:50:51	0.064371	0.009411	14:50:51	0.058388	0.017642	22:50:51	0.055746	0.0278
7:00:51	0.063946	0.00929	15:00:50	0.05826	0.017794	23:00:50	0.055131	0.027859
7:10:51	0.064382	0.009683	15:10:51	0.05807	0.01775	23:10:50	0.056547	0.028529
7:20:50	0.064456	0.010095	15:20:50	0.058498	0.01838	23:20:50	0.055649	0.028654
7:30:51	0.063623	0.009742	15:30:51	0.057769	0.018487	23:30:51	0.055247	0.028327
7:40:51	0.064281	0.010085	15:40:51	0.057799	0.018648	23:40:51	0.055732	0.028759
7:50:51	0.064078	0.010215	15:50:51	0.05731	0.018932	23:50:51	0.054946	0.028865

3 equivalent *p*-anisidine:

Time	Imine	Product	Time	Imine	Product	Time	Imine	Product
0:00:50	0.005411	-2.78E-05	8:00:50	0.075555	0.003959	16:00:50	0.081709	0.00679
0:10:50	0.015717	0.001314	8:10:50	0.076108	0.003815	16:10:51	0.081859	0.007066
0:20:51	0.018407	0.001093	8:20:51	0.076186	0.003862	16:20:51	0.081597	0.007114
0:30:50	0.021064	0.00128	8:30:50	0.076323	0.003931	16:30:51	0.081705	0.007148
0:40:51	0.023543	0.001343	8:40:51	0.076484	0.00396	16:40:50	0.081378	0.007306
0:50:51	0.02573	0.001333	8:50:50	0.076894	0.004216	16:50:51	0.081364	0.00715
1:00:51	0.02813	0.001644	9:00:51	0.077	0.004388	17:00:51	0.081182	0.007059
1:10:50	0.030632	0.001361	9:10:51	0.077311	0.004084	17:10:51	0.080648	0.007007
1:20:50	0.03269	0.001614	9:20:51	0.077536	0.004337	17:20:51	0.081228	0.007264
1:30:51	0.034833	0.001707	9:30:51	0.077939	0.004191	17:30:50	0.081009	0.007278
1:40:51	0.03721	0.001784	9:40:51	0.077998	0.004442	17:40:51	0.081131	0.007624
1:50:50	0.039462	0.001876	9:50:51	0.078169	0.004477	17:50:51	0.081433	0.007564
2:00:51	0.041195	0.001793	10:00:51	0.07865	0.004804	18:00:51	0.081125	0.007895
2:10:50	0.043124	0.00188	10:10:51	0.078699	0.004484	18:10:51	0.081355	0.00761
2:20:50	0.044702	0.00196	10:20:51	0.078965	0.004469	18:20:50	0.081362	0.007865
2:30:51	0.046663	0.002043	10:30:50	0.079132	0.0049	18:30:51	0.080977	0.007882
2:40:51	0.048138	0.001993	10:40:51	0.078986	0.004928	18:40:51	0.081131	0.007842
2:50:50	0.049387	0.002149	10:50:50	0.079117	0.004812	18:50:51	0.081221	0.008076
3:00:51	0.051195	0.002235	11:00:51	0.078988	0.004995	19:00:51	0.081302	0.008208
3:10:51	0.052606	0.002324	11:10:51	0.079206	0.004955	19:10:50	0.081456	0.008277
3:20:50	0.053784	0.002252	11:20:50	0.079137	0.004772	19:20:51	0.081506	0.008095
3:30:51	0.055373	0.002204	11:30:51	0.07954	0.005082	19:30:51	0.081132	0.008452
3:40:50	0.056396	0.002288	11:40:51	0.079254	0.005074	19:40:50	0.080943	0.008413
3:50:50	0.057854	0.002578	11:50:51	0.079715	0.005187	19:50:51	0.080839	0.008473
4:00:51	0.058805	0.0023	12:00:51	0.079665	0.005099	20:00:50	0.080708	0.008495
4:10:50	0.060283	0.002492	12:10:51	0.079701	0.005199	20:10:51	0.080607	0.00839
4:20:51	0.060855	0.002643	12:20:51	0.079756	0.005273	20:20:50	0.080641	0.008545
4:30:50	0.061963	0.002611	12:30:51	0.0799	0.005263	20:30:51	0.080394	0.008938
4:40:50	0.062925	0.002674	12:40:51	0.080146	0.005279	20:40:50	0.080825	0.008749
4:50:51	0.064066	0.002589	12:50:51	0.079917	0.005334	20:50:51	0.080826	0.009178
5:00:50	0.064812	0.002793	13:00:51	0.08016	0.005463	21:00:50	0.081037	0.009071
5:10:50	0.065631	0.003	13:10:51	0.080406	0.005578	21:10:50	0.0807	0.008978
5:20:51	0.066451	0.002929	13:20:50	0.080167	0.005765	21:20:51	0.080934	0.009332
5:30:51	0.06766	0.00287	13:30:51	0.080413	0.005511	21:30:50	0.081037	0.009313
5:40:50	0.068449	0.003063	13:40:51	0.080568	0.005701	21:40:51	0.080483	0.009335
5:50:51	0.068904	0.003206	13:50:51	0.080237	0.005746	21:50:50	0.080951	0.009248
6:00:51	0.069462	0.003353	14:00:51	0.080466	0.005778	22:00:51	0.080699	0.009502
6:10:50	0.070558	0.003175	14:10:51	0.08037	0.005993	22:10:51	0.080645	0.009398
6:20:51	0.071156	0.003196	14:20:51	0.080843	0.006018	22:20:50	0.0803	0.009679
6:30:51	0.071792	0.003359	14:30:51	0.081011	0.006124	22:30:51	0.080723	0.009719
6:40:50	0.072619	0.003399	14:40:51	0.081327	0.006282	22:40:51	0.080562	0.009833
6:50:51	0.072862	0.003607	14:50:51	0.08127	0.006344	22:50:51	0.080413	0.009795
7:00:51	0.073435	0.003547	15:00:50	0.081444	0.006341	23:00:50	0.080014	0.010172
7:10:51	0.073929	0.003814	15:10:51	0.081473	0.006703	23:10:50	0.080268	0.00977
7:20:50	0.074528	0.003631	15:20:50	0.081689	0.006513	23:20:50	0.079977	0.010283
7:30:51	0.075066	0.003628	15:30:51	0.081888	0.006923	23:30:51	0.079774	0.010266
7:40:51	0.075429	0.003691	15:40:51	0.081554	0.006659	23:40:51	0.079697	0.010097
7:50:51	0.075181	0.003823	15:50:51	0.081217	0.006888	23:50:51	0.079608	0.010382

4. Reaction Profile

The amount of *p*-anisidine, imine and product present in the reaction over time was determined according to the following procedure. An 8 mL oven dried vial equipped

with a magnetic stir bar was charged with catalyst (37.0 mg, 0.0427 mmol, 0.1 eq), *p*-anisidine (53 mg, 0.427 mmol, 1.0 eq), Hantzsch ester (130.0 mg, 0.513 mmol, 1.2 eq) and 4,4'-dimethylbiphenyl (77.8 mg, 0.427 mmol, 1.0 eq) as internal standard. Benzene (4.25 mL) and 5 Å molecular sieves (425 mg) were added and the reaction mixture was heated with stirring to 50 °C. After 5 minutes at 50 °C, acetophenone (212 µL mg, 1.28 mmol, 3.0 eq) was added in one portion. The reaction was sampled by flushing a small aliquot through a silica plug and diluting with Et₂O. The amount of conversion was determined by GLC using an achiral B-DM column (100 °C isotherm for 15 minutes, ramp to 170 °C at 40 °C/min, 170 °C isotherm for 25 minutes, 1 mL/min); *p*-anisidine *t_r* = 22.1 min, imine *t_r* = 37.8 min, product *t_r* = 34.2 min and internal standard *t_r* = 26.5 min.

Reaction Data:

Time (h)	<i>p</i> -anisidine	% imine	product
0	100	0	0
0.5	73	21	6
1	53	39	8
2	23	65	13
4	4	64	34
6	2	49	49
8	2	40	58
10	2	33	65
11	2	29	69
23	1	15	83
36	1	9	89
48	1	5	94

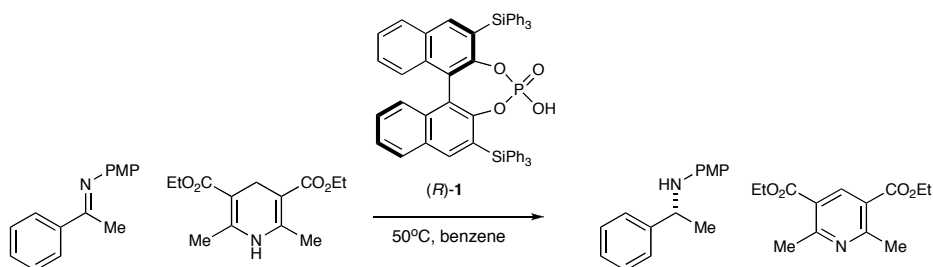
5. Nonlinear Effect Studies

A 4 mL vial equipped with a magnetic stir bar was charged with *p*-anisidine (15.0 mg, 0.122), Hantzsch ester (37.0 mg, 0.146) and 5Å molecular sieves (122 mg). Previously prepared 0.1 M stock solutions of (*R*)-**1** and (*S*)-**1** in benzene were added to create a total volume of 1.2 mL with the appropriate catalyst enantiopurity. Acetophenone (29 µL, 0.244 mmol) was added and the reaction was heated to 50 °C for

25 h. The reactions were sampled by flushing a small aliquot through a silica plug and diluting with Et₂O. The enantiomeric ratio of the product was determined by GLC using a Chirasil-Dex-CB column (150 °C isotherm for 150 minutes, 1 mL/min); major enantiomer t_r = 81.43 min and minor enantiomer t_r = 79.91 min.¹²

Catalyst	Enantiopurity (%)	
	Product (experimental)	Product (theoretical)
0	7	0.00
17	24	15.98
33	38	31.02
50	52	47.00
67	65	62.98
83	79	78.02
100	94	94.00
0	-4	0.00
-17	-21	-15.98
-33	-35	-31.02
-50	-50	-47.00
-67	-64	-62.98
-83	-79	-78.02
-100	-94	-94.00

Representative Procedure II: Determination of k_{initial} of imine reduction with (R)-1



An 8 mL oven dried vial equipped with a magnetic stir bar was charged with catalyst (10.6 mg, 0.012 mmol, 0.1 eq), imine (27.5 mg, 0.122 mmol, 1.0 eq) and 4,4'-dimethylbiphenyl (22.2mg, 0.122 mmol, 1.0 eq) as internal standard. Benzene (2.4 mL)

¹² Theoretical product enantiopurity determined using the equation: $EE_{\text{theoretical}} = (EE_0)(ee_{\text{catalyst}})$ where EE_0 is the observed enantioselectivity at 100% catalyst enantiopurity. See Kagan, H. B.; Guillaneux, D.; Zhao, S-H.; Samuel, O.; Rainford, D. *J. Am. Chem. Soc.* **1994**, 116(21) 9430.

was added and the reaction mixture was heated with stirring to 50 °C. After 5 minutes at 50 °C, Hantzsch ester (37.3 mg, 0.146 mmol, 1.2 eq) was added in one portion. The reaction was sampled by flushing a small aliquot through a silica plug and diluting with Et₂O. The amount of conversion was determined by GLC using a Chirasil-Dex-CB column (160 °C isotherm for 50 minutes, 1 mL/min); product t_r = 41.6 min and internal standard t_r = 10.0 min.

Determination of Conversion Factor for GLC analysis

To determine the conversion factor for GLC analysis, 0.047 M solutions of the product and 4,4'-dimethylbiphenyl in d₆-benzene were prepared. From these two solutions were prepared five mixed solutions with varying product, 4,4'-dimethylbiphenyl ratios. These solutions were analyzed by ¹HNMR to determine the exact ratio and then analyzed twice by GLC using a Chirasil-Dex-CB column (160 °C isotherm for 50 minutes, 1 mL/min). The conversion factor used in all kinetics experiments to determine absolute product concentration, 1.3319, is the average of the ten conversion factors obtained from the five solutions.

Solution	1HNMR		GC		Conversion factor
	#H (pdt)	#H (std)	Area (pdt)	Area (std)	
A	11.04	3	2007.580	691.078	1.26678241
	11.04	3	2210.430	750.204	1.24896553
B	8.64	3	551.193	280.683	1.46657712
	8.64	3	690.634	340.835	1.42131032
C	3.65	3	402.788	411.717	1.24363757
	3.65	3	507.752	515.096	1.23426449
D	1.88	3	292.253	600.762	1.28819044
	1.88	3	368.765	762.593	1.29592454
E	1.43	3	287.058	861.965	1.43131347
	1.43	3	338.684	1010.080	1.42159496

6. Determination of Catalyst Order:

The reaction order in catalyst was determined by measuring the initial kinetic rate constant at various catalyst loadings. Following representative procedure II, a constant amount of imine (31.1 mg, 0.139 mmol), Hantzsch ester (42.3 mg, 0.167 mmol) and 4,4'-dimethylbiphenyl (25.3mg, 0.139 mmol) as internal standard were used while the catalyst loading was varied from 5-30%. Results are summarized in the table below.

Time (min)	% Conversion					
	30 mol%	25 mol%	20 mol%	15 mol%	10 mol%	5 mol%
5	9.90	7.50	7.76	4.87	5.03	3.34
10	13.80	8.67	9.45	7.19	5.91	3.61
15	15.95	12.68	11.52	8.69	6.78	3.74
20	18.01	15.09	13.75	10.30	7.92	3.90
25	20.86	17.39	15.00	12.24	8.81	4.00
30	21.69	19.68	17.24	13.07	10.07	4.28
35	23.52	21.72	19.47	14.93	11.46	4.06
40	24.27	22.18	21.23	15.76	12.33	4.61
50	25.85	25.89	23.67	18.23	13.38	5.03
60	29.55	28.72		19.86	15.78	5.28
70				22.48	17.15	6.24
80					18.60	6.76
90					20.44	7.67
100						7.82

7. Determination of Imine Order

The reaction order in imine was determined by measuring the initial kinetic rate constant at various imine concentrations. For these experiments, a constant amount of catalyst (0.012 mmol), Hantzsch ester (0.146 mmol) and 4,4'-dimethylbiphenyl (0.122 mmol) was used while the starting imine concentration was varied from 0.05 M to 0.25 M.

Imine concentration: 0.05 M

Run #1:

Following representative procedure II, imine (27.8 mg, 0.123 mmol), catalyst (11.0 mg, 0.0127 mmol) and 4,4'-dimethylbiphenyl (22.0 mg, 0.121 mmol) in benzene heated to 50 °C and Hantzsch ester (37.0 mg, 0.146 mmol) added. Reaction sampled every ten minutes for 180 minutes.

Reaction data:

$$k_{\text{initial}} = 6.502 \times 10^{-5} \text{ M/min}^{-1}$$

Time (min)	Area std	Area pdt	[pdt]
10	691.21500	36.30460	0.003566
20	1442.28000	106.13400	0.004996
30	893.28700	71.61030	0.005443
40	769.07400	69.49260	0.006135
50	1071.76000	108.20200	0.006855
60	1443.45000	154.09500	0.007248
70	1058.68000	125.41500	0.008043
80	1033.82000	126.62100	0.008316
90	1046.77000	123.89900	0.008036
100	1122.64000	140.88000	0.008520
110	859.82100	106.16400	0.008383
123	961.14300	123.74200	0.008741

Run #2:

Following representative procedure II, imine (27.7 mg, 0.123 mmol), catalyst (10.6 mg, 0.0122 mmol) and 4,4'-dimethylbiphenyl (22.3 mg, 0.122 mmol) in benzene heated to 50 °C and Hantzsch ester (37.0 mg, 0.146 mmol) added. Reaction sampled every five minutes for 90 minutes.

Reaction data:

$$k_{\text{initial}} = 5.322 \times 10^{-5} \text{ M/min}^{-1}$$

Time (min)	Area (std)	Area (pdt)	[pdt] (M)
5	699.78967	37.02760	0.00359259
10	654.70581	36.83265	0.00381977
15	680.05182	42.94444	0.00428761
20	671.02979	45.13659	0.00456706
25	736.71301	55.89746	0.00515162
30	729.24829	49.07700	0.00456933
35	653.93262	50.16903	0.00520898
40	754.08197	60.72097	0.00546727
45	732.68872	63.53251	0.00588744
50	754.28027	65.91985	0.00593381
55	662.66730	57.27132	0.00586802
60	683.57446	63.56899	0.00631407
65	750.89154	70.50550	0.00637523
70	745.73016	67.91352	0.00618336
75	628.87823	59.64135	0.00643919
80	716.75482	68.27473	0.00646754
85	775.93097	76.15811	0.00666412
90	659.17279	64.10954	0.00660349

Run #3:

Following representative procedure II, imine (28.2 mg, 0.125 mmol), catalyst (10.8 mg, 0.0124 mmol) and 4,4'-dimethylbiphenyl (21.6 mg, 0.119 mmol) in benzene heated to 50 °C and Hantzsch ester (37.0 mg, 0.146 mmol) added. Reaction sampled every five minutes for 80 minutes.

Reaction data:

$$k_{\text{initial}} = 7.103 \times 10^{-5} \text{ M/min}^{-1}$$

Time (min)	Area (std)	Area (pdt)	[pdt] (M)
5	866.3710	47.4890	0.00360486
10	704.7120	51.4325	0.00479982
15	846.6420	58.8385	0.00457047
20	732.7060	54.5403	0.00489538
25	732.5410	56.4805	0.00507067
30	733.3820	62.2593	0.00558307
35	645.6510	60.9410	0.00620741
40	560.2790	58.5122	0.00686817
45	806.7720	93.4232	0.00761558
50	707.5280	85.8249	0.00797753
55	837.9550	103.6430	0.00813426
60	765.6470	96.8783	0.00832141
65	790.7740	105.9970	0.00881536
70	781.5510	106.6400	0.00897350
75	877.4860	107.2250	0.00803628
80	827.6600	107.5750	0.00854788

Imine concentration: 0.10 M**Run #1:**

Following representative procedure II, imine (54.8 mg, 0.243 mmol), catalyst (10.6 mg, 0.0122 mmol) and 4,4'-dimethylbiphenyl (22.2 mg, 0.122 mmol) in benzene heated to 50 °C and Hantzsch ester (37.0 mg, 0.146 mmol) added. Reaction sampled every five minutes for 100 minutes.

Reaction data:

$$k_{\text{initial}} = 1.236 \times 10^{-4} \text{ M/min}^{-1}$$

Time (min)	Area (std)	Area (pdt)	[pdt] (M)
5	797.45490	61.58949	0.00522034
10	787.07300	71.91210	0.00617568
15	793.99811	80.04166	0.00681388
20	794.83685	87.75176	0.00746236
25	853.78503	111.49759	0.00882704
30	950.38348	114.14977	0.00811847
35	849.75336	113.43935	0.00902337
40	823.62738	114.95933	0.00943434
45	883.89349	131.82076	0.01008050
50	916.09448	139.53244	0.01029516
55	845.90515	137.64198	0.01099835
60	838.68408	144.16763	0.01161897
65	1015.95477	161.81003	0.01076538
70	1166.08202	202.12523	0.01171628
75	836.28168	153.63379	0.01241745
80	798.00427	147.78139	0.01251736
85	842.05798	152.36288	0.01223025
90	1056.74072	191.66281	0.01225935
95	822.94348	143.40224	0.01177834
100	993.64966	188.39729	0.01281562

Run #2:

Following representative procedure II, imine (54.8 mg, 0.243 mmol), catalyst (10.6 mg, 0.0122 mmol) and 4,4'-dimethylbiphenyl (22.3 mg, 0.122 mmol) in benzene heated to 50 °C and Hantzsch ester (37.0 mg, 0.146 mmol) added. Reaction sampled every five minutes for 90 minutes.

Reaction data:

$$k_{\text{initial}} = 1.058 \times 10^{-4} \text{ M/min}^{-1}$$

Time (min)	Area (std)	Area (pdt)	[pdt] (M)
5	968.38324	74.04478	0.00519155
10	799.19086	66.35152	0.00563703
15	751.09454	69.96082	0.00632427
20	911.67566	88.95468	0.00662489
25	907.93127	98.18820	0.00734271
30	1088.84949	117.12968	0.00730380
35	973.69824	109.89849	0.00766333
40	841.49957	101.63097	0.00820016
45	882.89423	107.14925	0.00824006
50	890.44324	120.65168	0.00919977
55	1112.13550	145.80888	0.00890177
60	791.92139	104.75525	0.00898139
65	988.08960	135.09055	0.00928279
70	849.25616	122.37055	0.00978336
75	968.54053	138.51801	0.00971043
80	925.26611	129.20178	0.00948095
85	919.14142	132.71152	0.00980339
90	869.53979	123.75616	0.00966334

Imine concentration: 0.15 M

Run #1:

Following representative procedure II, imine (81.1 mg, 0.360 mmol), catalyst (10.6 mg, 0.0122 mmol) and 4,4'-dimethylbiphenyl (22.1 mg, 0.121 mmol) in benzene heated to 50 °C and Hantzsch ester (37.0 mg, 0.146 mmol) added. Reaction sampled every five minutes for 90 minutes.

Reaction data:

$$k_{\text{initial}} = 1.767 \times 10^{-4} \text{ M/min}^{-1}$$

Time (min)	Area (std)	Area (pdt)	[pdt] (M)
5	781.95135	62.84783	0.00540814
10	795.57776	74.69628	0.00631762
16	784.16010	83.01175	0.00712315
20	933.62512	114.08335	0.00822218
25	756.95947	106.78931	0.00949276
30	820.64508	124.80861	0.01023356
35	823.70850	135.19722	0.01104413
40	756.42780	135.51053	0.01205433
46	749.91516	144.31157	0.01294871
50	816.26794	160.56363	0.01323585
55	642.89014	133.55807	0.01397883
60	742.37579	163.27904	0.01479940
65	705.31586	160.20485	0.01528373
70	692.14111	161.62711	0.01571292
75	597.01489	145.62108	0.01641257
80	755.21039	188.62505	0.01680617
85	760.89270	192.99673	0.01706727
90	924.23987	241.40289	0.01757500

Run #2:

Following representative procedure II, imine (81.2 mg, 0.360 mmol), catalyst (10.6 mg, 0.0122 mmol) and 4,4'-dimethylbiphenyl (22.2 mg, 0.122 mmol) in benzene heated to 50 °C and Hantzsch ester (37.0 mg, 0.146 mmol) added. Reaction sampled every five minutes for 80 minutes.

Reaction data:

$$k_{\text{initial}} = 1.782 \times 10^{-4} \text{ M/min}^{-1}$$

Time (min)	Area (std)	Area (pdt)	[pdt] (M)
5	711.71381	52.40118	0.00497661
10	697.08594	62.32901	0.00604369
15	642.42480	67.42709	0.00709431
20	671.69836	83.16372	0.00836870
25	750.80945	101.44749	0.00913292
30	677.98370	101.25871	0.01009512
35	725.72919	117.91233	0.01098203
40	699.60645	121.47045	0.01173586
45	742.85791	138.56313	0.01260782
50	790.06018	153.71352	0.01315074
55	638.69000	131.02284	0.01386612
60	759.07983	160.64540	0.01430471
65	756.61896	167.98988	0.01500735
70	803.23853	185.30405	0.01559332
75	731.50909	172.25592	0.01591668
80	758.58533	184.83427	0.01646934

Imine concentration: 0.25 M**Run #1:**

Following representative procedure II, imine (135.0 mg, 0.600 mmol), catalyst (10.6 mg, 0.0122 mmol) and 4,4'-dimethylbiphenyl (22.1 mg, 0.121 mmol) in benzene heated to 50 °C and Hantzsch ester (37.0 mg, 0.146 mmol) added. Reaction sampled every five minutes for 80 minutes.

Reaction data:

$$k_{\text{initial}} = 2.409 \times 10^{-4} \text{ M/min}^{-1}$$

Time (min)	Area (std)	Area (pdt)	[pdt] (M)
5	548.90820	49.17182	0.00602773
10	642.85730	68.71110	0.00719200
15	576.29340	74.53334	0.00870251
20	631.46356	94.65869	0.01008671
25	588.10602	100.45442	0.01149346
30	605.07031	112.84402	0.01254903
35	609.71869	127.64349	0.01408661
40	727.19482	161.26416	0.01492191
45	623.50281	147.52975	0.01592130
50	677.34015	171.17633	0.01700491
55	680.24933	183.70435	0.01817142
60	776.35553	223.26321	0.01935058
65	687.51300	208.39621	0.02039606
70	637.49506	200.39688	0.02115201
75	682.99286	228.39397	0.02250121
80	685.26123	229.16153	0.02250210

Run #2:

Following representative procedure II, imine (135.3 mg, 0.601 mmol), catalyst (10.6 mg, 0.0122 mmol) and 4,4'-dimethylbiphenyl (22.2 mg, 0.122 mmol) in benzene heated to 50 °C and Hantzsch ester (37.0 mg, 0.146 mmol) added. Reaction sampled every five minutes for 70 minutes.

Reaction data:

$$k_{\text{initial}} = 2.139 \times 10^{-4} \text{ M/min}^{-1}$$

Time (min)	Area (std)	Area (pdt)	[pdt] (M)
5	590.06537	48.98928	0.00561176
10	575.13586	51.79704	0.00608741
15	581.46436	66.22800	0.00769869
20	564.47241	73.54892	0.00880708
25	622.47943	89.36082	0.00970332
30	653.85858	103.47855	0.01069707
35	602.90302	106.91950	0.01198692
40	585.86316	111.41827	0.01285459
45	642.36169	128.97588	0.01357147
50	616.05951	130.16507	0.01428137
55	709.90302	157.81540	0.01502618
60	758.54657	176.15627	0.01569690
65	484.38434	118.79407	0.01657688
70	702.22333	177.22768	0.01705903

8. Determination of Eyring Activation Parameters

The Eyring activation parameters were determined by measuring the initial kinetic rate constant at various temperatures. For these experiments, a constant amount of imine (27.5 mg, 0.122 mmol), catalyst (0.012 mmol), Hantzsch ester (0.146 mmol) and 4,4'-dimethylbiphenyl (0.122 mmol) were used while the reaction temperature was varied from 40-80 °C.

Reaction Temperature: 40 °C

Run #1:

Following representative procedure II, imine (27.3 mg, 0.121 mmol), catalyst (10.5 mg, 0.0122 mmol) and 4,4'-dimethylbiphenyl (22.4 mg, 0.123 mmol) in benzene heated to 40 °C and Hantzsch ester (37.0 mg, 0.146 mmol) added. Reaction sampled every 30 minutes for 480 minutes.

Reaction data:

$$k_{\text{initial}} = 2.006 \times 10^{-5} \text{ M/min}^{-1}$$

Time(min)	Area (std)	Area (pdt)	[pdt] (M)
30	571.16064	28.63650	0.00340917
60	739.62482	47.83702	0.00439784
90	739.17700	54.37664	0.00500208
120	738.77411	62.40548	0.00574378
150	676.88782	60.70488	0.00609809
182	708.31818	70.85033	0.00680143
210	918.88727	95.71320	0.00708266
240	595.88153	60.47773	0.00690117
274	760.07910	85.23110	0.00762476
303	589.78748	66.06036	0.00761609
335	662.28540	77.47519	0.00795434
365	685.24219	79.03014	0.00784216
390	661.15332	75.26059	0.00774020
420	734.01233	87.73637	0.00812762
451	643.59277	72.93298	0.00770548
481	605.86108	69.16721	0.00776272

Run #2:

Following representative procedure II, imine (27.8 mg, 0.123 mmol), catalyst (10.9 mg, 0.0126 mmol) and 4,4'-dimethylbiphenyl (22.2 mg, 0.122 mmol) in benzene heated to 40 °C and Hantzsch ester (37.0 mg, 0.146 mmol) added. Reaction sampled every 30 minutes for 420 minutes.

Reaction data:

$$k_{\text{initial}} = 2.404 \times 10^{-5} \text{ M/min}^{-1}$$

Time(min)	Area (std)	Area (pdt)	[pdt] (M)
30	661.83038	30.89101	0.00315489
60	690.81958	43.81554	0.00428708
90	732.95386	55.38557	0.00510761
120	679.08875	57.74845	0.00574794
150	632.50317	57.25140	0.00611817
180	652.28784	68.62114	0.00711077
210	817.65674	92.75174	0.00766742
240	658.97498	72.08146	0.00739355
270	654.32349	75.95528	0.00784628
300	693.91241	85.69823	0.00834767
330	687.77521	87.02325	0.00855238
360	632.43024	76.94823	0.00822402
390	681.70782	85.79404	0.00850662
420	737.25519	95.06595	0.00871576

Reaction Temperature: 60 °C**Run #1:**

Following representative procedure II, imine (27.5 mg, 0.122 mmol), catalyst (10.6 mg, 0.0122 mmol) and 4,4'-dimethylbiphenyl (22.4 mg, 0.123 mmol) in benzene heated to 60 °C and Hantzsch ester (37.0 mg, 0.146 mmol) added. Reaction sampled every five minutes for 90 minutes.

Reaction data:

$$k_{\text{initial}} = 1.450 \times 10^{-4} \text{ M/min}^{-1}$$

Time (min)	Area (std)	Area (pdt)	[pdt] (M)
5	556.53485	33.91317	0.00415594
10	594.31775	46.72368	0.00536181
15	675.60614	60.65401	0.00612293
20	633.40344	69.09070	0.00743931
25	830.34100	91.53220	0.00751814
30	704.86432	89.77643	0.00868660
35	761.09015	102.94744	0.00922513
40	666.64917	95.90195	0.00981123
45	823.32886	123.21080	0.01020631
50	740.96149	116.04078	0.01068091
55	573.40259	89.63885	0.01066178
60	672.44574	109.04047	0.01105920
65	831.33185	137.36177	0.01126898
70	663.74988	111.84735	0.01149250
75	757.57892	142.25775	0.01280682
80	493.36359	101.12933	0.01397987
85	973.29749	169.85378	0.01190208
90	901.10315	164.64977	0.01246177

Run #2:

Following representative procedure II, imine (27.6 mg, 0.123 mmol), catalyst (10.7 mg, 0.0124 mmol) and 4,4'-dimethylbiphenyl (22.2 mg, 0.122 mmol) in benzene heated to 60 °C and Hantzsch ester (37.0 mg, 0.146 mmol) added. Reaction sampled every five minutes for 90 minutes.

Reaction data:

$$k_{\text{initial}} = 1.631 \times 10^{-4} \text{ M/min}^{-1}$$

Time (min)	Area (std)	Area (pdt)	[pdt] (M)
5	657.35828	39.42118	0.00405346
10	709.71381	58.92029	0.00561151
16	660.88824	66.31219	0.00678209
21	662.74268	75.49848	0.00770001
26	615.57300	77.67064	0.00852856
30	769.30121	104.77410	0.00920568
35	602.81635	88.16499	0.00988574
40	797.27917	119.32735	0.01011644
45	830.81256	132.85574	0.01080875
50	695.06378	114.65273	0.01114956
55	864.50323	146.66768	0.01146743
61	710.49152	127.65093	0.01214404
65	1233.17261	224.46019	0.01230307
70	1268.59363	236.36865	0.01259405
75	752.16809	145.87318	0.01310867
80	718.05096	143.20180	0.01348005
85	632.59271	126.99739	0.01356965
90	904.48389	181.35330	0.01355261

Reaction Temperature: 70 °C

Run #1:

Following representative procedure II, imine (27.6 mg, 0.123 mmol), catalyst (10.7 mg, 0.0124 mmol) and 4,4'-dimethylbiphenyl (22.0 mg, 0.121 mmol) in benzene heated to 70 °C and Hantzsch ester (37.1 mg, 0.146 mmol) added. Reaction sampled every five minutes for 80 minutes.

Reaction data:

$$k_{\text{initial}} = 2.456 \times 10^{-4} \text{ M/min}^{-1}$$

Time (min)	Area (std)	Area (pdt)	[pdt] (M)
5	637.25000	44.97359	0.00472733
10	689.00189	63.68411	0.00619125
15	772.63025	88.25743	0.00765151
20	756.18048	100.67318	0.00891777
26	796.07037	120.53885	0.01014246
30	657.48315	106.45162	0.01084515
35	828.71082	143.24217	0.01157806
40	709.09210	131.97591	0.01246694
45	692.25793	137.78471	0.01333217
50	664.04102	138.87616	0.01400879
55	935.95801	201.74026	0.01443790
60	932.32135	206.94873	0.01486843
65	727.99359	168.20663	0.01547688
71	1124.30078	268.56339	0.01600045
76	960.14856	233.94205	0.01632066
80	752.71295	184.20399	0.01639221

Run #2:

Following representative procedure II, imine (27.5 mg, 0.122 mmol), catalyst (10.6 mg, 0.0122 mmol) and 4,4'-dimethylbiphenyl (23.5 mg, 0.128 mmol) in benzene heated to 70 °C and Hantzsch ester (37.0 mg, 0.146 mmol) added. Reaction sampled every five minutes for 80 minutes.

Reaction data:

$$k_{\text{initial}} = 2.925 \times 10^{-4} \text{ M/min}^{-1}$$

Time (min)	Area (std)	Area (pdt)	[pdt] (M)
5	768.06104	51.74697	0.00482061
10	806.44208	70.41950	0.00624788
15	714.68463	82.97021	0.00830655
20	731.63214	99.10799	0.00969235
25	797.47461	122.24255	0.01096778
30	661.48212	110.47239	0.01194947
35	1005.08905	179.77223	0.01279768
40	755.33002	140.56276	0.01331517
45	860.69678	169.27330	0.01407185
50	790.83331	163.46867	0.01478981
55	768.13000	165.06395	0.01537555
60	983.75159	216.52663	0.01574849
65	841.84491	190.67165	0.01620567
70	827.12939	192.19307	0.01662560
75	825.90002	195.34904	0.01692376
80	1214.34338	290.77887	0.01713304

Reaction Temperature: 80 °C

Run #1:

Following representative procedure II, imine (27.5 mg, 0.122 mmol), catalyst (10.8 mg, 0.0125 mmol) and 4,4'-dimethylbiphenyl (22.0 mg, 0.121 mmol) in benzene heated to 80 °C and Hantzsch ester (37.0 mg, 0.146 mmol) added. Reaction sampled every three minutes for 60 minutes.

Reaction data:

$$k_{\text{initial}} = 3.986 \times 10^{-4} \text{ M/min}^{-1}$$

Time (min)	Area (std)	Area (pdt)	[pdt] (M)
3	542.65576	40.97087	0.00505730
6	637.28119	54.83144	0.00576324
9	533.42596	59.52266	0.00747440
12	528.64917	70.32658	0.00891086
15	621.76929	90.50343	0.00974998
18	742.84161	119.19634	0.01074817
21	591.12476	105.04902	0.01190367
24	606.50189	115.72050	0.01278045
27	643.28564	126.06865	0.01312717
30	657.46960	139.44626	0.01420689
33	695.28430	153.90181	0.01482686
36	596.22296	136.53131	0.01533880
39	679.49054	164.63652	0.01622971
42	742.92554	184.98158	0.01667827
45	706.30072	179.34540	0.01700860
51	586.16479	156.22090	0.01785202
54	586.37146	161.52534	0.01845167
57	653.39240	183.54283	0.01881617
60	621.92627	177.22200	0.01908739

Run #2:

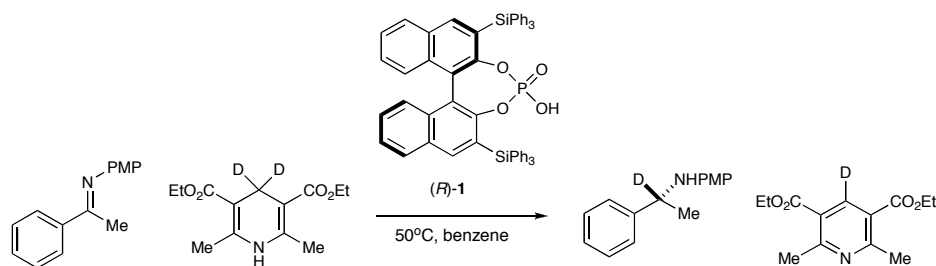
Following representative procedure II, imine (27.7 mg, 0.123 mmol), catalyst (10.6 mg, 0.0122 mmol) and 4,4'-dimethylbiphenyl (22.4 mg, 0.123 mmol) in benzene heated to 80 °C and Hantzsch ester (37.2 mg, 0.147 mmol) added. Reaction sampled every three minutes for 54 minutes.

Reaction data:

$$k_{\text{initial}} = 4.033 \times 10^{-4} \text{ M/min}^{-1}$$

Time (min)	Area (std)	Area (pdt)	[pdt] (M)
3	620.47766	38.58028	0.00424065
6	689.02136	59.01572	0.00584155
9	639.89447	69.24717	0.00738052
12	686.61377	86.29246	0.00857144
15	697.48114	96.53794	0.00943971
18	697.21069	105.42374	0.01031259
21	724.37848	121.95189	0.01148196
24	743.62408	134.38722	0.01232531
27	666.14703	128.75459	0.01318214
30	710.73840	142.82671	0.01370544
33	716.71729	154.09712	0.01466357
36	661.80835	146.81409	0.01512964
39	575.18158	131.88947	0.01563862
42	676.16553	162.62137	0.01640279
45	654.90045	156.52789	0.01630083
48	489.85712	121.12298	0.01686360
51	719.46234	184.74223	0.01751263
54	494.70078	129.47331	0.01784970

9. Determination of Kinetic Isotope Effect



The kinetic isotope effect for the imine reduction was determined by measuring the initial kinetic rate constant using d₂-Hantzsch ester. For these experiments, a constant amount of imine (27.5 mg, 0.122 mmol), catalyst (0.012 mmol), d₂-Hantzsch ester (0.146 mmol) and 4,4'-dimethylbiphenyl (0.122 mmol) was used at a reaction temperature of 50 °C.

Run #1:

Following representative procedure II, imine (27.8 mg, 0.123 mmol), catalyst (10.9 mg, 0.0125 mmol) and 4,4'-dimethylbiphenyl (22.3 mg, 0.122 mmol) in benzene heated to 50 °C and d₂-Hantzsch ester (37.3 mg, 0.146 mmol) added. Reaction sampled every 15 minutes for 660 minutes.

Reaction data:

$$k_{\text{initial}} = 2.004 \times 10^{-5} \text{ M/min}^{-1}$$

Time (min)	Area (std)	Area (pdt)	[pdt] (M)
15	638.9340	22.2052	0.00235966
30	670.0000	25.1513	0.00254880
45	503.2830	20.4579	0.00275993
60	708.0670	37.7414	0.00361904
75	781.3910	42.9312	0.00373039
90	555.7040	31.7661	0.00388124
105	734.1340	42.7515	0.00395390
138	639.5070	37.6282	0.00399501
165	567.0860	34.9934	0.00418974
195	527.6200	32.0411	0.00412322
225	766.5450	52.3752	0.00463915
285	713.7330	49.2035	0.00468069
315	584.4080	38.7237	0.00449895
349	631.9990	43.5442	0.00467804
391	764.0940	54.1225	0.00480929
540	688.3840	48.9562	0.00482866
600	760.9630	56.2021	0.00501463
660	701.3720	52.0436	0.00503813

Run #2:

Following representative procedure II, imine (27.8 mg, 0.123 mmol), catalyst (10.6 mg, 0.0122 mmol) and 4,4'-dimethylbiphenyl (21.9 mg, 0.120 mmol) in benzene heated to 50 °C and d₂-Hantzsch ester (37.4 mg, 0.146 mmol) added. Reaction sampled every ten minutes for 200 minutes.

Reaction data:

$$k_{\text{initial}} = 2.099 \times 10^{-5} \text{ M/min}^{-1}$$

Time (min)	Area (std)	Area (pdt)	[pdt] (M)
10	690.15765	23.24573	0.00231765
20	625.43146	23.05176	0.00253617
30	696.83105	32.60260	0.00321943
40	787.00824	37.50846	0.00327947
50	715.69849	37.95883	0.00364952
60	593.61041	31.43805	0.00364425
70	674.42041	38.54656	0.00393286
80	708.46643	42.19925	0.00409863
90	700.37579	44.60698	0.00438253
100	647.24048	41.92595	0.00445729
110	972.90436	63.63365	0.00450060
120	863.24170	59.34525	0.00473050
130	735.77557	49.22034	0.00460313
140	852.14404	58.18955	0.00469879
150	974.64984	66.66962	0.00470688
160	846.35492	59.90904	0.00487072
170	796.18079	57.08291	0.00493342
180	872.55255	60.64148	0.00478225
190	779.34674	54.05262	0.00477243
200	988.78424	68.95824	0.00479886

Run #3:

Following representative procedure II, imine (27.2 mg, 0.121 mmol), catalyst (10.6 mg, 0.0122 mmol) and 4,4'-dimethylbiphenyl (22.6 mg, 0.124 mmol) in benzene heated to 50 °C and d₂-Hantzsch ester (37.4 mg, 0.146 mmol) added. Reaction sampled every ten minutes for 180 minutes.

Reaction data:

$$k_{\text{initial}} = 2.068 \times 10^{-5} \text{ M/min}^{-1}$$

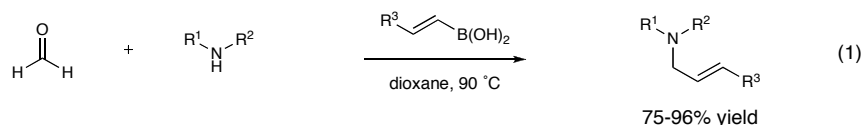
Time (min)	Area (std)	Area (pdt)	[pdt] (M)
10	730.61603	21.94008	0.00206634
20	714.24066	25.19121	0.00242693
30	739.54297	31.88877	0.00296707
40	711.86267	32.03493	0.00309657
50	802.75745	40.33631	0.00345753
60	865.05591	44.60720	0.00354825
70	642.85370	37.51810	0.00401589
80	854.58337	45.65367	0.00367599
90	817.24689	49.99718	0.00420965
100	732.03918	44.71857	0.00420346
110	1031.63513	62.69551	0.00418181
120	743.28094	49.82743	0.00461285
133	719.29401	46.83632	0.00448054
141	785.47107	53.79211	0.00471240
152	889.96545	64.53924	0.00499004
170	921.52527	65.09480	0.00486063
180	954.10663	72.80413	0.00525065

Chapter 4

Development of an Acid Promoted Addition of Organotrifluoroborates to Non-Activating Electrophiles

I. Introduction

Initially reported by Petasis in 1997, the boronic acid-Mannich reaction has proven to be a versatile three component coupling reaction, generating highly functionalized amine products from simple aldehyde, amine and boronic acid precursors (eq. 1).¹ In the years following this work, the Petasis reaction has seen widespread use in the chemical community where it has been applied to synthesis of both natural products and pharmaceutical agents.² A great deal of investigation has extended this methodology to include a wide range of primary and secondary amines along with aromatic, heteroaromatic and vinyl boronic acids. However, the aldehyde component of this transformation has been effectively limited to those containing a pendant heteroatom such as glyoxylate³, α -hydroxy⁴ and salicylaldehyde⁵ species (eq. 2-4). This limitation is



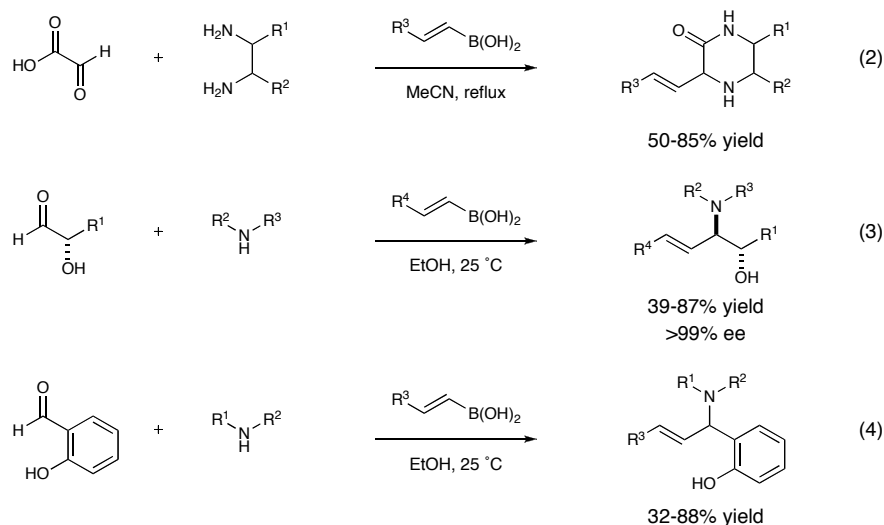
¹ Petasis, N. A.; Akritopoulou, I. *Tetrahedron Lett.* **1993**, 34, 583.

² For application to synthesis see: (a) Davis, A. S.; Pyne, S. G.; Skelton, B. W.; White, A. H. *J. Org. Chem.* **2004**, 69, 3139. (b) Sugiyama, S.; Arai, A.; Kiriya, M.; Ishii, K. *Chem. Pharm. Bull.* **2005**, 55, 100.

³ (a) Petasis, N. A. *J. Am. Chem. Soc.* **1997**, 119, 445. (b) Petasis, N. A.; Patel, Z. D. *Tetrahedron Lett.* **2000**, 41, 9607. (c) Piettre, S. R.; Jourdan, H.; Gouhier, G.; Hijfte, L. V.; Angibaud, P. *Tetrahedron Lett.* **2005**, 46, 8027. (d) Hutton, C. A.; Southwood, T. J.; Curry, M. C. *Tetrahedron* **2006**, 62, 236.

⁴ Petasis, N. A.; Zavialov, I. A. *J. Am. Chem. Soc.* **1998**, 120, 11798.

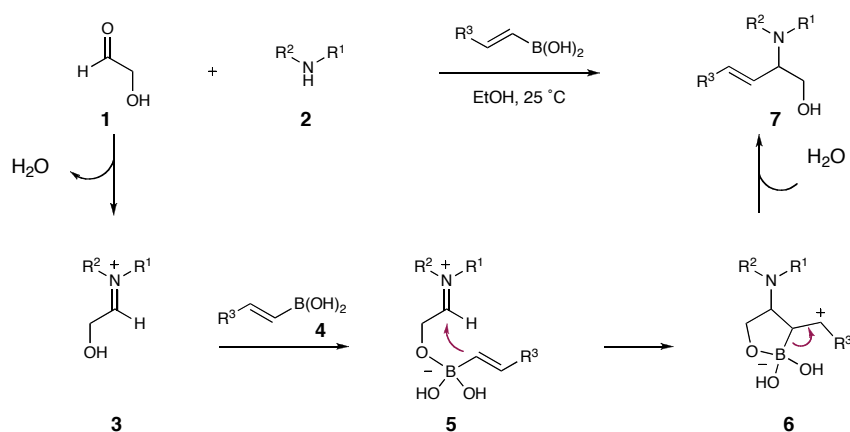
⁵ (a) Petasis, N. A.; Boral, S. *Tetrahedron Lett.* **2001**, 42, 539. (b) Finn, M. G.; Wang, Q. *Org. Lett.* **2000**, 2, 4063.



an inherent feature of this transformation, as illustrated by the reaction mechanism in Figure 1.

Following condensation of the aldehyde and amine starting materials **1** and **2**, the boronic acid **4** is coordinated by the α -heteroatom of iminium ion **3** to form the activated boronate complex **5**. Upon activation, intramolecular transfer of the boronic acid substituent to the iminium ion occurs to generate allylic amine product **7** following rehybridization and hydrolysis. The key mechanistic feature of the Petasis reaction is that

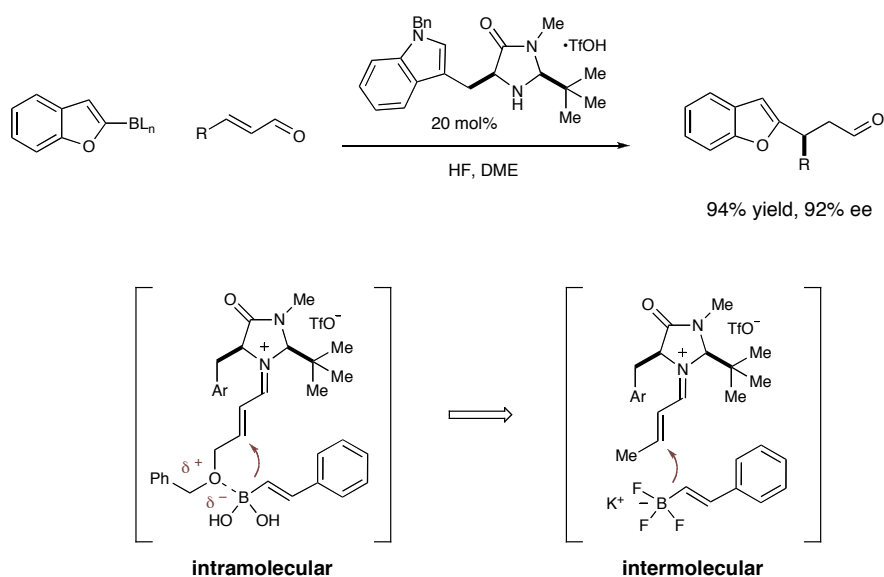
Figure 1: Mechanism of the Petasis reaction



intramolecular addition takes place only upon formation of the boronate complex, as a direct consequence, when non-coordinating aldehydes are used, no product was observed. In light of these observations, we postulated that starting from a preactivated boron species, such as an organotrifluoroborate salt,⁶ might circumvent this requirement and thereby expand the scope and utility of this transformation. Earlier reports from our lab on the organocatalytic Friedel-Crafts alkylation of α,β -unsaturated aldehydes with trifluoroborate salts⁷ effectively demonstrated the ability of these species to behave in such a manner, undergoing 1,4-addition to non-heteroatom functionalized iminium ions (Scheme 1).

While previous work has shown that trifluoroborate salts will undergo π -nucleophilic addition reactions through the proposed intermediacy of their dihalogenated

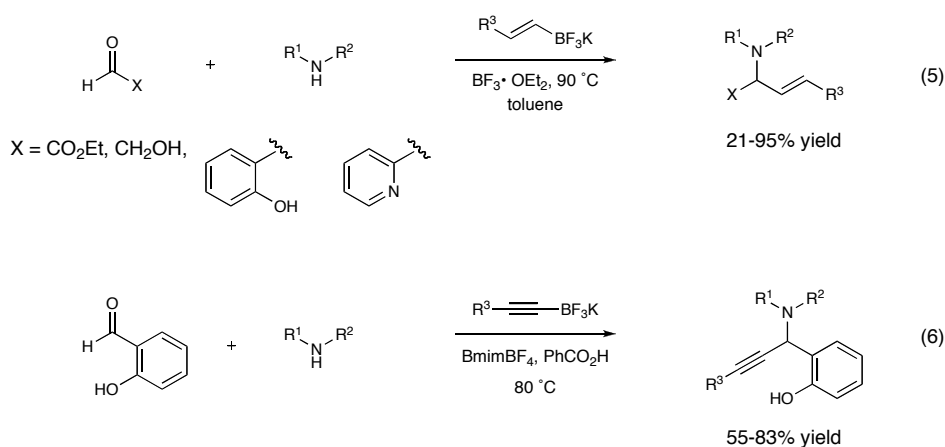
Scheme 1: Organocatalyzed Friedel-Crafts addition of organotrifluoroborates



⁶ For a recent review of organotrifluoroborates, see: Darses, S.; Genet, J-P. *Chem. Rev.* **2008**, *108*, 288.

⁷ Lee, S.; MacMillan, D. W. C. *J. Am. Chem. Soc.* **2007**, *129*, 15438.

equivalents under Lewis acid catalysis,⁸ this activation mode faces the same limitation as more traditional Petasis systems in that preassociation with the electrophile is required before addition occurs (eq. 5, 6). We wondered if the electrophile was instead subjected to Brønsted acid activation and the trifluoroborate salt was allowed to remain as the boronate species, one could overcome this limitation and obtain reactivity with non-heteroatom functionalized electrophiles.



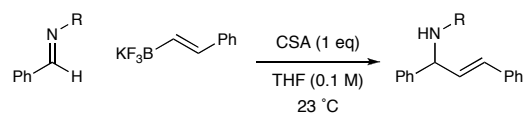
II. Development of an Organotrifluoroborate Petasis Reaction

Initial studies of the reaction of potassium *trans*-styryltrifluoroborate with variously protected aromatic aldimines and camphorsulfonic acid (CSA) indicated that the electronics of the non-activating electrophile plays a key role in determining the reactivity of the system (Table 1). It was found that only the carbamate protected imine gave appreciable amounts of the desired product, electron-rich protecting groups (PMP, Bn, entries 1, 3) and electron-poor protecting groups (tosyl, entry 2) gave no detectable

⁸ Lewis acid catalyzed organotrifluoroborate additions: (a) Raeppel S.; Tremblay-Morin, J-P. *Tetrahedron Lett.* **2004**, 45, 3471. (b) Kabalka, G. W.; Venkataiah, B.; Dong, G. *Tetrahedron. Lett.* **2004**, 45, 729. (c) Hansen, T. K.; Schlienger, N.; Bryce, M. R. *Tetrahedron Lett.* **2000**, 41, 1303.

amounts of the Petasis product. In addition to the Boc protecting group, the Cbz and methyl carbamate protecting groups were shown to perform equally well.

Table 1: Evaluation of nitrogen protecting groups

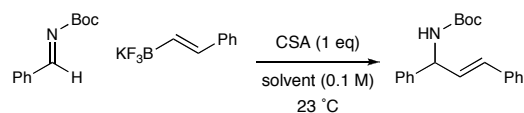


entry	R	solvent	time (h)	% conv. ^a
1	PMP	THF	24	0
2	Ts	THF	24	0
3	benzyl	THF	24	0
4	Boc	THF	24	12

^a Conversion determined by GLC analysis relative to an internal standard.

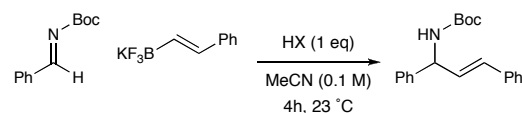
Solvent polarity was also found to play a key role in the observed levels of reactivity with highly polar solvents such as acetonitrile giving the greatest levels of conversion over shorter reaction times (Table 2, entry 7, 55% conv.). This result can be directly attributed to solubility effects as homogenous solutions of potassium trifluoroborate salt are only obtained in solvents with a high dielectric constant. Further examination of the Brønsted acid promoter revealed the importance of pKa trends in reaction efficiency (Table 3). A sufficiently acidic promoter is required for high levels of reactivity as protonation of the imine nitrogen is necessary for intermolecular addition of

Table 2: Effect of solvent on reactivity



entry	solvent	time (h)	% conv. ^a
1	THF	24	12
2	CH ₂ Cl ₂	24	36
3	CHCl ₃	24	48
4	toluene	24	16
5	Et ₂ O	24	21
6	DMF	24	0
7	MeCN	2	55

^a Conversion determined by GLC analysis relative to an internal standard.

Table 3: Evaluation of achiral Brønsted acids

entry	HX	pK _a ^a	% conv. ^b
1	camphorsulfonic acid	-2.17	40
2	trifluoroacetic acid	-0.25	86
3	dichloroacetic acid	1.29	68
4	2,4-dinitrobenzoic acid	1.42	54
5	benzoic acid	4.2	4
6	PPTS	5.21	42

^a Values in H₂O ^b Conversion determined by GLC analysis relative to an internal standard.

the trifluoroborate substituent (entries 2-7, 4-86% conv.). However, a highly acidic reaction media gives rise to a competing hydrodeboration reaction pathway, resulting in decomposition of the organotrifluoroborate starting material and low product yields (entry 1, 40% conv.). Trifluoroacetic acid (TFA) seems to be an ideal acid promoter; it is acidic enough to protonate the imine electrophile but at the same time does not exhibit appreciable amounts of hydrodeboration over the lifetime of the reaction (entry 2, 86% conv.).

While *trans*-styryl boronic acid derivatives are known to be particularly reactive in Petasis systems, we were pleased to find that a diverse range of trifluoroborate salts also participate in this reaction (Table 4). The less electron-rich *cis* and *trans* methyl vinyl organotrifluoroborates both undergo intermolecular addition in this system (entries 2-3, 63-68% yield) with retention of olefin geometry. Electron-rich heterocycles such as furan, *N*-Boc-pyrrole and 4-methylthiophene also undergo addition with good levels of reactivity (entries 5-7, 73-82% yield) with the use of cryogenic conditions serving to retard the rate of competing hydrodeboration of the trifluoroborate starting material. Similarly, in the case of electron-rich aromatics such as 4-methoxyphenyl trifluoroborate,

Table 4: Scope of vinyl and aryl trifluoroborate salt nucleophiles

entry	product	yield	entry	product	yield
1		94%	5 ^a		82%
2		63%	6 ^{a,b}		73%
3 ^a		68%	7 ^b		79%
4		85%	8 ^a		79%

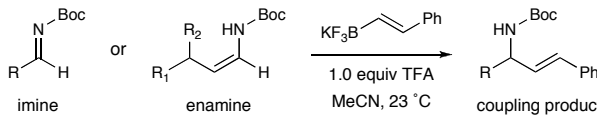
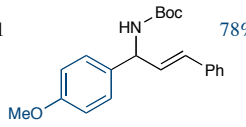
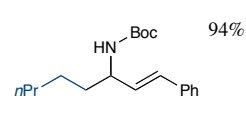
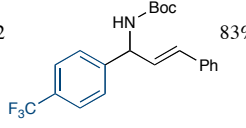
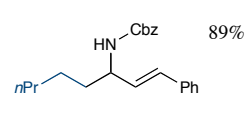
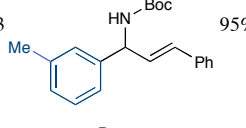
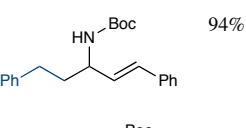
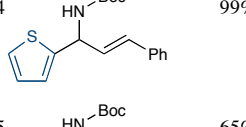
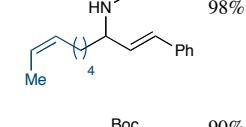
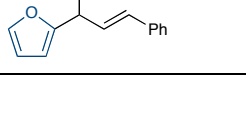
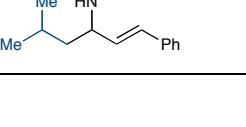
^a Performed with dichloroacetic acid ^b Performed at -20 °C.

dichloroacetic acid is used in place of TFA to limit this competing hydrodeboration pathway (entry 8, 79% yield).

Having shown that benzaldehyde derived imines react well with a variety of organotrifluoroborate nucleophiles, we next turned our attention to the goal of exploring the applicability of this methodology to diverse electrophile frameworks. In addition to the parent benzaldehyde imine, both the electron-rich 4-methoxy and electron-poor 4-trifluoromethyl substituted imines undergo reaction with good levels of efficiency (Table 5, entries 1-2, 78-83% yield) while substitution at the *meta* position is also well tolerated (entry 3, 95% yield). In addition to substituted phenyl systems, heteroaromatic imines also undergo net styrene addition with good levels of reactivity (Table 5, entries 4-5, 65-99% yield).

We next turned our attention toward applying this methodology to nonaromatic systems with the aim of accomplishing our goal of expanding the scope of this reaction to a wide range electrophiles. To our immense satisfaction, it was found that easily prepared alkyl enamines undergo reaction with styryl trifluoroborate (through their imine tautomer) upon exposure to trifluoroacetic acid in excellent yields and relatively short reaction times (Table 5, entries 6-10, 89-98% yield). It should also be noted that both the *tert*butyl and benzyl carbamate *N*-protecting groups can be used, with both furnishing the desired addition products with high levels of reactivity (entries 6-7). The use of such alkyl enamines represents a particularly valuable transformation, as this opens up an entirely new class of previously non-reactive substrates to Petasis functionalization.

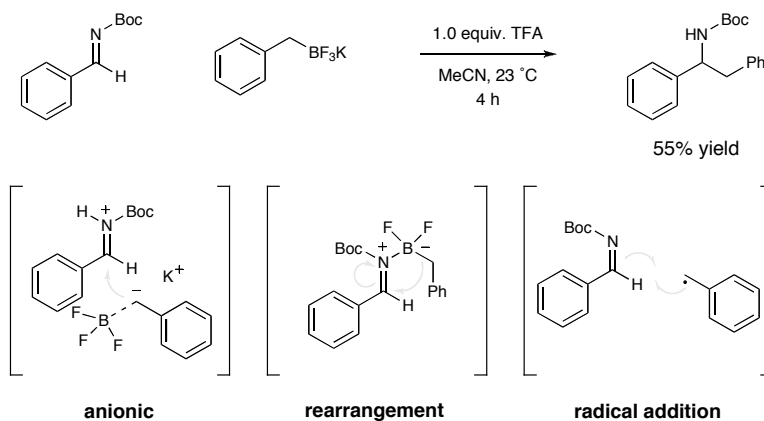
Table 5: Reaction scope with aryl imines and aliphatic enamines

					
entry	product	yield	entry	product	yield
1		78%	6		94%
2		83%	7		89%
3		95%	8		94%
4		99%	9		98%
5		65%	10		90%

III. Investigations into Reaction Mechanism

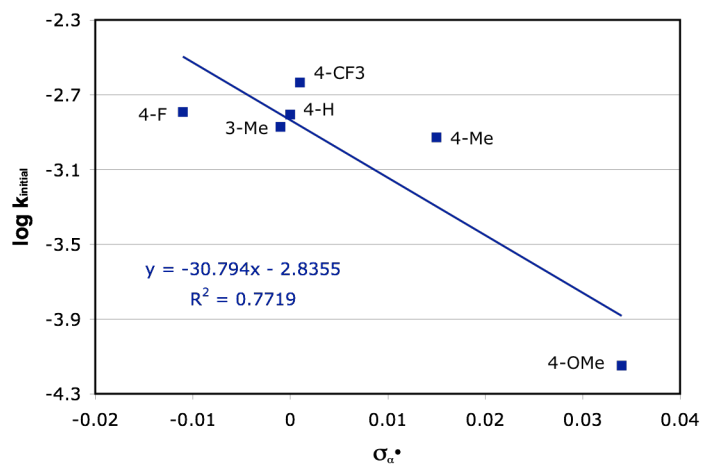
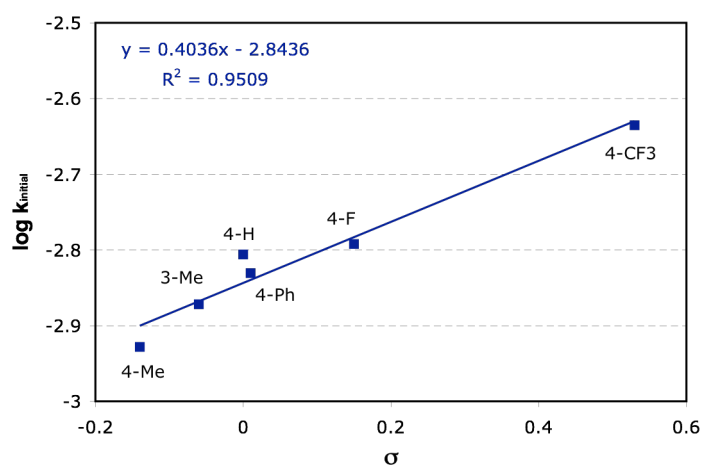
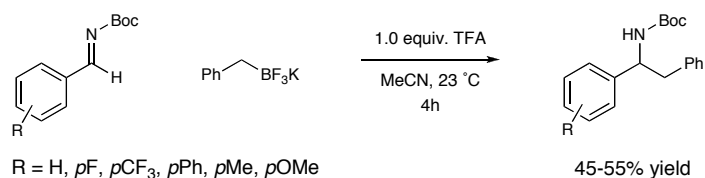
Much to our surprise, initial results revealed that potassium benzyltrifluoroborate also undergoes Petasis-type addition, albeit in moderate yield (Scheme 2). Due to the inability of this substrate to participate in a Friedel-Crafts type mechanism, this intriguing result raises the possibility of alternative mechanisms for trifluoroborate addition including anionic, rearrangement and radical addition pathways. In the anionic mechanism, polarization of the boron-carbon bond would lead to a localization of negative charge on the benzylic carbon, which could behave as a carbanionic nucleophile. An alternative mechanism, reminiscent of the classical Petasis mechanism, is that of intramolecular rearrangement of the benzylic group following coordination to the imine nitrogen. There is also the possibility of a one-electron radical addition mechanism, as it has been shown that a similar class of imine electrophiles are susceptible to such radical fragmentation pathways.⁹ In order to determine which reaction mechanism is in effect, a Hammett study probing the role of imine electronics on the rate of addition was undertaken (Figure 2).

Scheme 2: Acid promoted addition of benzyltrifluoroborate



⁹ Tan, K.L.; Jacobsen, E. N. *Angew. Chem. Int. Ed.* **2007**, *46*, 1315.

Figure 2: Hammett study of benzyl trifluoroborate addition

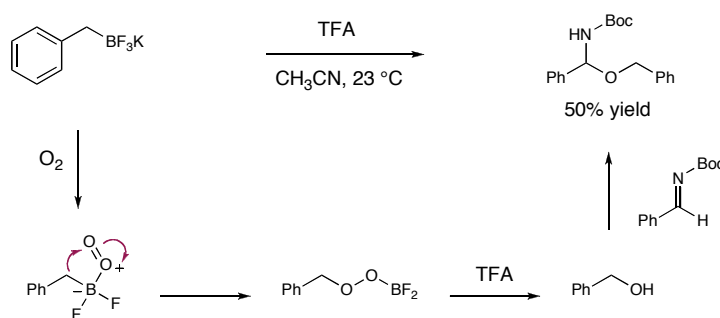


For this study a number of variously substituted imines were synthesized and the initial rate of their reaction with benzyl trifluoroborate at 0 °C was measured. If this reaction is proceeding through a two-electron mechanism, one would expect to see correlation with two electron Hammett constant σ . Conversely, if it proceeds through a one-electron mechanism, then better correlation should be seen with the single-electron

Hammett constant $\sigma_{\alpha^{\bullet}}$. As seen in Figure 2, better correlation is obtained with σ , indicating that this addition proceeds through a two-electron pathway. This suggests that either the anionic or rearrangement pathways are in effect for the addition of benzyltrifluoroborate.

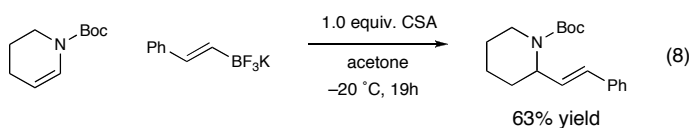
Additional evidence for the rearrangement pathway comes from the appearance of a significant amount of hemiaminal byproduct arising from the addition of benzyl alcohol to the imine electrophile (Figure 3). The appearance of benzyl alcohol from exposure of benzyltrifluoroborate to TFA at room temperature was confirmed by ^1H NMR and a possible mechanism for its formation is illustrated in Figure 3. Such a pathway has been proposed for the formation stable boronate radicals in the initiation phase of living polymerization,¹⁰ with the requirement that the concentration of oxygen remains lower than that of the boronate species. To test the validity of this alcohol formation mechanism, the reaction was run following extensive purging with argon to remove any remaining atmospheric oxygen in solution. Following this purging procedure, the formation of hemiaminal was completely repressed, however, product formation did not increase beyond the previously observed levels.

Figure 3: Mechanism of hemiaminal formation



¹⁰ Chung, T. C.; Janvikul, W.; Lu, H. L. *J. Am. Chem. Soc.* **1996**, *118*, 705.

In light of these mechanistic insights into the nature of benzyltrifluoroborate addition, the mechanism of π -nucleophilic organotrifluoroborate additions was examined. It was shown that a fully substituted cyclic enamine, containing no open coordination sites, also undergoes styryl addition under the standard reaction conditions (eq. 8). This result illustrates that while a rearrangement pathway is likely in effect for the addition of non π -nucleophilic trifluoroborates, traditional Petasis substrates are most likely undergoing a true intermolecular addition of the trifluoroborate substituent.

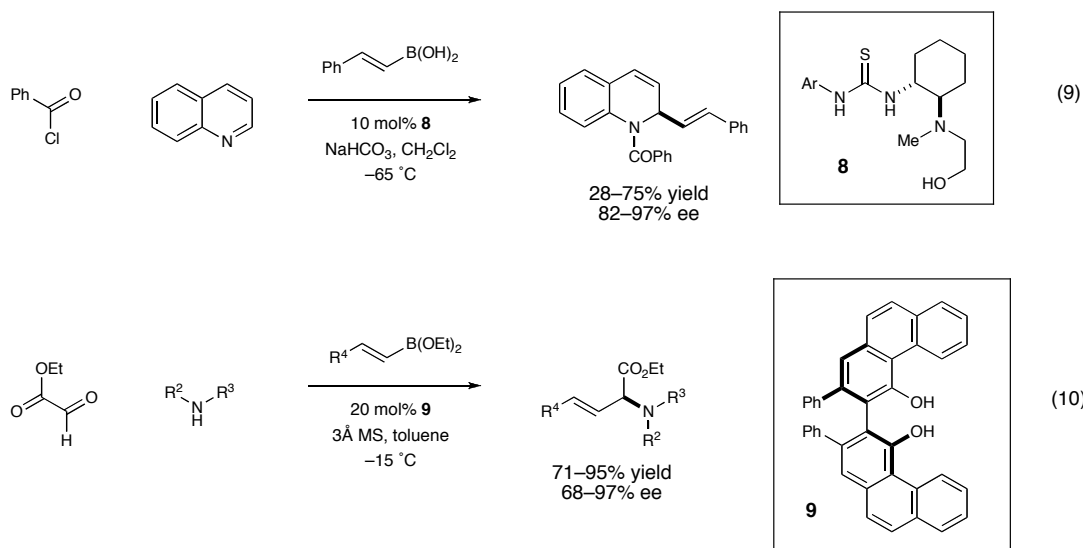


IV. Enantioselective Induction

As a direct consequence of the intramolecular transition state in the traditional Petasis system, high levels of diastereoselective induction can be achieved when starting from chiral aldehyde, amine and boronic ester starting materials.¹¹ Recent reports from the labs of Schaus and Takemoto have also described enantioselective variants of this transformation that rely on the creation of a chiral environment around the boron nucleophile through chelation of the boronic acid with a chiral catalyst (eq. 9, 10).¹² In the addition of organotrifluoroborates to non-activating electrophiles, the key protonation step to activate the imine to the iminium species was seen as a possible means to introduce enantioselectivity through the mediation of a Brønsted acid catalyst.

¹¹ (a) Scobie, M.; Koolmeister, T.; Soedergren, M. *Tetrahedron Lett.* **2002**, 43, 5969. (b) Hutton, C. A.; Southwood, T. J.; Curry, M. C. *Tetrahedron* **2006**, 62, 236.

¹² (a) Takemoto, Y.; Yamaoka, Y.; Miyabe, H. *J. Am. Chem. Soc.* **2007**, 129, 6686. (b) Schaus, S. E.; Lou, S. J. *J. Am. Chem. Soc.* **2008**, 130, 6922.



The addition of potassium styryltrifluoroborate to enamine **10** was used as the model system for initial investigations into enantioinduction. A preliminary examination of a number of differentially substituted (*R*)-BINOL derived phosphoric acid catalysts revealed that in addition to low levels of reactivity, no enantioinduction was achieved (Table 6).

Following these results, a number of structurally diverse classes of chiral

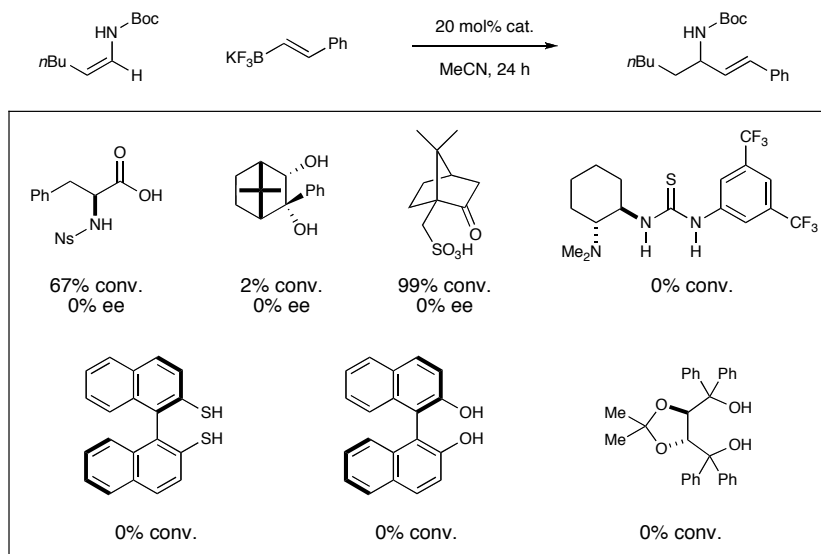
Table 6: Examination of chiral phosphoric acid catalysts

entry	cat.	cat. substitution (R)	temp (°C)	% conv. ^a	% ee ^b
1	11	SiPh ₃	23	24	0
2	12	1-naphthyl	23	15	2
3	13	3,5-OMe-phenyl	23	17	3
4	14	3,5-CF ₃ -phenyl	23	57	1
5	15	4-NO ₂ -phenyl	23	23	2
6	16	4-mesityl-phenyl	23	32	1
7	17	adamantyl	23	17	0

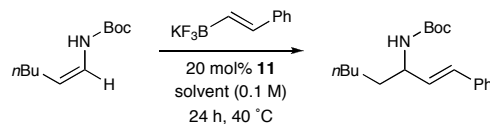
^a Determined by GLC analysis relative to an internal standard. ^b Determined by chiral SFC analysis.

hydrogen bonding and Brønsted acid catalysts such as (*R*)-BINOL, (–)-TADDOL, (+)-camphorsulfonic acid, thioureas and amino acids were investigated (Scheme 3). However, most of these catalysts were even less reactive than the previously examined phosphoric acids and those that did exhibit reactivity were completely non-selective.

Scheme 3: Evaluation of diverse acid catalyst structures



Returning to the more reactive class of chiral phosphoric acid catalysts, it was decided to examine the effect of solvent on reaction efficiency and enantioselectivity. Previous work on the reductive amination of ketones (Ch. 2) had revealed the dramatic effect of solvent polarity on the selectivity of transformations mediated by this family of catalysts. This is to be expected in the case of hydrogen bonding and acid mediated chiral induction as the necessary formation of hydrogen bonds and ion pairs is difficult to achieve in highly polar media. The use of non-polar aromatic solvents such as benzene and toluene with these BINOL derived acids also leads to higher conversion due to their

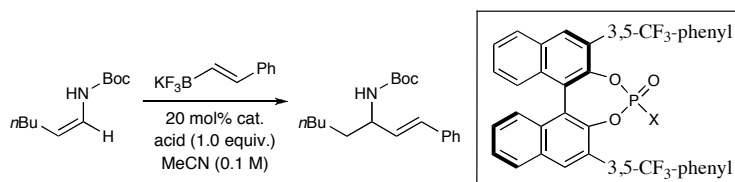
Table 7: The effect of solvent on acid catalyzed trifluoroborate addition

entry	solvent	% conv. ^a	% ee ^b
1	CH ₂ Cl ₂	26	0
2	benzene	10	0
3	acetone	29	0
4	toluene	11	0
5	MeCN	67	0

^a Determined by GLC analysis relative to an internal standard. ^b Determined by chiral SFC analysis.

increased solubility as homogenous reaction mixtures are generally not seen when these catalysts are used with non-aromatic solvents such as ethers and alkanes. Unfortunately, the use of benzene and toluene, even at elevated temperatures, led to a dramatic drop-off in reactivity (most likely attributable to insolubility of the organotrifluoroborate salt) and no enantioinduction was observed.

One possible explanation for these low observed levels of reactivity is the lack of a proton source for catalyst turnover. It was hypothesized that use of an achiral acid

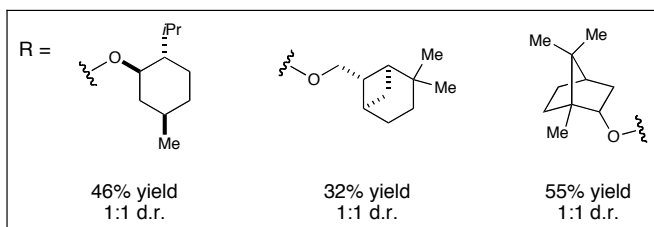
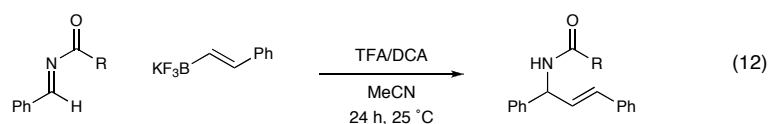
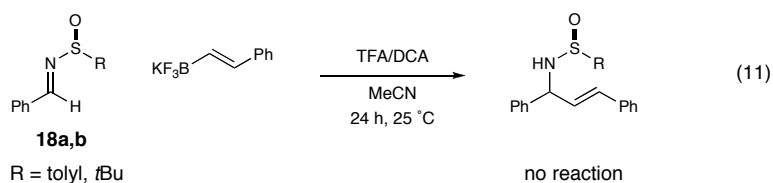
Table 8: Investigation into achiral acid additives to aid turnover

entry	achiral acid	X	temp (°C)	% conv. ^a	% ee ^b
1	camphorsulfonic acid	OH	23	46	0
2		NHTf	23	60	0
3	benzoic acid	OH	23	43	0
4		NHTf	23	33	0
5	<i>p</i> -toluenesulfonic acid	OH	23	28	0
6		NHTf	23	25	0
7	<i>p</i> -NO ₂ -benzoic acid	OH	23	37	0
8		NHTf	23	30	0

^a Determined by GLC analysis relative to an internal standard. ^b Determined by chiral SFC analysis.

additive could provide this necessary proton, leading to increased levels of reactivity. This hypothesis was examined using a combination of phosphoric acid or phosphoramidate catalysts as shown in Table 8 along with a number of achiral proton sources. Even though conversion levels improved with the use of achiral acid additives, the lack of enantioselectivity remained unchanged.

In light of these unsuccessful attempts to render organotrifluoroborate addition enantioselective via chiral acid catalysis, chiral auxiliary approaches were also explored. The chiral sulfinimines **18a-b**, used extensively by Ellman for the addition of a wide range of carbon nucleophiles,¹³ were synthesized and exposed to the standard reaction conditions (eq. 11). Neither TFA nor DCA were successful in mediating formation of the desired product; in both cases the unreacted sulfinimine starting material was recovered unchanged, even at temperatures up to 60 °C. The chiral carbamate protected substrates in equation 12 were able to undergo trifluoroborate addition with moderate levels of reactivity, however, no diastereomeric preference was observed.



¹³ Ellman, J. A.; Owens, T. D.; Tang, T. P. *Acc. Chem. Res.* **2002**, *35*, 984.

V. Conclusion

In conclusion, the first use of organotrifluoroborate salts as nucleophiles in the boronic acid-Mannich reaction has been demonstrated. This versatile reaction has a wide substrate scope with various aromatic, heteroaromatic and vinyl trifluoroborate species undergoing addition with high levels of efficiency. Through the use of these commercially available, air and moisture stable boronate salts, we have been able to greatly expand the scope of electrophiles used in this synthetically valuable and versatile transformation to include non-activating imines and enamines. Additional mechanistic studies have revealed that π -nucleophilic trifluoroborates undergo intermolecular addition to iminium electrophiles while the non- π -nucleophilic benzyl trifluoroborate undergoes intramolecular rearrangement following coordination to the imine nitrogen. Attempts to render the transformation enantioselective through chiral acid catalysis and chiral auxiliary approaches have proven to be unsuccessful.

Supporting Information

General Information. Commercially available organotrifluoroborates and trifluoroacetic acid were used without any further purification. Aromatic imines were prepared according to the procedure of Jacobsen¹⁴ while enamines were prepared according to the method of Terada.¹⁵ Tosyl imine was prepared according to the procedure of Kim¹⁶ while chiral sulfinimines were prepared according to the method of Ellman.¹³ Chiral carbamates were prepared according to literature procedure.¹⁷ All solvents were purified according to the method of Grubbs.¹⁸ Organic solutions were concentrated under reduced pressure on a Büchi rotary evaporator. Chromatographic purification of products was accomplished using flash chromatography on Silicycle 230-400 mesh silica gel. Thin-layer chromatography (TLC) was carried out on Silicycle 0.25mm silica gel plates. Visualization of the developed chromatogram was performed by fluorescence quenching or CAM staining.

¹H and ¹³C NMR spectra were recorded on Varian Mercury 300, 400 and Bruker 500 Spectrometers, and are internally referenced to residual protic solvent signals (CHCl₃ = 7.24 ppm). Data for ¹H are reported as follows: chemical shift (δ ppm), multiplicity (s = singlet, d = doublet, t = triplet, q = quartet, m = multiplet), integration, coupling

¹⁴ Jacobsen, E. N; Wenzel, A. G. *J. Am. Chem. Soc.* **2002**, *124*, 12964.

¹⁵ Terada, M.; Sorimachi, K. *J. Am. Chem. Soc.* **2007**, *129*, 292.

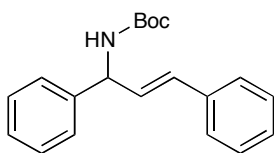
¹⁶ Kim, J. N.; Lee, K. Y.; Lee, C. G. *Tetrahedron Lett.* **2003**, *44*, 1231.

¹⁷ Synthesis of (–)-menthol derived carbamate: Hajra, S.; Bhowmick, M.; Maji, B.; Sinha, D. *J. Org. Chem.* **2007**, *72*, 4872.

¹⁸ Pangborn, A. B; Giardello, M.A.; Grubbs, R. H.; Rosen, R.K.; Timmers, F.J. *Organometallics* **1996**, *15*, 1518.

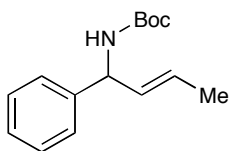
constant (Hz) and assignment. Data for ^{13}C NMR are reported in terms of chemical shift. IR spectra were recorded on a Perkin Elmer Paragon 1000 spectrometer and are reported in terms of frequency of absorption (cm^{-1}). Mass spectra were obtained from the Princeton Mass Spectroscopy Facility. Gas liquid chromatography (GLC) was carried out on a Hewlett-Packard 6850 Series gas chromatograph equipped with a splitmode capillary injection system and flame ionization detectors using a Varian HP-1 column (30 m x 0.25 mm).

General Procedure: A 20 mL oven-dried vial equipped with a magnetic stir bar was charged with imine (0.952 mmol, 2.0 equiv.) and acetonitrile (4.8 mL, 0.1 M) was added. Potassium organotrifluoroborate (0.476 mmol, 1.0 equiv.) was added followed by dropwise addition of either trifluoroacetic or dichloroacetic acid (0.476 mmol, 1.0 equiv.) and the reaction was stirred at room temperature until completion as determined by TLC monitoring. The crude reaction mixture was poured into a separatory funnel containing NaHCO_3 (sat. aq.) and extracted with CH_2Cl_2 (3 x 25 mL). The combined organic phase was dried (Na_2SO_4) and concentrated *in vacuo*. The product was purified by silica gel chromatography (solvents noted) to yield the title compounds.

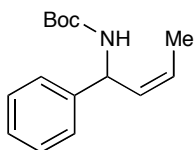


(E)-tert-butyl 1,3-diphenylallylcarbamate (Table 4, entry 1): Prepared according to the general procedure from potassium *trans*-styryltrifluoroborate (100 mg, 0.476 mmol) and benzaldehyde *N*-(*tert*-butoxycarbonyl)imine (195 mg, 0.952 mmol) at 23 °C for 4 h to

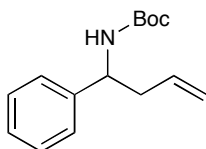
provide the title compound as a white solid (139 mg, 94% yield) following silica gel chromatography (5% Et₂O/petroleum ether). IR (film) 3376, 2976, 2926, 1680, 1502, 1456, 1362, 1295, 1234, 1163, 1156, 1025, 1039, 1012, 967, 886, 767, 738, 705 cm⁻¹; ¹H NMR (400 MHz, CDCl₃) δ 1.46 (s, 9H, -C(CH₃)₃), 4.98 (brs, 1H, -CHNH), 5.48 (brs, 1H, -CHNH), 6.33 (dd, 1H, *J* = 6.4, 16 Hz, -CHCHC₆H₅), 6.55 (d, 1H, *J* = 15.6 Hz, -CHCHC₆H₅), 7.39-7.24 (m, 10H, ArH); ¹³C NMR (125 MHz, CDCl₃) δ 27.27, 28.40, 126.54, 127.01, 127.58, 127.72, 128.56, 128.75, 129.59, 130.93; HRMS (EI) exact mass calculated for (C₂₀H₂₃NO₂) requires *m/z* 332.16265, found *m/z* 332.16222 [M+Na]⁺.



(*E*)-tert-butyl 1-phenylbut-2-enylcarbamate (Table 4, entry 2): Prepared according to the general procedure from potassium *trans*-methylvinyltrifluoroborate (100 mg, 0.676 mmol) and benzaldehyde *N*-(*tert*-butoxycarbonyl)imine (277 mg, 1.35 mmol) at 23 °C for 4 h to provide the title compound as a white solid (105 mg, 63% yield) following silica gel chromatography (3% Et₂O/petroleum ether). IR (film) 3354, 2979, 2934, 1682, 1513, 1494, 1449, 1389, 1364, 1293, 1246, 1165, 1041, 1016, 966, 744 cm⁻¹; ¹H NMR (400 MHz, CDCl₃) δ 1.44 (s, 9H, -C(CH₃)₃), 1.78 (d, 3H, *J* = 4.8 Hz, -CH₃), 4.86 (brs, 1H, -CHNH), 5.22 (brs, 1H, -CHNH), 5.64-5.60 (m, 2H, -CHCHCH₃), 7.36-7.24 (m, 5H, ArH); ¹³C NMR (125 MHz, CDCl₃) δ 17.74, 18.00, 28.17, 28.39, 56.19, 125.43, 126.79, 127.25, 128.55, 131.13; HRMS (EI) exact mass calculated for (C₁₅H₂₁NO₂) requires *m/z* 270.14700, found *m/z* 270.14649 [M+Na]⁺.

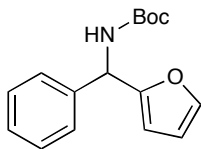


(Z)-tert-butyl 1-phenylbut-2-enylcarbamate (Table 4, entry 3): Prepared according to the general procedure from potassium *cis*-methylvinyltrifluoroborate (57.0 mg, 0.385 mmol) and benzaldehyde *N*-(*tert*-butoxycarbonyl)imine (158 mg, 0.770 mmol) at 23 °C for 4 h to provide the title compound as a white solid (64.9 mg, 68% yield) following silica gel chromatography (3% Et₂O/petroleum ether). IR (film) 3356, 2976, 2920, 1688, 1510, 1389, 1360, 1230, 1165, 1040, 1018, 799, 755, 697 cm⁻¹; ¹H NMR (300 MHz, CDCl₃) δ 1.44 (s, 9H, -C(CH₃)₃), 1.77 (d, 3H, *J* = 6.3 Hz, -CH₃), 4.83 (brs, 1H, -CHNH), 5.46-5.70 (m, 3H, -CHNH, -CHCHCH₃), 7.22-7.36 (m, 5H, ArH); ¹³C NMR (125 MHz, CDCl₃) δ 13.40, 17.74, 28.41, 126.34, 126.80, 127.14, 128.62, 130.74; HRMS (EI) exact mass calculated for (C₁₅H₂₁NO₂) requires *m/z* 270.14700, found *m/z* 270.14636 [M+Na]⁺.

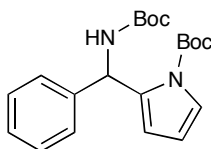


tert-butyl 1-phenylbut-3-enylcarbamate (Table 4, entry 4): To a solution of potassium allyltrifluoroborate (60.0 mg, 0.405 mmol) and benzaldehyde *N*-(*tert*-butoxycarbonyl)imine (108 mg, 0.527 mmol) in acetonitrile (8.1 mL, 0.05 M) at 0 °C was added dropwise trifluoroacetic acid (30.0 μL, .405 mmol). The reaction was let come to 23 °C and stirred for 1 h to provide the title compound as a white solid (85.0 mg,

85% yield) following standard workup procedure and silica gel chromatography (5% Et₂O/hexanes). ¹H NMR and ¹³C NMR data in accord with literature values.¹⁹



tert-butyl furan-2-yl(phenyl)methylcarbamate (Table 4, entry 5): Prepared according to the general procedure from potassium 2-furantrifluoroborate (127.1 mg, 0.731 mmol) and benzaldehyde *N*-(*tert*-butoxycarbonyl)imine (100 mg, 0.487 mmol) in acetonitrile (1.9 mL, 0.25 M) at 23 °C for 24 h to provide the title compound as a white solid (109 mg, 82% yield) following silica gel chromatography (5% Et₂O/petroleum ether). IR (film) 3367, 2979, 2932, 1687, 1515, 1499, 1457, 1389, 1368, 1299, 1241, 1168, 1149, 1130, 1076, 1043, 1021, 1006, 946, 872, 753 cm⁻¹; ¹H NMR (500 MHz, CDCl₃) δ 1.41 (s, 9H, -C(CH₃)₃), 5.96 (brd, 1H, *J* = 8.5 Hz, -CHNH), 6.17 (d, 1H, *J* = 3.0 Hz, ArH), 6.35 (t, 1H, *J* = 3.0 Hz, ArH), 6.90 (brs, 1H, -CHNH), 7.30 (m, 1H, ArH), 7.33-7.38 (m, 4H, ArH), 7.47 (s, 1H, ArH); ¹³C NMR (125 MHz, CDCl₃) δ 28.38, 52.66, 107.32, 110.24, 126.93, 127.74, 128.62, 142.39; HRMS (EI) exact mass calculated for (C₁₆H₁₉NO₃) requires *m/z* 273.13649 found *m/z* 273.13719 [M+Na]⁺.

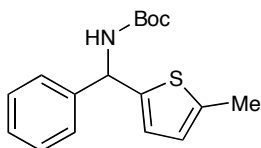


tert-butyl-2[(*tert*-butyl-carbonylamino)-phenylmethyl]-1H-pyrrole-1-carboxylate

(Table 4, entry 6): Prepared according to the general procedure from potassium 2-*N*-

¹⁹ Vilaivan, T.; Winotapan, C.; Banphavichit, V.; Shinada, T.; Ohfuné, Y. *J. Org. Chem.* **2005**, *70*, 3464.

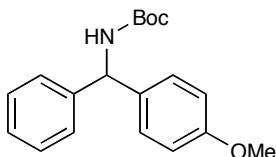
Boc-pyrroletetrafluoroborate (96.1 mg, 0.352 mmol) and benzaldehyde *N*-(*tert*-butoxycarbonyl)imine (108 mg, 0.528 mmol) in acetonitrile (2.3 mL, 0.15 M) at $-20\text{ }^{\circ}\text{C}$ for 24 h to provide the title compound as a white solid (95.4 mg, 73% yield) following silica gel chromatography (5% Et₂O/petroleum ether). IR (film) 3434, 2976, 2933, 1738, 1714, 1486, 1368, 1332, 1258, 1164, 1142, 1113, 1066, 1044, 1018, 882, 847, 770, 728, 700 cm^{-1} ; ¹H NMR (400 MHz, CDCl₃) δ 1.39 (s, 9H, -C(CH₃)₃), 1.48 (s, 9H, -C(CH₃)₃), 5.75 (brs, 1H, -CHNH), 6.15 (t, 1H, $J = 3.2\text{ Hz}$, ArH), 6.26 (brs, 1H, -CHNH), 6.38 (brd, 1H, $J = 9.2\text{ Hz}$, ArH), 7.12-7.29 (m, 6H, ArH); ¹³C NMR (125 MHz, CDCl₃) δ 27.69, 27.97, 28.48, 52.26, 109.95, 114.26, 122.56, 126.52, 126.93, 128.16, 132.15; HRMS (EI) exact mass calculated for (C₂₁H₂₈N₂O₂) requires m/z 411.16861, found m/z 411.18898 [M+K]⁺.



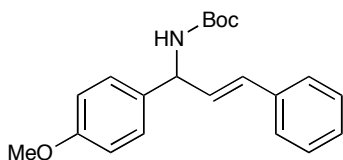
***tert*-butyl(5-methylthiophen-2-yl)(phenyl)methylcarbamate**

(Table 4, entry 7): Prepared according to the general procedure from potassium 2-(5-methyl)thiophenetetrafluoroborate (102.8 mg, 0.501 mmol) and benzaldehyde *N*-(*tert*-butoxycarbonyl)imine (154.2 mg, 0.751 mmol) at $-20\text{ }^{\circ}\text{C}$ for 24 h to provide the title compound as a white solid (120.4 mg, 79% yield) following silica gel chromatography (5% Et₂O/petroleum ether). IR (film) 3383, 2976, 2933, 1679, 1510, 1456, 1366, 1295, 1249, 1165, 1153, 1011, 869, 842, 757, 712 cm^{-1} ; ¹H NMR (400 MHz, CDCl₃) δ 1.45 (s, 9H, -C(CH₃)₃), 2.43 (s, 3H, -CH₃), 5.22 (brs, 1H, -CHNH), 6.03 (brs, 1H, -CHNH), 6.57 (m, 2H, ArH), 7.27-7.37 (m, 5H, ArH); ¹³C NMR (125 MHz, CDCl₃) δ 15.36, 28.37,

54.57, 119.72, 124.74, 125.10, 125.30, 126.82, 126.97, 127.40, 127.65, 128.59; HRMS (EI) exact mass calculated for (C₁₇H₂₁NO₂S) requires m/z 326.11907 found m/z 326.11847 [M+Na]⁺.



tert-butyl (4-methoxyphenyl)(phenyl)-1-methylcarbamate (Table 4, entry 8): To a solution of potassium 4-methoxyphenyltrifluoroborate (192.0 mg, 0.934 mmol) and benzaldehyde *N*-(*tert*-butoxycarbonyl)imine (100 mg, 0.467 mmol) at 23 °C was added dropwise dichloroacetic acid (115 μ L, 1.40 mmol). The reaction was stirred for 24 h to provide the title compound as a white solid (115.7 mg, 79% yield) following standard workup procedure and silica gel chromatography (5% Et₂O/hexanes). ¹H NMR and ¹³C NMR data in accord with literature values.²⁰

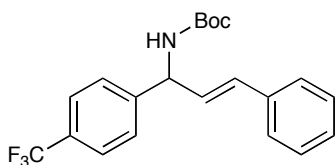


(E)-tert-butyl 1-(4-methoxyphenyl)-3-phenylallylcarbamate (Table 5, entry 1):

Prepared according to the general procedure from potassium *trans*-styryltrifluoroborate (100 mg, 0.476 mmol) and 4-methoxybenzaldehyde *N*-(*tert*-butoxycarbonyl)imine (224 mg, 0.952 mmol) at 23 °C for 24 h to provide the title compound as a white solid (126.6 mg, 78% yield) following silica gel chromatography (5–10% Et₂O/petroleum ether). IR (film) 3362, 2978, 2932, 2834, 1682, 1608, 1507, 1461, 1447, 1364, 1298, 1161, 1030,

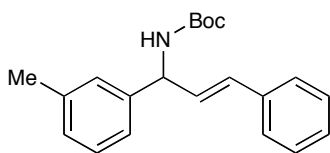
²⁰ Ellman, J. A.; Nakagawa, H.; Rech, J. C.; Sindelar, R. W. *Org. Lett.* **2007**, 9, 5155.

965, 885, 857, 830, 748, 727, 694 cm^{-1} ; ^1H NMR (500 MHz, CDCl_3) δ 1.46 (s, 9H, $-\text{C}(\text{CH}_3)_3$), 3.82 (s, 3H, $-\text{OCH}_3$), 4.93 (brs, 1H, $-\text{CHNH}$), 5.43 (brs, 1H, $-\text{CHNH}$), 6.32 (dd, 1H $J = 5, 15$ Hz, $-\text{CHCHC}_6\text{H}_5$), 6.53 (d, 1H, $J = 15$ Hz, $-\text{CHCHC}_6\text{H}_5$), 6.90 (d, 2H, $J = 5$ Hz, ArH), 7.31-7.23 (m, 5H, ArH), 7.37-7.39 (m, 2H, ArH); ^{13}C NMR (125 MHz, CDCl_3) δ 28.45, 55.36, 114.12, 114.39, 126.55, 127.67, 128.25, 128.58, 129.82, 130.66, 132.05, 133.55, 136.67, 159.03; HRMS (EI) exact mass calculated for $(\text{C}_{21}\text{H}_{25}\text{NO}_3)$ requires m/z 339.18344, found m/z 362.17285 $[\text{M}+\text{Na}]^+$.



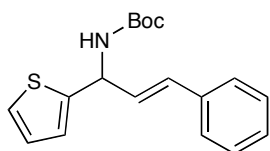
***E*)-tert-butyl 1-(4-trifluoromethylphenyl)-3-phenylallylcarbamate (Table 5, entry 2):**

Prepared according to the general procedure from potassium *trans*-styryltrifluoroborate (100 mg, 0.476 mmol) and 4-trifluoromethylbenzaldehyde *N*-(*tert*-butoxycarbonyl)imine (260 mg, 0.952 mmol) at 23 °C for 4 h to provide the title compound as a white solid (148.9 mg, 83% yield) following silica gel chromatography (5–10% Et_2O /petroleum ether). IR (film) 3363, 2980, 1683, 1619, 1513, 1448, 1421, 1390, 1366, 1323, 1296, 1158, 1120, 1108, 1067, 1017, 961, 896, 867, 840, 780, 767, 689 cm^{-1} ; ^1H NMR (500 MHz, CDCl_3) δ 1.48 (s, 9H, $-\text{C}(\text{CH}_3)_3$), 5.05 (brs, 1H, $-\text{CHNH}$), 5.54 (brs, 1H, $-\text{CHNH}$), 6.33 (dd, 1H $J = 20, 10$ Hz, $-\text{CHCHC}_6\text{H}_5$), 6.55 (d, 1H, $J = 20$ Hz, $-\text{CHCHC}_6\text{H}_5$), 7.28 (m, 1H, ArH), 7.34 (m, 2H, ArH), 7.39 (m, 2H, ArH), 7.50 (d, 2H, $J = 10$ Hz, ArH), 7.65 (d, 2H, $J = 10$ Hz, ArH); ^{13}C NMR (125 MHz, CDCl_3) δ 28.38, 56.10, 65.92, 125.71, 125.74, 126.58, 127.23, 128.11, 128.40, 128.68, 132.13; HRMS (EI) exact mass calculated for $(\text{C}_{21}\text{H}_{22}\text{F}_3\text{NO}_2)$ requires m/z 377.16026, found m/z 400.14942 $[\text{M}+\text{Na}]^+$.



(*E*)-tert-butyl 1-(3-methylphenyl)-3-phenylallylcarbamate (Table 5, entry 3):

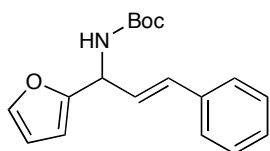
Prepared according to the general procedure from potassium *trans*-styryltrifluoroborate (100 mg, 0.476 mmol) and 3-methylbenzaldehyde *N*-(*tert*-butoxycarbonyl)imine (209 mg, 0.952 mmol) at 23 °C for 4 h to provide the title compound as a white solid (145.6 mg, 95% yield) following silica gel chromatography (5–10% Et₂O/petroleum ether). IR (film) 3343, 2978, 2933, 1678, 1606, 1511, 1448, 1391, 1366, 1333, 1281, 1252, 1164, 1040, 1017, 968, 865, 836, 780, 765, 736, 694 cm⁻¹; ¹H NMR (500 MHz, CDCl₃) δ 1.46 (s, 9H, -C(CH₃)₃), 2.36 (s, 3H, -CH₃), 4.96 (brs, 1H, -CHNH), 5.43 (brs, 1H, -CHNH), 6.32 (dd, 1H *J* = 5, 15 Hz, -CHCHC₆H₅), 6.55 (d, 1H, *J* = 15 Hz, -CHCHC₆H₅), 7.11 (m, 1H, ArH), 7.15 (m, 2H, ArH), 7.25 (m, 2H, ArH), 7.32 (m, 2H, ArH), 7.39 (m, 2H, ArH); ¹³C NMR (125 MHz, CDCl₃) δ 21.52, 28.43, 56.31, 65.92, 124.02, 126.56, 127.69, 127.77, 128.37, 128.57, 128.68, 129.72, 130.66; HRMS (EI) exact mass calculated for (C₂₁H₂₅NO₂) requires *m/z* 323.18853, found *m/z* 346.17758 [M+Na]⁺.



(*E*)-tert-butyl 1-(2-thiophenyl)-3-phenylallylcarbamate (Table 5, entry 4):

Prepared according to the general procedure from potassium *trans*-styryltrifluoroborate (100 mg, 0.476 mmol) and thiophene-2-carboxaldehyde *N*-(*tert*-butoxycarbonyl)imine

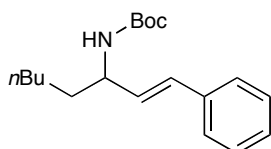
(203 mg, 0.952 mmol) at 23 °C for 24 h to provide the title compound as a white solid (134.1 mg, 99% yield) following silica gel chromatography (3–10% Et₂O/petroleum ether). IR (film) 3348, 2979, 2932, 1692, 1493, 1390, 1366, 1300, 1234, 1155, 1045, 1017, 964, 878, 846, 827, 765, 752, 742 cm⁻¹; ¹H NMR (500 MHz, CDCl₃) δ 1.48 (s, 9H, -C(CH₃)₃), 5.02 (brs, 1H, -CHNH), 5.71 (brs, 1H, -CHNH), 6.36 (dd, 1H *J* = 6, 16 Hz, -CHCHC₆H₅), 6.65 (d, 1H, *J* = 16 Hz, -CHCHC₆H₅), 6.98 (m, 2H, ArH), 7.25 (m, 2H, ArH), 7.33 (m, 2H, ArH), 7.40 (m, 2H, ArH); ¹³C NMR (125 MHz, CDCl₃) δ 28.41, 52.12, 124.77, 124.93, 126.68, 127.03, 127.91, 128.62, 128.67, 131.31, 136.37, 145.45, 154.79; HRMS (EI) exact mass calculated for (C₁₈H₂₁NO₂S) requires *m/z* 315.1293, found *m/z* 315.12976 [M+Na]⁺.



(*E*)-tert-butyl 1-(2-furanyl)-3-phenylallylcarbamate (Table 5, entry 5):

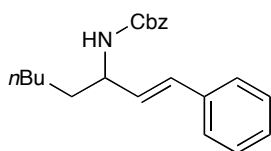
Prepared according to the general procedure from potassium *trans*-styryltrifluoroborate (53.8 mg, 0.256 mmol) and furfural *N*-(*tert*-butoxycarbonyl)imine (75.0 mg, 0.384 mmol) at -10 °C for 5 h to provide the title compound as a white solid (49.9 mg, 65% yield) following silica gel chromatography (10–20% Et₂O/petroleum ether). IR (film) 3360, 2975, 2933, 1685, 1513, 1499, 1389, 1364, 1308, 1240, 1163, 1152, 1076, 1044, 1011, 962, 950, 877, 862, 692 cm⁻¹; ¹H NMR (500 MHz, CDCl₃) δ 1.48 (s, 9H, -C(CH₃)₃), 5.05 (brs, 1H, -CHNH), 5.59 (brs, 1H, -CHNH), 6.25 (d, 1H, *J* = 4 Hz, ArH) 6.30–6.35 (m, 2H, ArH, -CHCHC₆H₅), 6.58 (d, 1H, *J* = 16 Hz, -CHCHC₆H₅), 7.25 (d, 1H, *J* = 7 Hz, ArH), 7.32 (t, 2H, *J* = 7 Hz, ArH), 7.39 (m, 3H, ArH); ¹³C NMR (125 MHz, CDCl₃) δ

28.42, 106.63, 110.34, 126.64, 126.97, 127.86, 128.59, 131.35, 136.49, 142.33, 153.53, 154.91; HRMS (EI) exact mass calculated for (C₁₈H₂₁NO₃) requires m/z 299.15214, found m/z 299.15316 [M+Na]⁺.



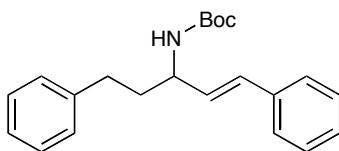
(E)-tert-butyl 1-phenyloct-1-en-3-ylcarbamate (Table 5, entry 6):

Prepared according to the general procedure from potassium *trans*-styryltrifluoroborate (100 mg, 0.476 mmol) and *tert*-butyl hex-1-enylcarbamate (mixture of *E* and *Z* isomers) (190.0 mg, 0.952 mmol) at 23 °C for 4 h to provide the title compound as a clear oil (137.1 mg, 94% yield) following silica gel chromatography (2.5% EtOAc/petroleum ether). IR (film) 3363, 2955, 2929, 2858, 1683, 1512, 1453, 1390, 1369, 1303, 1277, 1246, 1165, 1116, 1042, 1017, 964, 864, 777, 747, 693 cm⁻¹; ¹H NMR (400 MHz, CDCl₃) δ 0.89 (t, 3H, *J* = 6 Hz, -CH₃), 1.46 (s, 9H, -C(CH₃)₃), 1.31-1.50 (m, 8H, -(CH₂)₄), 4.26 (brs, 1H, -CHNH), 4.53 (brs, 1H, -CHNH), 6.09 (dd, 1H, *J* = 10, 16Hz, -CHCHC₆H₅), 6.51 (d, 1H, *J* = 16 Hz, -CHCHC₆H₅), 7.21-7.38 (m, 5H, ArH); ¹³C NMR (125 MHz, CDCl₃) δ 14.01, 22.61, 24.45, 25.53, 28.44, 31.65, 35.63, 126.37, 127.44, 128.54, 129.81, 136.91, 195.53; HRMS (EI) exact mass calculated for (C₁₉H₂₉NO₂) requires m/z 303.21983, found m/z 303.2205 [M+Na]⁺.



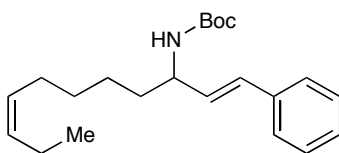
(E)-benzyl 1-phenyloct-1-en-3-ylcarbamate (Table 5, entry 7):

Prepared according to the general procedure from potassium *trans*-styryltrifluoroborate (100 mg, 0.476 mmol) and benzyl hex-1-enylcarbamate (mixture of *E* and *Z* isomers) (222.0 mg, 0.952 mmol) at 23 °C for 6 h to provide the title compound as a clear oil (142.4 mg, 89% yield) following silica gel chromatography (5–10% Et₂O/petroleum ether). IR (film) 3304, 3032, 2950, 2926, 2856, 1682, 1553, 1495, 1466, 1454, 1300, 1247, 1114, 1044, 1027, 964, 909, 832, 748, 727, 693 cm⁻¹; ¹H NMR (400 MHz, CDCl₃) δ 0.83–0.90 (m, 5H, -CH₂CH₃), 1.30–1.38 (m, 6H, -(CH₂)₃), 4.34 (brs, 1H, -CHNH), 4.76 (brs, 1H, -CHNH), 5.13 (brs, 2H, -OCH₂Ph), 6.10 (dd, 1H, *J* = 8, 20 Hz, -CHCHC₆H₅) 6.55 (d, 1H, *J* = 20 Hz, -CHCHC₆H₅), 7.21–7.37 (m, 10H, ArH); ¹³C NMR (125 MHz, CDCl₃) δ 14.09, 22.58, 25.47, 31.61, 35.50, 53.10, 66.77, 126.41, 127.57, 128.56, 130.22, 136.50, 136.70, 195.54; HRMS (EI) exact mass calculated for (C₂₂H₂₇NO₂) requires *m/z* 337.20418, found *m/z* 337.20465 [M+Na]⁺.

**(E)-tert-butyl 1,5-diphenylpent-1-en-3-ylcarbamate (Table 5, entry 8):**

Prepared according to the general procedure from potassium *trans*-styryltrifluoroborate (100 mg, 0.476 mmol) and *tert*-butyl 3-phenylprop-1-enylcarbamate (mixture of *E* and *Z* isomers) (222.0 mg, 0.952 mmol) at 23 °C for 4 h to provide the title compound as a white solid (149.9 mg, 94% yield) following silica gel chromatography (5% Et₂O/petroleum ether). IR (film) 3318, 2980, 2932, 1679, 1524, 1494, 1453, 1433, 1391, 1365, 1246, 1163, 1045, 1026, 969, 866, 742, 693 cm⁻¹; ¹H NMR (500 MHz, CDCl₃) δ

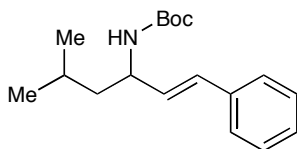
1.47 (s, 9H, $-\text{C}(\text{CH}_3)_3$), 1.92 (brs, 2H, $-\text{CH}_2\text{CH}_2\text{Ph}$), 2.72 (m, 2H, $-\text{CH}_2\text{CH}_2\text{Ph}$), 4.34 (brs, 1H, $-\text{CHNH}$), 4.59 (brs, 1H, $-\text{CHNH}$), 6.13 (dd, 1H, $J = 10, 15$ Hz, $-\text{CHCHC}_6\text{H}_5$) 6.55 (d, 1H, $J = 15$ Hz, $-\text{CHCHC}_6\text{H}_5$), 7.20-7.22 (m, 3H, ArH), 7.24-7.32 (m, 5H, ArH), 7.37-7.38 (m, 2H, ArH); ^{13}C NMR (125 MHz, CDCl_3) δ 28.33, 28.37, 28.45, 32.29, 37.17, 37.34, 52.35, 125.99, 126.08, 126.42, 127.59, 128.44, 128.51, 128.58, 128.78, 130.36, 136.80, 141.60; HRMS (EI) exact mass calculated for $(\text{C}_{22}\text{H}_{27}\text{NO}_2)$ requires m/z 337.20418, found m/z 337.20447 $[\text{M}+\text{Na}]^+$.



***tert*-butyl (1*E*, 8*Z*)-1-phenylundeca-1,8-dien-3-ylcarbamate (Table 5, entry 9):**

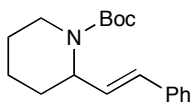
Prepared according to the general procedure from potassium *trans*-styryltrifluoroborate (100 mg, 0.476 mmol) and *tert*-butyl nona-1,8-dienylcarbamate (mixture of *E* and *Z* isomers) (228.0 mg, 0.952 mmol) at 23 °C for 4 h to provide the title compound as a clear oil (161.0 mg, 98% yield) following silica gel chromatography (1–5% Et_2O /petroleum ether). IR (film) 3377, 2978, 2965, 2934, 2856, 1687, 1504, 1460, 1447, 1388, 1364, 1304, 1235, 1165, 1053, 1003, 985, 914, 862, 750, 693 cm^{-1} ; ^1H NMR (500 MHz, CDCl_3) δ 0.94–0.97 (m, 3H, $-\text{CH}_3$), 1.39 (m, 4H, $-(\text{CH}_2)_2$), 1.45 (s, 9H, $-\text{C}(\text{CH}_3)_3$), 2.00–2.04 (m, 6H, $-(\text{CH}_2)_3$), 4.26 (brs, 1H, $-\text{CHNH}$), 4.54 (brs, 1H, $-\text{CHNH}$), 5.34 (m, 2H, $-\text{CH}_2\text{CHCHCH}_2-$), 6.09 (dd, 2H, $J = 5, 15$ Hz, $-\text{CHCHC}_6\text{H}_5$) 6.51 (d, 1H, $J = 15$ Hz, $-\text{CHCHC}_6\text{H}_5$), 7.23 (dd, 1H, $J = 10$ Hz, ArH), 7.30 (dd, 2H, $J = 5, 10$ Hz, ArH), 7.37 (d, 2H, $J = 10$ Hz, ArH); ^{13}C NMR (125 MHz, CDCl_3) δ 14.39, 20.54, 25.49, 26.99, 28.31, 28.45, 29.55, 35.58, 126.39, 127.46, 128.54, 128.88, 129.91, 130.76, 131.88, 136.93;

HRMS (EI) exact mass calculated for ($C_{22}H_{33}NO_2$) requires m/z 343.25113, found m/z 343.25176 $[M+Na]^+$.



(*E*)-tert-butyl 5-methyl-1-phenylhex-1-en-3-ylcarbamate (Table 5, entry 10):

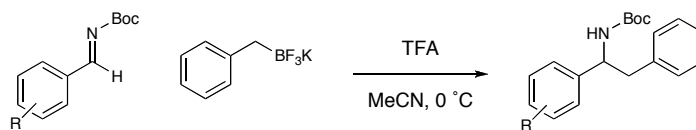
Prepared according to the general procedure from potassium *trans*-styryltrifluoroborate (100 mg, 0.476 mmol) and *tert*-butyl 4-methylpent-1-enylcarbamate (mixture of *E* and *Z* isomers) (176.0 mg, 0.952 mmol) at 23 °C for 4 h to provide the title compound as a clear oil (123.8.0 mg, 90% yield) following silica gel chromatography (3% Et₂O/petroleum ether). IR (film) 3321, 2976, 2951, 2934, 1685, 1534, 1494, 1389, 1364, 1273, 1249, 1166, 1124, 1049, 1027, 966, 877, 741, 690 cm⁻¹; ¹H NMR (500 MHz, CDCl₃) δ 0.956 (dd, 6H, J = 2, 25 Hz, -CH(CH₃)₂), 1.06 (dd, 2H, J = 5, 25, Hz, -CH₂CH(CH₃)₂), 1.46 (s, 9H, -C(CH₃)₃), 1.71 (m, 1H, -CH₂CH(CH₃)₂), 4.33 (brs, 1H, -CHNH), 4.49 (brs, 1H, -CHNH), 6.07 (dd, 1H, J = 15, 10Hz, -CHCHC₆H₅) 6.52 (d, 1H, J = 15 Hz, -CHCHC₆H₅), 7.23 (m, 1H, ArH), 7.31 (m, 2H, ArH), 7.37 (d, 2H, J = 10 Hz, ArH); ¹³C NMR (125 MHz, CDCl₃) δ 22.63, 22.92, 24.78, 24.97, 25.34, 27.19, 28.36, 28.38, 28.44, 44.81, 50.76, 126.37, 127.44, 128.53, 129.71, 130.97; HRMS (EI) exact mass calculated for ($C_{18}H_{27}NO_2$) requires m/z 289.20418, found m/z 289.20432 $[M+Na]^+$.



tert-butyl 2-styrylpiperidine-1-carboxylate: Prepared according to the general procedure from potassium *trans*-styryltrifluoroborate (15.0 mg, 0.0714 mmol) and *N*-

(*tert*-butoxycarbonyl)-1,2,3,4-tetrahydropyridine²¹ (26.2 mg, 0.143 mmol) at –20 °C for 19 h to provide the title compound as a clear oil (123.8.0 mg, 90% yield) following silica gel chromatography (3% Et₂O/petroleum ether). Reaction conversion determined by achiral GLC analysis on a Varian HP-1 column IR relative to 4,4'-dimethylbiphenyl. (film) 2940, 2920, 2855, 1681, 1449, 1398, 1364, 1326, 1275, 1252, 1240, 1157, 1117, 1090, 1039, 1012, 969, 961, 929, 870, 769, 757, 748, 708 cm⁻¹; ¹H NMR (500 MHz, CDCl₃) δ 1.49 (s, 9H, -C(CH₃)₃), 1.52-1.63 (m, 4H, -CH(CH₂)₃CH₂NH-), 1.74-1.86 (m, 2H, -CH(CH₂)₃CH₂NH-), 2.92 (t, 1H, *J* = 13 Hz, -CH(CH₂)₃CH₂NH-), 4.01 (brd, 1H, *J* = 12 Hz, -CH(CH₂)₃CH₂NH), 4.97 (brs, 1H, -CHNH), 6.19 (dd, 1H, *J* = 16, 5 Hz, -CHCHC₆H₅) 6.40 (d, 1H, *J* = 16 Hz, -CHCHC₆H₅), 7.22-7.25 (m, 1H, ArH), 7.31-7.38 (m, 4H, ArH); ¹³C NMR (125 MHz, CDCl₃) δ 19.71, 25.58, 28.50, 29.54, 79.49, 126.25, 127.39, 128.58, 128.74, 130.70; HRMS (EI) exact mass calculated for (C₁₈H₂₇NO₂) requires *m/z* 287.18853, found *m/z* 310.17767 [M+Na]⁺.

Reactions with Potassium Benzyltrifluoroborate

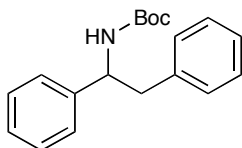


General procedure: To a rigorously degassed solution of potassium benzyltrifluoroborate (50.0 mg, 0.252 mmol) and benzaldehyde *N*-(*tert*-butoxycarbonyl)imine (104 mg, 0.505 mmol) in acetonitrile (2.5 mL, 0.1 M) at 23 °C was added dropwise trifluoroacetic acid (19 µL, 0.252 mmol). The reaction was stirred at

²¹ Prepared according to: Dieter, K. R.; Sharma, R. R. *J. Org. Chem.* **1996**, 61, 4180.

23 °C for 4 h, then the crude reaction mixture was poured into a separatory funnel containing NaHCO₃ (sat. aq.) and extracted with CH₂Cl₂ (3 × 25 mL). The combined organic phase was dried (Na₂SO₄), concentrated *in vacuo* and purified via silica gel chromatography (5% Et₂O/hexanes) to give the desired product as a white solid (39.6 mg, 50% yield).

Determination of initial reaction rates: To an oven dried vial was added standardized solutions of benzyl trifluoroborate (0.300 mmol, 0.74 mL), 4,4'-dimethylbiphenyl (0.075 mmol, 0.88 mL) and imine (0.450 mmol, 0.62 mL) in acetonitrile. The reaction was diluted to a total volume of 3.0 mL with acetonitrile, sealed with a septa cap, cooled to 0 °C and purged with argon for 20 minutes. Trifluoroacetic acid (0.300 mmol, 22.3 µL) was added dropwise and the reaction was sampled at the indicated time periods. Sampling was accomplished by withdrawing 0.10 mL of crude reaction mixture via syringe and filtering through a plug of silica gel with Et₂O. The amount of product present was determined via GLC analysis relative to the internal standard on a Varian HP-1 column.



(N)-tert-butoxycarbonyl α-benzyl-benzylamine: ¹H NMR and ¹³C NMR data in accord with literature values.²² Conversion factor for initial rate determination: 0.6182833 mmol product / 4,4'-dimethylbiphenyl.

²² Beak, P.; Park, Y. S.; Boys, M.L. *J. Am. Chem. Soc.* **1996**, *118*, 3757.

Run #1: $k_{\text{initial}} = 1.57 \times 10^{-3} \text{ M/min}^{-1}$

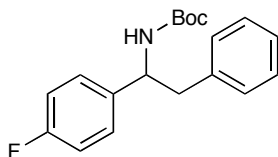
Time (min)	Area std	Area pdt	% pdt	mmol pdt
0	0	0	0	0
2	989.206	95.6969	1.49533553	0.00448601
4	2830.88	492.046	2.68665419	0.00805996
6	1634.67	408.59	3.8635378	0.01159061
8	1888.07	593.887	4.86198094	0.01458594
10	1858.37	672.771	5.59580538	0.01678742
12	2901.9	1189.1	6.33378711	0.01900136
14	1847.43	845.485	7.07400627	0.02122202
16	2192.12	1076.99	7.59407481	0.02278222
20	1495.66	836.098	8.64075777	0.02592227
25	2666.8	869.129	5.03757262	0.01511272
30	2194.6	1403.8	9.88729263	0.02966188

Run #2: $k_{\text{initial}} = 1.59 \times 10^{-3} \text{ M/min}^{-1}$

Time (min)	Area std	Area pdt	% pdt	mmol pdt
0	0	0	0	0
2	1431.19	155.688	1.68145547	0.00504437
4	1440.64	251.977	2.70354098	0.00811062
6	1622.65	406.255	3.86991468	0.01160974
8	1831.56	550.617	4.6468215	0.01394046
10	1966.86	686.274	5.39326329	0.01617979
12	2207.34	838.733	5.8732978	0.01761989
14	2132.35	882.219	6.39507204	0.01918522
16	2404.74	1034.01	6.64636421	0.01993909
20	2268.55	1053.62	7.17898713	0.02153696
25	1648.72	826.923	7.75256989	0.02325771
30	1558.63	825.312	8.18469789	0.02455409

Run #3: $k_{\text{initial}} = 1.53 \times 10^{-3} \text{ M/min}^{-1}$

Time (min)	Area std	Area pdt	% pdt	mmol pdt
0	0	0	0	0
2	1325.6	138.062	1.609864	0.00482959
4	1674.45	295.69	2.72955581	0.00818867
6	1185.44	286.882	3.74068594	0.01122206
8	1608.4	467.73	4.49498955	0.01348497
10	1493.23	504.836	5.22578016	0.01567734
12	1800.9	668.496	5.7376855	0.01721306
14	1724.49	689.1	6.17659456	0.01852978
16	1962.18	836.461	6.5892256	0.01976768
20	2573.9	1164.89	6.9955324	0.0209866
25	2383.14	1154.78	7.48992075	0.02246976
30	2024.87	1041.908	7.95352685	0.02386058



(N)-tert-butoxycarbonyl α-benzyl-4-fluorobenzylamine: IR (film) 3383, 2976, 2908, 1675, 1604, 1506, 1455, 1442, 1391, 1365, 1350, 1296, 1266, 1250, 1223, 1168, 1158, 1097, 1081, 1044, 1014, 876, 837, 819, 730, 699 cm^{-1} ; ^1H NMR (500 MHz, CDCl_3) δ 1.38 (s, 9H, $-\text{C}(\text{CH}_3)_3$), 3.00 (brs, 2H, $-\text{CH}_2\text{Ph}$), 4.88 (brs, 2H, $-\text{CHNH}$), 6.96-6.99 (m, 2H, ArH), 7.01-7.03 (m, 2H, ArH), 7.12-7.15 (m, 2H, ArH), 7.18-7.25 (m, 3H, ArH); ^{13}C NMR (125 MHz, CDCl_3) δ 28.32, 43.35, 115.18, 115.34, 126.62, 127.95, 128.01, 128.38, 129.40, 137.04; HRMS (EI) exact mass calculated for $(\text{C}_{19}\text{H}_{22}\text{FNO}_2)$ requires m/z 315.16346, found m/z 338.15347 $[\text{M}+\text{Na}]^+$. Conversion factor for initial rate determination: 0.818235 mmol product/4,4'-dimethylbiphenyl.

Run #1: $k_{\text{initial}} = 1.62 \times 10^{-3} \text{ M/min}^{-1}$

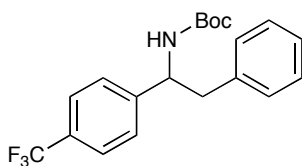
Time (min)	Area std	Area pdt	% pdt	mmol pdt
0	0	0	0	0
2	1472.79	106.221	1.47532472	0.00442597
4	1571.33	207.437	2.70045461	0.00810136
6	1310.42	249.41	3.89333174	0.01168
8	2074.01	483.968	4.7733564	0.01432007
10	1926.55	534.701	5.67739058	0.01703217
12	2016.9	631.417	6.40397998	0.01921194
14	2087.06	726.588	7.12149785	0.02136449
16	2692.8	985.214	7.4841854	0.02245256
18	1342.05	554.635	8.45389086	0.02536167
20	1632.04	706.03	8.84933055	0.02654799

Run #2: $k_{\text{initial}} = 1.59 \times 10^{-3} \text{ M/min}^{-1}$

Time (min)	Area std	Area pdt	% pdt	mmol pdt
0	0	0	0	0
2	1226.71	93.9261	1.56625491	0.00469876
4	2262.88	299.328	2.70585102	0.00811755
6	2446.21	451.769	3.77781556	0.01133345
8	2203.03	509.159	4.72771268	0.01418314
10	1470.71	422.736	5.8797688	0.01763931
12	2299.83	731.335	6.50487094	0.01951461
14	2239.32	788.038	7.19861691	0.02159585
16	2948.97	916.794	6.35944871	0.01907835
18	1448.46	587.945	8.30325271	0.02490976
20	2089.22	887.642	8.69103962	0.02607312

Run #3: $k_{\text{initial}} = 1.63 \times 10^{-3} \text{ M/min}^{-1}$

Time (min)	Area std	Area pdt	% pdt	mmol pdt
0	0	0	0	0
2	1114.47	87.5502	1.60696649	0.0048209
4	2062.88	281.093	2.78736682	0.0083621
6	2128.29	405.899	3.90126308	0.01170379
8	2520.53	611.233	4.96058601	0.01488176
10	2407.91	683.659	5.80787614	0.01742363
12	1951.32	633.944	6.64569585	0.01993709
14	2036.95	730.884	7.33983247	0.0220195
16	2178	854.954	8.02976683	0.0240893



(*N*)-*tert*-butoxycarbonyl α -benzyl-4-trifluoromethylbenzylamine: IR (film) 3380, 2979, 1675, 1619, 1519, 1496, 1443, 1367, 1325, 1267, 1251, 1162 1123, 1108, 1067, 1046, 1016, 850, 839, 779, 752, 732, 699 cm^{-1} ; ^1H NMR (500 MHz, CDCl_3) δ 1.38 (s, 9H, $-\text{C}(\text{CH}_3)_3$), 3.03 (brs, 2H, $-\text{CH}_2\text{Ph}$), 4.96 (brs, 2H, $-\text{CHNH}$), 7.02-7.04 (m, 2H, ArH), 7.21-7.24 (m, 3H, ArH), 7.29-7.31 (m, 2H, ArH), 7.55-7.56 (m, 2H, ArH); ^{13}C NMR (125 MHz, CDCl_3) δ 28.04, 28.29, 125.42, 126.68, 126.86, 128.54, 129.33, 155.01; HRMS (EI) exact mass calculated for $(\text{C}_{20}\text{H}_{22}\text{F}_3\text{NO}_2)$ requires m/z 364.12863, found m/z 365.13562 $[\text{M}+\text{H}]^+$. Conversion factor for initial rate determination: 0.8526336 mmol

product / 4,4'-dimethylbiphenyl.

Run #1: $k_{\text{initial}} = 2.29 \times 10^{-3} \text{ M/min}^{-1}$

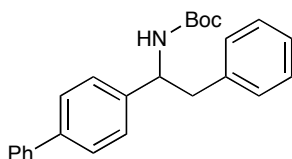
Time (min)	Area std	Area pdt	% pdt	mmol pdt
0	0	0	0	0
2	1615.58	174.818	2.30653543	0.00691961
4	1627.38	343.351	4.49729933	0.0134919
6	1852.71	504.142	5.80026567	0.0174008
8	3474	1046.13	6.41886577	0.0192566
10	2257.12	844.279	7.97322078	0.02391966
12	1790.91	758.101	9.02309978	0.0270693
14	1116.73	525.649	10.0334458	0.03010034
16	2144.88	1052.02	10.4549858	0.03136496
18	2162.61	1114.35	10.9836292	0.03295089
20	2948.02	1574.72	11.3861099	0.03415833

Run #2: $k_{\text{initial}} = 2.40 \times 10^{-3} \text{ M/min}^{-1}$

Time (min)	Area std	Area pdt	% pdt	mmol pdt
0	0	0	0	0
2	1990.79	267.38	2.8628983	0.00858869
4	1927.93	426.558	4.71616816	0.0141485
6	2222.73	639.109	6.12901485	0.01838704
8	2211.4	755.08	7.27826918	0.02183481
10	2444.55	950.011	8.28384876	0.02485155
12	1819.7	790.147	9.25572733	0.02776718
14	1385.19	660.172	10.1589823	0.03047695
16	1369.3	699.906	10.8954096	0.03268623
18	1562.3	842.2	11.4908791	0.03447264
20	1923.3	1080.86	11.9791186	0.03593736

Run #3: $k_{\text{initial}} = 2.26 \times 10^{-3} \text{ M/min}^{-1}$

Time (min)	Area std	Area pdt	% pdt	mmol pdt
0	0	0	0	0
2	2086.27	297.532	3.03994426	0.00911983
4	1613.24	363.3	4.80030539	0.01440092
6	2410.13	666.702	5.89649237	0.01768948
8	2343.86	775.736	7.0548004	0.0211644
10	2023.92	751.613	7.91595639	0.02374787
12	738.867	308.725	8.90651863	0.02671956
14	1864.3	824.316	9.42497879	0.02827494
16	1648.38	776.833	10.0455283	0.03013658
18	1313.37	650.461	10.5569052	0.03167072
20	2304.33	1161.54	10.744642	0.03223393



(N)-tert-butoxycarbonyl α -benzyl-4-phenylbenzylamine: IR (film) 3382, 2874, 2923, 1679, 1602, 1514, 1488, 1453, 1442, 1390, 1364, 1290, 1265, 1247, 1167, 1081, 1043, 1021, 1007, 851, 838, 760, 728, 719, 692 cm^{-1} ; ^1H NMR (500 MHz, CDCl_3) δ 1.39 (s, 9H, $-\text{C}(\text{CH}_3)_3$), 3.10 (brs, 2H, $-\text{CH}_2\text{Ph}$), 4.94 (brs, 2H, $-\text{CHNH}$), 7.08-7.09 (m, 2H, ArH), 7.20-7.28 (m, 5H, ArH), 7.33-7.36 (m, 1H, ArH), 7.44-7.47 (m, 2H, ArH), 7.53-7.54 (m, 2H, ArH), 7.58-7.59 (m, 2H, ArH); ^{13}C NMR (125 MHz, CDCl_3) δ 28.35, 43.31, 126.55, 126.84, 127.06, 127.20, 127.26, 127.37, 128.36, 128.78, 129.45, 137.33, 140.04; HRMS (EI) exact mass calculated for ($\text{C}_{25}\text{H}_{27}\text{NO}_2$) requires m/z 373.20418, found m/z 396.19325 $[\text{M}+\text{Na}]^+$. Conversion factor for initial rate determination: 1.0763331 mmol product / 4,4'-dimethylbiphenyl.

Run #1: $k_{\text{initial}} = 1.50 \times 10^{-3} \text{ M/min}^{-1}$

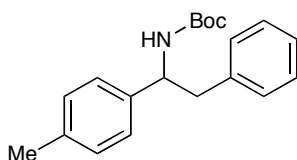
Time (min)	Area std	Area pdt	% pdt	mmol pdt
0	0	0	0	0
2	1648.68	74.3869	1.21407858	0.00364224
4	2736.1	206.199	2.02787552	0.00608363
6	2791.96	314.332	3.02946618	0.0090884
8	2328.09	341.801	3.95057461	0.01185172
10	1777.07	341.015	5.16363638	0.01549091
12	2310.38	468.956	5.46179487	0.01638538
14	2292.65	529.962	6.22004713	0.01866014
16	2659.42	855.03	8.65129512	0.02595389
18	2952.53	758.271	6.91061713	0.02073185
20	3090.43	891.881	7.76559444	0.02329678

Run #2: $k_{\text{initial}} = 1.46 \times 10^{-3} \text{ M/min}^{-1}$

Time (min)	Area std	Area pdt	% pdt	mmol pdt
0	0	0	0	0
2	2447.28	101.731	1.11855246	0.00335566
4	2719.02	209.548	2.0737568	0.00622127
6	2679.84	311.412	3.12689417	0.00938068
8	2145.71	332.021	4.16371728	0.01249115
10	2859.69	506.79	4.7686537	0.01430596
12	2780.41	567.492	5.49208951	0.01647627
14	3030.12	677.673	6.017929	0.01805379
16	3345.04	819.382	6.59131108	0.01977393
18	3117.09	808.698	6.98109796	0.02094329
20	2883.57	789.472	7.36703847	0.02210112

Run #3: $k_{\text{initial}} = 1.47 \times 10^{-3} \text{ M/min}^{-1}$

Time (min)	Area std	Area pdt	% pdt	mmol pdt
0	0	0	0	0
2	2163.21	94.0562	1.16997196	0.00350992
4	2203.65	180.588	2.20512379	0.00661537
6	1735.09	218.012	3.38099943	0.010143
8	2735.37	412.761	4.06040432	0.01218121
10	2560.26	465.694	4.89444301	0.01468333
12	3047.31	801.505	7.07744175	0.02123233
14	3052.27	670.319	5.90942583	0.01772828
16	2059.69	556.528	7.27062698	0.02181188
18	2171.77	626.935	7.76775271	0.02330326
20	3060.91	856.993	7.53378842	0.02260137



(N)-tert-butoxycarbonyl α -benzyl-4-methylbenzylamine: IR (film) 3384, 2979, 2911, 1681, 1512, 1455, 1440, 1389, 1362, 1314, 1293, 1265, 1248, 1167, 1043, 1020, 850, 804, 778, 730, 719, 697 cm^{-1} ; ^1H NMR (500 MHz, CDCl_3) δ 1.37 (s, 9H, $-\text{C}(\text{CH}_3)_3$), 2.32 (s, 3H, $-\text{CH}_3$), 3.04 (brs, 2H, $-\text{CH}_2\text{Ph}$), 4.89 (brs, 2H, $-\text{CHNH}$), 7.05-7.11 (m, 6H, ArH), 7.18-7.24 (m, 3H, ArH); ^{13}C NMR (125 MHz, CDCl_3) δ 21.12, 28.33, 126.33, 126.42, 128.27, 129.15, 129.44, 136.81, 137.57; HRMS (EI) exact mass calculated for $(\text{C}_{20}\text{H}_{25}\text{NO}_2)$ requires m/z 311.18853, found m/z 334.17781 $[\text{M}+\text{Na}]^+$. Conversion factor

for initial rate determination: 0.8700065 mmol product / 4,4'-dimethylbiphenyl.

Run #1: $k_{\text{initial}} = 1.17 \times 10^{-3} \text{ M/min}^{-1}$

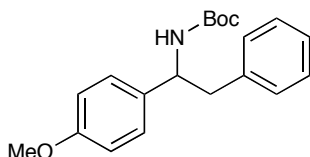
Time (min)	Area std	Area pdt	% pdt	mmol pdt
0	0	0	0	0
5	2492.3	284.427	2.4821785	0.00744654
10	1876.84	395.861	4.58752002	0.01376256
20	1626.6	628.623	8.40566359	0.02521699
25	1587.23	712.389	9.76202347	0.02928607
30	2614.38	1302.04	10.8322362	0.03249671
35	2209.4	1246.58	12.2718012	0.0368154
40	1815.63	1120.13	13.4184881	0.04025546
45	2280.5	1472.3	14.0419927	0.04212598
50	2910.38	1922.13	14.3646671	0.043094
55	1700.85	1225.64	15.6732629	0.04701979
60	2925.5	2127.56	15.8177323	0.0474532

Run #2: $k_{\text{initial}} = 1.19 \times 10^{-3} \text{ M/min}^{-1}$

Time (min)	Area std	Area pdt	% pdt	mmol pdt
0	0	0	0	0
5	2159.92	236.97	2.38626246	0.00715879
10	2633.02	559.128	4.61869825	0.01385609
15	1622.31	502.634	6.73876829	0.0202163
20	1476.88	577.566	8.50587343	0.02551762
25	2497.3	1126.83	9.81409346	0.02944228
30	2375.97	1222.73	11.1931448	0.03357943
35	2964.36	1696.67	12.4488416	0.03734652
40	2159.99	1327.7	13.3693632	0.04010809
45	1770.4	1183.81	14.5436398	0.04363092
50	3434.54	2357.2	14.9276127	0.04478284
55	2539.18	1828.07	15.6589212	0.04697676
60	1692.6	1287.29	16.5418685	0.04962561

Run #3: $k_{\text{initial}} = 1.18 \times 10^{-3} \text{ M/min}^{-1}$

Time (min)	Area std	Area pdt	% pdt	mmol pdt
0	0	0	0	0
5	2174.41	268.353	2.6842782	0.00805283
10	1264.53	294.549	5.06630022	0.0151989
15	1469.87	467.972	6.92473963	0.02077422
20	2596	996.933	8.35264051	0.02505792
25	2400	1096.9	9.94073052	0.02982219
30	2406.15	1263.35	11.4199313	0.03425979
35	1780.08	1050.47	12.8353182	0.03850595
40	1722.7	1129.62	14.2621574	0.04278647
45	1982.96	1355.61	14.8690532	0.04460716
50	1099.23	812.575	16.0781986	0.0482346
55	2206.14	1686.1	16.6231286	0.04986939
60	1982.11	1577.81	17.3136828	0.05194105



(N)-tert-butoxycarbonyl- α -benzyl-4-methoxybenzylamine: IR (film) 3383, 2975, 2910, 2838, 1679, 1613, 1508, 1455, 1441, 1390, 1364, 1303, 1242, 1166, 1109, 1082, 1023, 971, 879, 849, 834, 808, 778, 750, 729, 698 cm^{-1} ; ^1H NMR (500 MHz, CDCl_3) δ 1.38 (s, 9H, $-\text{C}(\text{CH}_3)_3$), 3.02 (brs, 2H, $-\text{CH}_2\text{Ph}$), 3.79 (s, 3H, $-\text{OCH}_3$), 4.84 (brs, 2H, $-\text{CHNH}$), 6.83-6.82 (m, 2H, ArH), 7.03-7.05 (m, 2H, ArH), 7.09-7.11 (m, 2H, ArH), 7.18-7.24 (m, 3H, ArH); ^{13}C NMR (125 MHz, CDCl_3) δ 28.32, 55.27, 113.77, 113.92, 126.41, 127.58, 127.85, 128.26, 128.39, 129.46, 137.54; HRMS (EI) exact mass calculated for $(\text{C}_{20}\text{H}_{25}\text{NO}_3)$ requires m/z 327.18344, found m/z 350.1726 $[\text{M}+\text{Na}]^+$. Conversion factor for initial rate determination: 0.930085 mmol product / 4,4'-dimethylbiphenyl.

Run #1: $k_{\text{initial}} = 6.89 \times 10^{-5} \text{ M/min}^{-1}$

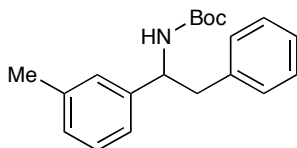
Time (min)	Area std	Area pdt	% pdt	mmol pdt
0	0	0	0	0
10	2614.04	27.3369	0.24316423	0.00072949
15	2268.21	34.1327	0.34990491	0.00104971
20	2577.82	52.4179	0.47281329	0.00141844
25	1733.99	46.4324	0.62264025	0.00186792
30	2480.12	73.5296	0.68936965	0.00206811
35	2727.74	98.8583	0.84269965	0.0025281
40	1061.26	49.9256	1.09386606	0.0032816
45	2101.74	97.8424	1.08245726	0.00324737
50	2591.82	122.639	1.10023742	0.00330071
55	2773.27	150.958	1.2656879	0.00379706
60	2960.67	173.504	1.36264315	0.00408793

Run #2: $k_{\text{initial}} = 6.86 \times 10^{-5} \text{ M/min}^{-1}$

Time (min)	Area std	Area pdt	% pdt	mmol pdt
0	0	0	0	0
5	2711.22	17.7384	0.15212911	0.00045639
10	2170.09	21.7364	0.23290163	0.0006987
15	1503.12	24.6404	0.38116828	0.0011435
20	2536.31	49.1952	0.45100675	0.00135302
25	2638.28	63.5088	0.55972624	0.00167918
30	1497.03	46.8724	0.7280301	0.00218409
35	2241.67	75.0817	0.77879843	0.0023364
40	1194.23	50.0488	0.9744697	0.00292341
45	2486.65	107.969	1.00959471	0.00302878
50	2530.91	123.648	1.13598617	0.00340796
55	1164.16	67.946	1.35710631	0.00407132
60	2897.52	166.27	1.33428961	0.00400287

Run #3: $k_{\text{initial}} = 7.50 \times 10^{-5} \text{ M/min}^{-1}$

Time (min)	Area std	Area pdt	% pdt	mmol pdt
0	0	0	0	0
5	1675.5	9.45473	0.13121012	0.00039363
10	2230.82	21.438	0.22345104	0.00067035
15	2120.44	33.2527	0.36463938	0.00109392
20	2842.6	55.4533	0.4536013	0.0013608
25	2791.64	69.4631	0.57857198	0.00173572
30	1757.26	58.9961	0.78063843	0.00234192
35	2993.95	104.693	0.81308463	0.00243925
40	3227.72	128.679	0.92698877	0.00278097
45	3125.1	145	1.07851438	0.00323554
50	2679.38	141.206	1.22541019	0.00367623
55	2217.13	137.066	1.43747808	0.00431243
60	1683.32	125.807	1.73780392	0.00521341



(*N*)-*tert*-butoxycarbonyl α -benzyl-3-methylbenzylamine: IR (film) 3383, 2980, 2920, 1682, 1606, 1517, 1495, 1443, 1389, 1363, 1349, 1264, 1244, 1159, 1083, 1044, 1027, 1012, 886, 853, 786, 776, 752, 730, 699 cm^{-1} ; ^1H NMR (500 MHz, CDCl_3) δ 1.37 (s, 9H, $-\text{C}(\text{CH}_3)_3$), 2.32 (s, 3H, $-\text{CH}_3$), 3.04 (brs, 2H, $-\text{CH}_2\text{Ph}$), 4.86 (brs, 2H, $-\text{CHNH}$), 6.98-7.00

(m, 2H, ArH), 7.04-7.07 (m, 3H, ArH), 7.17-7.20 (m, 2H, ArH), 7.22-7.24 (m, 2H, ArH); ^{13}C NMR (125 MHz, CDCl_3) δ 21.50, 28.33, 123.40, 126.45, 127.22, 127.98, 128.27, 128.35, 129.43, 137.54, 138.07; HRMS (EI) exact mass calculated for ($\text{C}_{20}\text{H}_{25}\text{NO}_3$) requires m/z 311.18853, found m/z 334.17782 $[\text{M}+\text{Na}]^+$. Conversion factor for initial rate determination: 0.8563388 mmol product / 4,4'-dimethylbiphenyl.

Run #1: $k_{\text{initial}} = 1.50 \times 10^{-3} \text{ M/min}^{-1}$

Time (min)	Area std	Area pdt	% pdt	mmol pdt
0	0	0	0	0
2	1157.99	94.9457	1.75531928	0.00526596
4	2554.1	361.433	3.02953194	0.0090886
6	1796.97	341.093	4.06366231	0.01219099
8	3099.82	763.281	5.27149266	0.01581448
10	1929.3	584.892	6.49025182	0.01947076
12	1863.59	638.089	7.3302117	0.02199064
14	2883.28	1086.83	8.06975648	0.02420927
16	2592.99	1070.42	8.83769488	0.02651308
18	1930.5	865.177	9.5944656	0.0287834
20	2113.16	1010.31	10.2354726	0.03070642

Run #2: $k_{\text{initial}} = 1.15 \times 10^{-3} \text{ M/min}^{-1}$

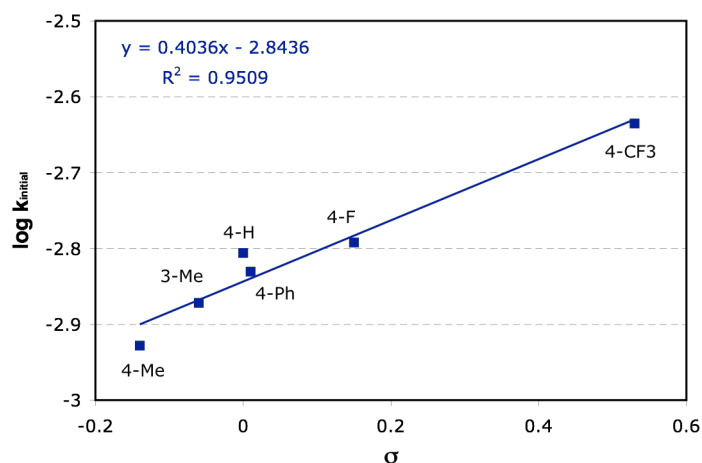
Time (min)	Area std	Area pdt	% pdt	mmol pdt
0	0	0	0	0
2	2691.31	207.22	1.64836572	0.0049451
4	1805.57	259.94	3.0820836	0.00924625
6	2823.89	533.886	4.04749562	0.01214249
8	1837.17	464.138	5.40858192	0.01622575
10	1951.35	569.904	6.25247787	0.01875743
12	1780.19	603.841	7.26175966	0.02178528
14	2466.7	894.27	7.76136233	0.02328409
16	3105.7	1202.7	8.29055185	0.02487166
18	3172.01	1336.41	9.01967314	0.02705902
20	2075.12	911.109	9.39967312	0.02819902

Run #3: $k_{\text{initial}} = 1.38 \times 10^{-3} \text{ M/min}^{-1}$

Time (min)	Area std	Area pdt	% pdt	mmol pdt
0	0	0	0	0
2	1907.59	139.714	1.56798	0.00470394
4	2632.65	315.678	2.56706474	0.00770119
6	1689.91	285.036	3.61095245	0.01083286
8	2951.1	602.181	4.36846392	0.01310539
10	2666.82	640.402	5.14096452	0.01542289
12	2170.8	588.227	5.80110562	0.01740332
14	1259.91	397.512	6.75454892	0.02026365
16	1721.94	564.335	7.01624268	0.02104873
18	911.633	329.203	7.73088792	0.02319266
20	2045.28	741.064	7.75690684	0.02327072

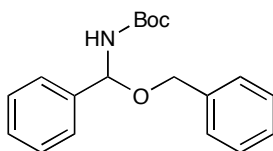
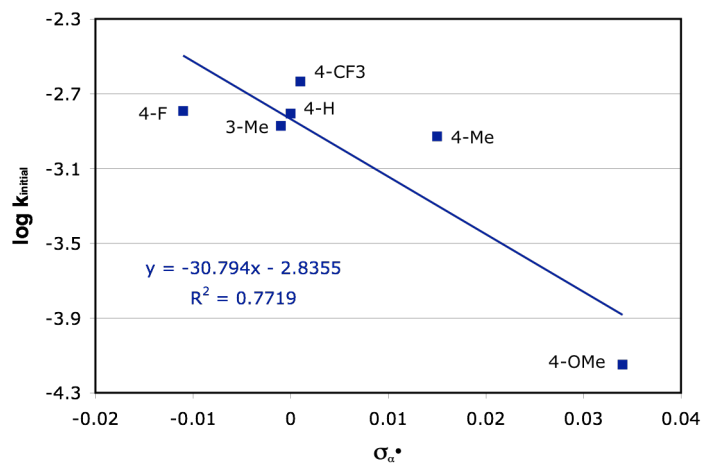
Hammett Plots: Values for the initial rate were averaged over the three runs and plotted versus σ^{23} and $\sigma_{\alpha}^{\bullet 24}$.

R	Initial Rate	log (Initial Rate)	σ	$\sigma_{\alpha}^{\bullet}$
4-OMe	7.08333E-05	-4.14976232	-0.12	0.034
4-Me	0.00118	-2.928117993	-0.14	0.015
3-Me	0.001343333	-2.871816209	-0.06	-0.001
H	0.001563333	-2.805948412	0	0
4-Ph	0.001476667	-2.830717528	0.01	
4-F	0.001613333	-2.792275893	0.15	-0.011
4-CF ₃	0.002316667	-2.63513645	0.53	0.001



²³ Values for σ taken from: *Modern Physical Organic Chemistry*; Anslyn, R. A.; Dougherty, D. A.; University Science Books: Sausalito, 2006.

²⁴ Value for $\sigma_{\alpha}^{\bullet}$ taken from: Arnold, D. R.; Dust, J. M. *J. Am. Chem. Soc.* **1983**, *105*, 1221.



(*N*)-*tert*-butoxycarbonyl α -benzyl-benzylamine: To a solution of potassium (50.0 mg, 0.252 mmol) and benzaldehyde *N*-(*tert*-butoxycarbonyl)imine (104 mg, 0.505 mmol) in acetonitrile (2.5 mL, 0.1 M) at 23 °C was added an O₂ containing balloon and oxygen was bubbled through the solution for 20 minutes. The balloon was removed and 19 μ L (0.252 mmol) of trifluoroacetic acid was added in a dropwise fashion. The reaction was stirred at 23 °C for 4 h to provide the title compound as a white solid (54.6 mg, 69% yield) following standard workup procedure and silica gel chromatography (5% Et₂O/hexanes). IR (film) 3387, 3270, 3064, 2973, 1720, 1689, 1541, 1518, 1497, 1454, 1362, 1266, 1248, 1170, 1053, 1026, 963, 914, 888, 856, 845, 750, 696 cm⁻¹; ¹H NMR (300 MHz, CDCl₃) δ 1.48 (s, 9H, -C(CH₃)₃), 5.07 (AB, 2H, *J* = 5, 11 Hz, -OCH₂Ph), 5.31 (brs, 1H, -CHNH), 6.52 (brs, 1H, -CHNH), 7.33-7.36 (m, 10H, ArH); ¹³C NMR (125 MHz, CDCl₃) δ 28.31, 85.13, 126.51, 128.41, 128.61, 128.99, 129.24, 135.66, 136.32;

HRMS (EI) exact mass calculated for (C₁₉H₂₃NO₃) requires m/z 352.13150, found m/z 352.15219 [M+K]⁺.